

Status of the Bonn-Gatchina partial-wave analysis

A. Sarantsev

HISKP (Bonn), PNPI (Russia)



Petersburg
Nuclear
Physics
Institute

PWA 2011

23-27 May 2011, GWU, USA

Bonn-Gatchina partial wave analysis group:

A. Anisovich, E. Klempt, V. Nikonov, A. Srantsev, U. Thoma

<http://pwa.hiskp.uni-bonn.de/>



Bonn-Gatchina Partial Wave Analysis



Address: Nussallee 14-16, D-53115 Bonn Fax: (+49) 228 / 73-2505

[Data Base](#)

[Meson Spectroscopy](#)

[Baryon Spectroscopy](#)

[NN-interaction](#)

[Formalism](#)

[Analysis of Other Groups](#)

- [SAID](#)
- [MAID](#)
- [Giessen Uni](#)

[BG PWA](#)

- [Publications](#)
- [Talks](#)
- [Contacts](#)

[Useful Links](#)

- [SPIRES](#)
- [PDG Homepage](#)
- [Durham Data Base](#)
- [Bonn Homepage](#)

[CB-ELSA Homepage](#)

Responsible: Dr. V. Nikonov, E-mail: nikonov@hiskp.uni-bonn.de
Last changes: January 26th, 2010.

Search for baryon states

1. Analysis of single meson and double meson photoproduction reactions.

$\gamma p \rightarrow \pi N, \eta N, K\Lambda, K\Sigma, \pi\pi N, \pi\eta N$, CB-ELSA, CLAS, GRAAL, LEPS.

2. Analysis of single meson and double meson pion-induced reactions.

$\pi N \rightarrow \pi N, \eta N, K\Lambda, K\Sigma, \pi\pi N$.

Search for meson states

1. Analysis of the $p\bar{p}$ annihilation at rest and $\pi\pi$ interaction data.
2. Analysis of the $p\bar{p}$ annihilation in flight into two and tree meson final state.
3. Analysis of the J/Ψ decays (BES III collaboration).

Analysis of NN interaction

1. Analysis of single and double meson production $NN \rightarrow \pi NN$ and $\pi\pi NN$
2. Analysis of hyperon production $NN \rightarrow K\Lambda p$

Energy dependent approach

In many cases an unambiguous partial wave decomposition at fixed energies is impossible. Then the energy and angular parts should be analyzed together:

$$A(s, t) = \sum_{\beta\beta'n} A_n^{\beta\beta'}(s) Q_{\mu_1 \dots \mu_n}^{(\beta)} F_{\nu_1 \dots \nu_n}^{\mu_1 \dots \mu_n} Q_{\nu_1 \dots \nu_n}^{(\beta')}$$

1. C. Zemach, Phys. Rev. 140, B97 (1965); 140, B109 (1965).
 2. S.U.Chung, Phys. Rev. D 57, 431 (1998).
 3. A.V. Anisovich *et al.* J. Phys. G 28 15 (2002)
 V. V. Anisovich, M. A. Matveev, V. A. Nikonov, J. Nyiri and A. V. Sarantsev,
Hackensack, USA: World Scientific (2008) 580 p
1. Correlations between angular part and energy part are under control.
 2. Unitarity and analyticity can be introduced from the beginning.
 3. Parameters are be fixed from combined fit of many reactions.

πN vertices

$$N_{\mu_1 \dots \mu_n}^+ = X_{\mu_1 \dots \mu_n}^{(n)} \quad N_{\mu_1 \dots \mu_n}^- = i\gamma_\nu \gamma_5 X_{\nu \mu_1 \dots \mu_n}^{(n+1)} \quad (1)$$

γN vertices

$$\begin{aligned} Q_{\alpha_1 \dots \alpha_n}^{(1+) \mu} &= \gamma_\mu i \gamma_5 X_{\alpha_1 \dots \alpha_n}^{(n)} , & Q_{\alpha_1 \dots \alpha_n}^{(1-) \mu} &= \gamma_\xi \gamma_\mu O_{\xi \alpha_1 \dots \alpha_n}^{(n+1)} , \\ Q_{\alpha_1 \dots \alpha_n}^{(2+) \mu} &= \gamma_\nu i \gamma_5 X_{\mu \nu \alpha_1 \dots \alpha_n}^{(n+2)} , & Q_{\alpha_1 \dots \alpha_n}^{(2-) \mu} &= X_{\mu \alpha_1 \dots \alpha_n}^{(n+1)} , \\ Q_{\alpha_1 \dots \alpha_n}^{(3+) \mu} &= \gamma_\nu i \gamma_5 X_{\nu \alpha_1 \dots \alpha_n}^{(n+1)} g_{\mu \alpha_n}^\perp , & Q_{\alpha_1 \dots \alpha_n}^{(3-) \mu} &= X_{\alpha_2 \dots \alpha_n}^{(n-1)} g_{\alpha_1 \mu}^\perp . \end{aligned}$$

Fermion propagator for $J = N + \frac{1}{2}$

$$\begin{aligned} F_{\nu_1 \dots \nu_L}^{\mu_1 \dots \mu_L}(p) &= (m + \hat{p}) O_{\alpha_1 \dots \alpha_L}^{\mu_1 \dots \mu_L} \frac{L+1}{2L+1} \left(g_{\alpha_1 \beta_1}^\perp - \frac{L}{L+1} \sigma_{\alpha_1 \beta_1} \right) \prod_{i=2}^L g_{\alpha_i \beta_i} O_{\nu_1 \dots \nu_L}^{\beta_1 \dots \beta_L} \\ \sigma_{\alpha_i \alpha_j} &= \frac{1}{2} (\gamma_{\alpha_i} \gamma_{\alpha_j} - \gamma_{\alpha_j} \gamma_{\alpha_i}) \end{aligned}$$

Combined analysis of pion- and photo-production data:

For pion induced reactions:

$$A_{1i} = K_{1j}(I - i\rho K)_{ji}^{-1}$$

and

$$K_{ij} = \sum_{\alpha} \frac{g_i^{\alpha} g_j^{\alpha}}{M_{\alpha}^2 - s} + f_{ij}(s) \quad f_{ij} = \frac{f_{ij}^{(1)} + f_{ij}^{(2)} \sqrt{s}}{s - s_0^{ij}}.$$

where f_{ij} is nonresonant transition part.

For the photoproduction:

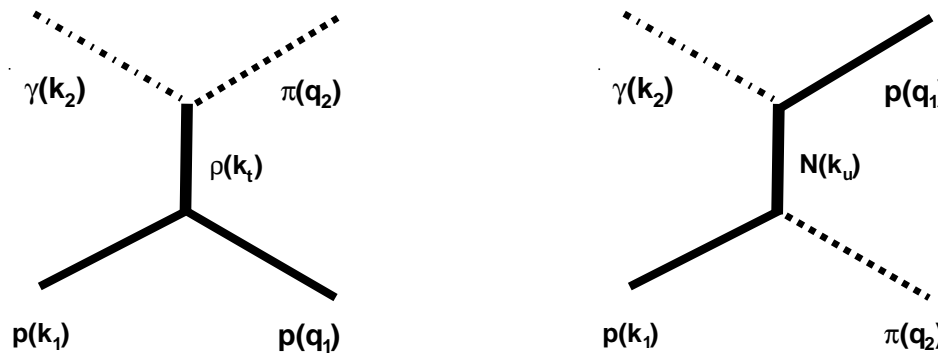
$$A_k = P_j(I - i\rho K)_{jk}^{-1}$$

The vector of the initial interaction has the form:

$$P_j = \sum_{\alpha} \frac{\Lambda^{\alpha} g_j^{\alpha}}{M_{\alpha}^2 - s} + F_j(s)$$

Here F_j is nonresonant production of the final state j .

Reggeized exchanges:



The amplitude for t-channel exchange:

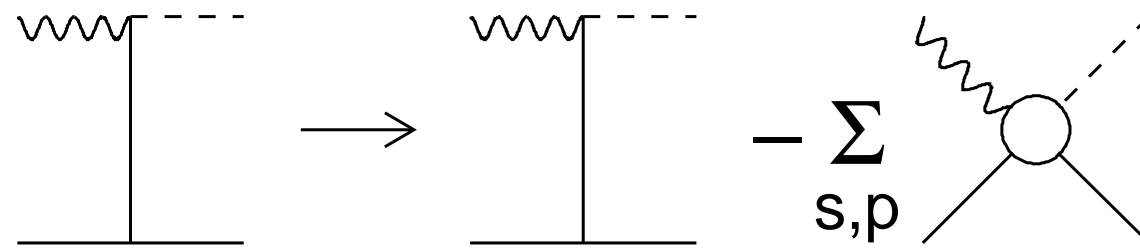
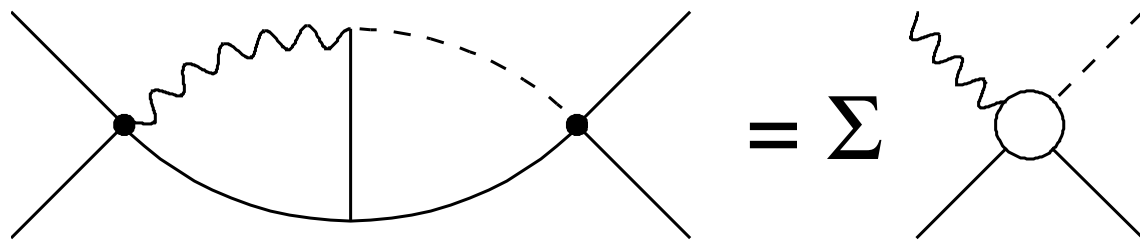
$$A = g_1(t)g_2(t)R(\xi, \nu, t) = g_1(t)g_2(t) \frac{1 + \xi \exp(-i\pi\alpha(t))}{\sin(\pi\alpha(t))} \frac{\nu}{\nu_0}^{\alpha(t)} \quad \nu = \frac{1}{2}(s - u).$$

Here $\alpha(t)$ is Reggeon trajectory, and ξ is its signature:

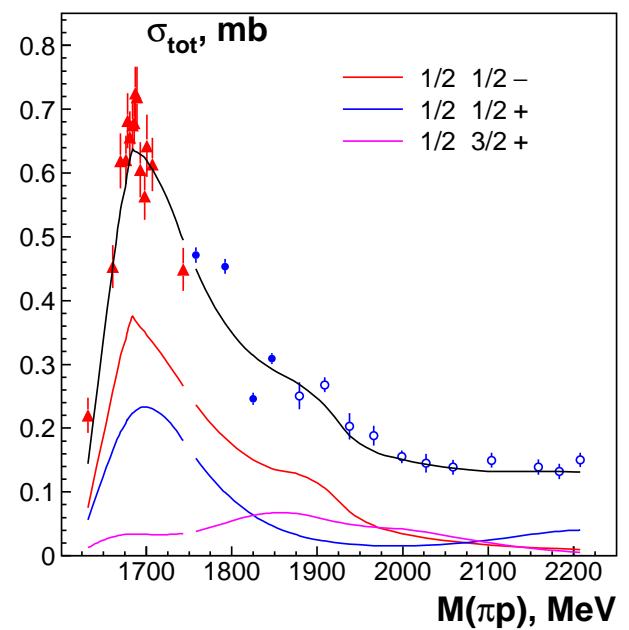
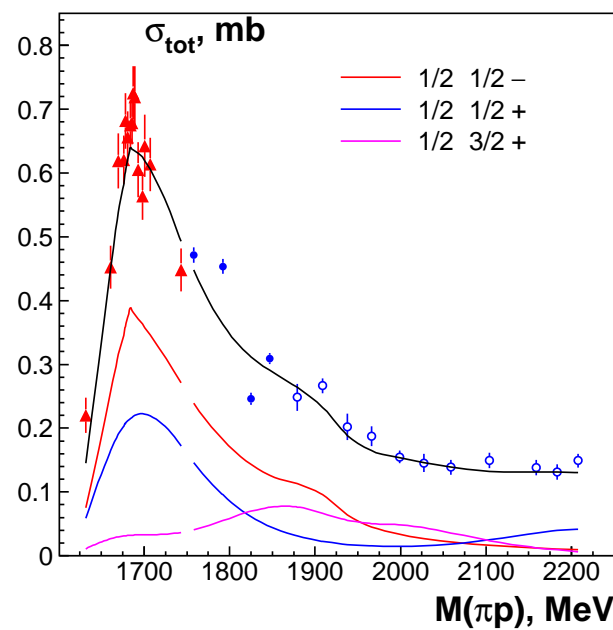
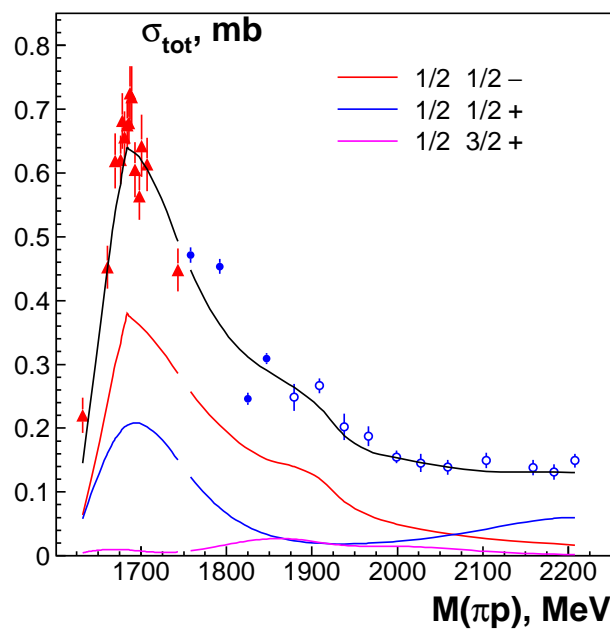
$$R(+, \nu, t) = \frac{e^{-i\frac{\pi}{2}\alpha(t)}}{\sin(\frac{\pi}{2}\alpha(t))\Gamma_{-\frac{\alpha(t)}{2}}} \frac{\nu}{\nu_0}^{\alpha(t)},$$

$$R(-, \nu, t) = \frac{ie^{-i\frac{\pi}{2}\alpha(t)}}{\cos(\frac{\pi}{2}\alpha(t))\Gamma_{-\frac{\alpha(t)}{2} + \frac{1}{2}}} \frac{\nu}{\nu_0}^{\alpha(t)}.$$

t,u-exchange subtraction procedure

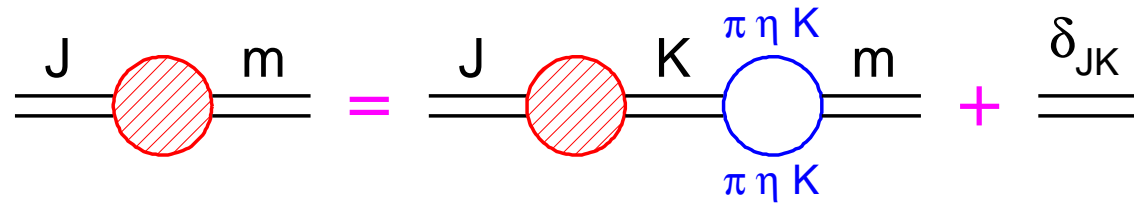


t,u-exchange subtraction procedure



N/D based (D-matrix) analysis of the data

In the case of resonance contributions only we have factorization and Bethe-Salpeter equation can be easily solved:



$$D_{jm} = D_{jk} \sum_{\alpha} B_{\alpha}^{km}(s) \frac{1}{M_m - s} + \frac{\delta_{jm}}{M_j^2 - s} \quad B_{\alpha}^{km}(s) = \int_{4m_{\alpha}^2}^{\infty} \frac{ds'}{\pi} \frac{g_{\alpha}^{(k)}(s') \rho_{\alpha}(s') g_{\alpha}^{(m)}(s')}{s' - s - i0}$$

$$\hat{D} = \hat{\kappa}(I - \hat{B}\hat{\kappa})^{-1} \quad \kappa_{ij} = \frac{\delta_{ij}}{M_i^2 - s} \quad B^{ij} = \sum_{\alpha} B_{\alpha}^{km}(s)$$

There is no factorization for non-resonant contributions: for every non-resonant transition to introduce a vertices and propagator (e.g. $R = 1$).

$$B_{\alpha}^{km}(s) = B_{\alpha}^{km}(M_s^2) + (s - M_s^2) \int_{4m_{\alpha}^2}^{\infty} \frac{ds'}{\pi} \frac{g_{\alpha}^{(k)}(s') \rho_{\alpha}(s') g_{\alpha}^{(m)}(s')}{(s' - s - i0)(s' - M_s^2)}$$

Meson spectroscopy. Two body reactions:

Reaction	Experiment	Reaction	Experiment
$\pi^+ \pi^- \rightarrow \pi^+ \pi^-$ (all waves)	CERN-Münich		
$\pi\pi \rightarrow \pi^0 \pi^0$ (S-wave)	GAMS	$\pi\pi \rightarrow \pi^0 \pi^0$ (S-wave)	E852
$\pi\pi \rightarrow \eta\eta$ (S-wave)	GAMS	$\pi\pi \rightarrow \eta\eta'$ (S-wave)	GAMS
$\pi\pi \rightarrow K\bar{K}$ (S-wave)	BNL	S-wave $\delta(\pi^+ \pi^-)$	Ke4

Three body reactions from Crystal Barrel: (**L**-liquid, **G**-gaseous targets).

Reaction	Target	Reaction	Target	Reaction	Target
$\bar{p}p \rightarrow \pi^0 \pi^0 \pi^0$	(L) H_2	$\bar{p}p \rightarrow \pi^+ \pi^0 \pi^-$	(L) H_2	$\bar{p}p \rightarrow K_S K_S \pi^0$	(L) H_2
$\bar{p}p \rightarrow \pi^0 \eta\eta$	(L) H_2	$\bar{p}n \rightarrow \pi^0 \pi^0 \pi^-$	(L) D_2	$\bar{p}p \rightarrow K^+ K^- \pi^0$	(L) H_2
$\bar{p}p \rightarrow \pi^0 \pi^0 \eta$	(L) H_2	$\bar{p}n \rightarrow \pi^- \pi^- \pi^+$	(L) D_2	$\bar{p}p \rightarrow K_L K^\pm \pi^\mp$	(L) H_2
$\bar{p}p \rightarrow \pi^0 \pi^0 \pi^0$	(G) H_2			$\bar{p}n \rightarrow K_S K_S \pi^-$	(L) D_2
$\bar{p}p \rightarrow \pi^0 \eta\eta$	(G) H_2			$\bar{p}n \rightarrow K_S K^- \pi^0$	(L) D_2
$\bar{p}p \rightarrow \pi^0 \pi^0 \eta$	(G) H_2				

Parameterization of the K-matrix for S-wave:

$$K_{ab}(s) = \left(\sum_{\alpha} \frac{g_a^{(\alpha)} g_b^{(\alpha)}}{M_{\alpha}^2 - s} + f_{ab} \frac{1 \text{ GeV}^2 + s_0}{s + s_0} \right) \frac{s - s_A}{s + s_{A0}} ,$$

where K_{ab} is a 5×5 matrix ($a, b = \pi\pi, K\bar{K}, \eta\eta, \eta\eta', 4pi + \dots$)

$$\rho_a(s) = \frac{\sqrt{(s - (m_{1a} + m_{2a})^2)(s - (m_{1a} - m_{2a})^2)}}{s} , \quad a = \pi, K, \eta, \eta'$$

The multi-meson phase space factor is defined as

$$\begin{aligned} \rho_{51} = \rho_0 \int \frac{ds_1}{\pi} \int \frac{ds_2}{\pi} M^2 \Gamma(s_1) \Gamma(s_2) \sqrt{(s + s_1 - s_2)^2 - 4ss_1} \times \\ \times s^{-1} [(M^2 - s_1)^2 + M^2 \Gamma^2(s_1)]^{-1} [(M^2 - s_2)^2 + M^2 \Gamma^2(s_2)]^{-1} , \end{aligned}$$

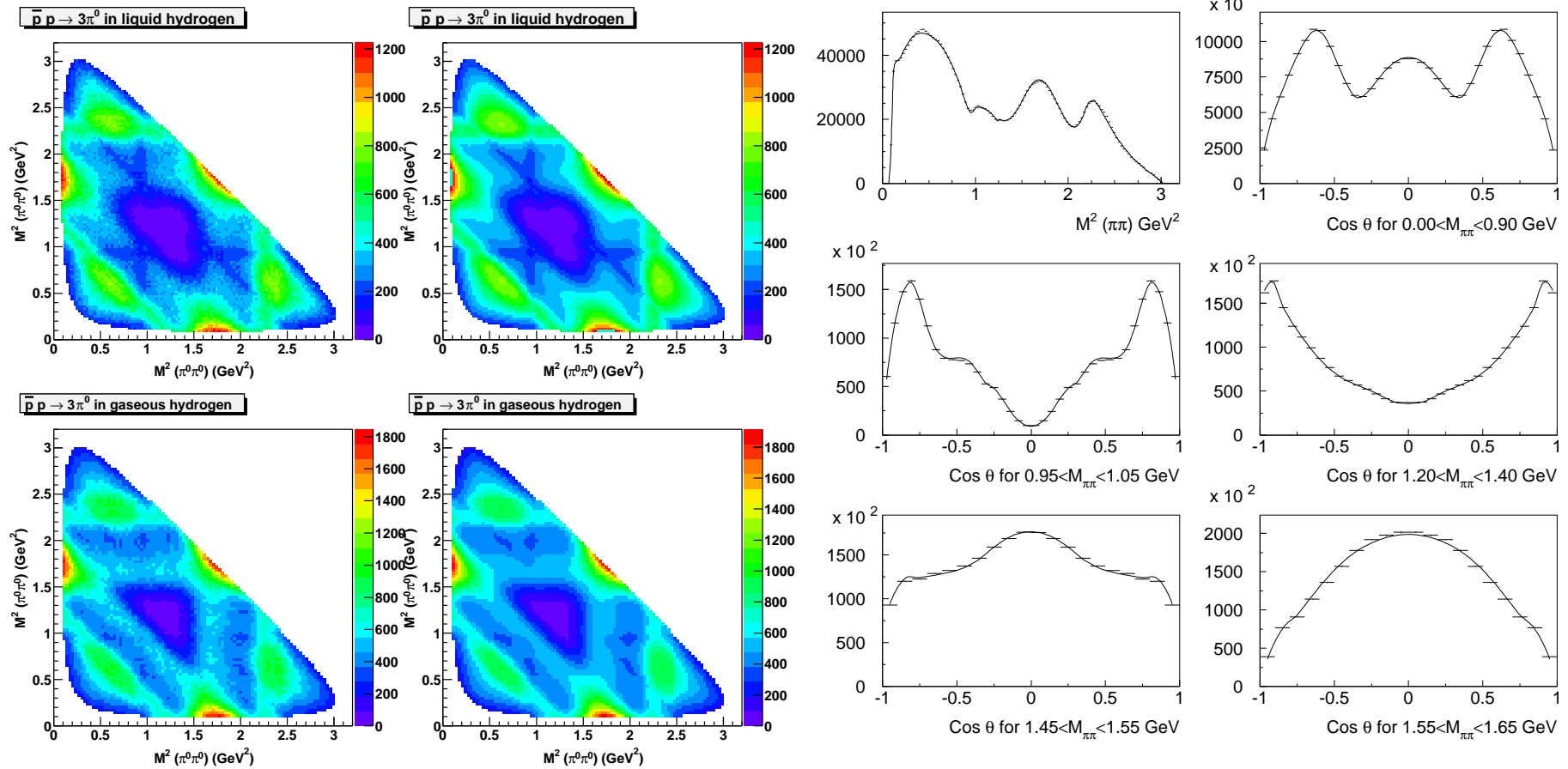
$$B_{\alpha\beta}^j(s) = g_a^{R(\alpha)} \left(b^j + (s - M_j^2) \int_{(m_{1a}+m_{2a})^2}^{\infty} \frac{ds'}{\pi} \frac{\rho_j(s', m_{1a}, m_{2a})}{(s' - s - i0)(s' - M_j^2)} \right) g_b^{L(\beta)} ,$$

Description of the data with K-matrix and D-matrix approaches

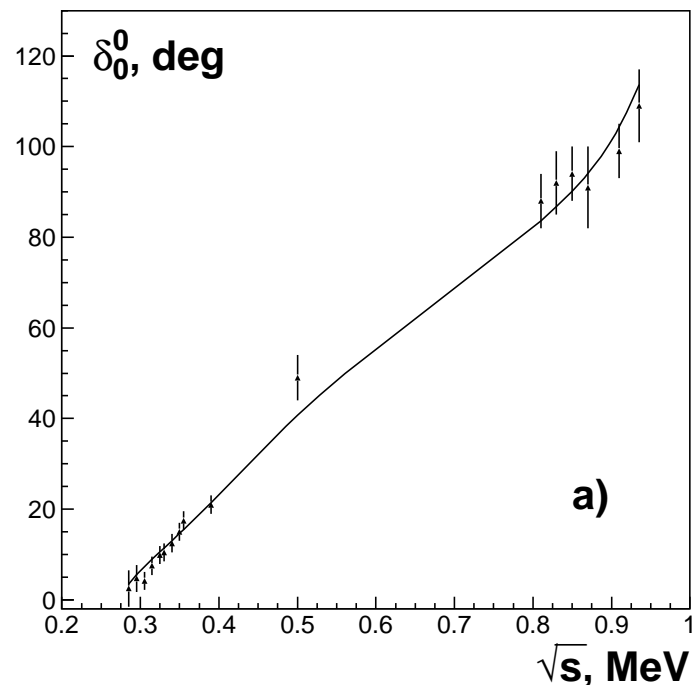
	K-matr.	D-matr.	N		K-matr.	D-matr.	N
$\bar{p}p \rightarrow \pi^0 \pi^0 \pi^0 (\text{L})$	1.32	1.37	7110	$\bar{p}p \rightarrow \pi^0 \pi^0 \pi^0 (\text{G})$	1.39	1.44	4891
$\bar{p}p \rightarrow \pi^0 \eta \eta (\text{L})$	1.33	1.34	3595	$\bar{p}p \rightarrow \pi^0 \eta \eta (\text{G})$	1.31	1.34	1182
$\bar{p}p \rightarrow \pi^0 \pi^0 \eta (\text{L})$	1.24	1.33	3475	$\bar{p}p \rightarrow \pi^0 \pi^0 \eta (\text{G})$	1.20	1.22	3631
$\bar{p}p \rightarrow \pi^+ \pi^0 \pi^- (\text{L})$	1.54	1.46	1334	$\bar{p}p \rightarrow K_S K_S \pi^0 (\text{L})$	1.09	1.10	394
$\bar{p}n \rightarrow \pi^0 \pi^0 \pi^-$	1.51	1.47	825	$\bar{p}n \rightarrow \pi^- \pi^- \pi^+$	1.61	1.54	823
$\bar{p}n \rightarrow K^+ K^- \pi^0$	0.98	1.00	521	$\bar{p}n \rightarrow K_L K^\pm \pi^\mp$	0.78	0.79	737
$\bar{p}p \rightarrow K_S K_S \pi^-$	1.66	1.64	396				
$\pi\pi \rightarrow (\pi^0 \pi^0)_S$	1.23	1.13	68	$\pi\pi \rightarrow (\eta\eta)_S$	1.02	1.05	15
$\pi\pi \rightarrow (\eta\eta')_S$	0.45	0.30	9	$\pi\pi \rightarrow (K\bar{K})_S$	1.32	1.13	35
$\delta_0^0(\pi^- \pi^+ \rightarrow \pi^- \pi^+)$	1.51	1.02	17	K_{e4} data			

Description of the $\bar{p}p \rightarrow 3\pi^0$ data (D-matrix method)

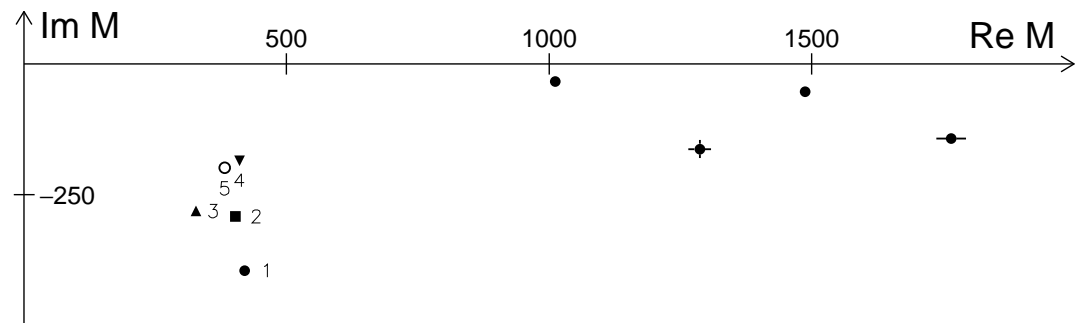
$\bar{p}p - 3\pi^0$ Liquid target



Pole position of the resonances



	K-matrix	D-matrix
σ -meson	420-i 395	407-i 281
$f_0(980)$	1014-i 31	1015-i 36
$f_0(1300)$	1302-i 180	1307-i 137
$f_0(1500)$	1487-i 58	1487-i 60
$f_0(1750)$	1738-i 152	1781-i 140



Masses and couplings of bare states

	K-matrix	D-matrix		K-matrix	D-matrix
M_1	671	685	$g_{4\pi}^{(1)}$	0*	0*
M_2	1205	1135	$g_{4\pi}^{(2)}$	0*	0*
M_3	1560	1561	$g_{4\pi}^{(3)}$	0.638	0.534
M_4	1210	1290	$g_{4\pi}^{(4)}$	0.997	0.790
M_5	1816	1850	$g_{4\pi}^{(5)}$	-0.901	-0.862
g_1	0.860	0.926	Φ_1	-74	-83
g_2	0.956	0.950	Φ_2	6	-2.6
g_3	0.373	0.290	Φ_3	9	5
g_4	0.447	0.307	Φ_4	38	31
g_5	0.458	0.369	Φ_5	-64	-71
$f_{\pi\pi \rightarrow \pi\pi}$	0.337	0.408	$f_{\pi\pi \rightarrow K\bar{K}}$	0.212	0.036
$f_{\pi\pi \rightarrow 4\pi}$	-0.199	-0.101	$f_{\pi\pi \rightarrow \eta\eta}$	0.389	0.438
$f_{\pi\pi \rightarrow \eta\eta'}$	0.394	0.518			

Baryon Data Base

Pion induced reactions (χ^2 analysis).

Observable	N_{data}	$\frac{\chi^2}{N_{\text{data}}}$		Observable	N_{data}	$\frac{\chi^2}{N_{\text{data}}}$	
$N_{1/2}^*$ S ₁₁ ($\pi N \rightarrow \pi N$)	112	2.05	SAID (2.10)	$\Delta_{1/2}^-$ S ₃₁ ($\pi N \rightarrow \pi N$)	112	2.31	SAID (2.10)
$N_{1/2}^*$ P ₁₁ ($\pi N \rightarrow \pi N$)	112	2.49	SAID (2.10)	$\Delta_{1/2}^+$ P ₃₁ ($\pi N \rightarrow \pi N$)	104	3.81	SAID (2.10)
$N_{3/2}^*$ P ₁₃ ($\pi N \rightarrow \pi N$)	112	1.33	SAID (2.20)	$\Delta_{3/2}^*$ P ₃₃ ($\pi N \rightarrow \pi N$)	120	2.79	SAID (2.20)
$N_{3/2}^*$ D ₁₃ ($\pi N \rightarrow \pi N$)	108	2.55	SAID (2.20)	$\Delta_{3/2}^*$ D ₃₃ ($\pi N \rightarrow \pi N$)	108	2.47	SAID (2.10)
$N_{5/2}^*$ D ₁₅ ($\pi N \rightarrow \pi N$)	140	2.37	SAID (2.40)	$N_{7/2}^*$ G ₁₇ ($\pi N \rightarrow \pi N$)	102	2.54	SAID (2.40)
$N_{5/2}^*$ F ₁₅ ($\pi N \rightarrow \pi N$)	88	1.72	SAID (2.20)	$\Delta_{5/2}^+$ F ₃₅ ($\pi N \rightarrow \pi N$)	62	1.45	SAID (2.10)
$N_{7/2}^*$ F ₁₇ ($\pi N \rightarrow \pi N$)	82	1.98	SAID (2.50)	$\Delta_{7/2}^+$ F ₃₇ ($\pi N \rightarrow \pi N$)	72	2.75	SAID (2.10)
$N_{9/2}^*$ G ₁₉ ($\pi N \rightarrow \pi N$)	74	2.82	SAID (2.50)	$N_{9/2}^*$ H ₁₉ ($\pi N \rightarrow \pi N$)	86	2.56	SAID (2.50)
$d\sigma/d\Omega(\pi^- p \rightarrow n\eta)$	70	1.58	Richards <i>et al.</i>	$d\sigma/d\Omega(\pi^- p \rightarrow n\eta)$	84	2.73	CBALL
$d\sigma/d\Omega(\pi^- p \rightarrow K\Lambda)$	598	1.67	RAL	$P(\pi^- p \rightarrow K\Lambda)$	355	1.67	RAL+ANL
$d\sigma/d\Omega(\pi^+ p \rightarrow K^+\Sigma)$	609	1.25	RAL	$\beta(\pi^- p \rightarrow K\Lambda)$	72	1.04	RAL
$d\sigma/d\Omega(\pi^- p \rightarrow K^0\Sigma^0)$	259	0.88	RAL	$P(\pi^+ p \rightarrow K^+\Sigma)$	307	1.43	RAL
				$\beta(\pi^+ p \rightarrow K^+\Sigma)$	7	2.08	RAL
				$P(\pi^- p \rightarrow K^0\Sigma^0)$	95	1.35	RAL

Baryon Data Base (SAID db: 2008)

π and η photoproduction reactions (χ^2 analysis).

Observable	N_{data}	$\frac{\chi^2}{N_{\text{data}}}$		Observable	N_{data}	$\frac{\chi^2}{N_{\text{data}}}$	
$d\sigma/d\Omega(\gamma p \rightarrow p\pi^0)$	1106	1.56	CB-ELSA	$d\sigma/d\Omega(\gamma p \rightarrow p\pi^0)$	861	1.58	GRAAL
$d\sigma/d\Omega(\gamma p \rightarrow p\pi^0)$	592	1.27	CLAS	$d\sigma/d\Omega(\gamma p \rightarrow p\pi^0)$	1692	2.00	TAPS@MAMI
$\Sigma(\gamma p \rightarrow p\pi^0)$	540	0.71	CB-ELSA	$\Sigma(\gamma p \rightarrow p\pi^0)$	1492	2.48	SAID db
$E(\gamma p \rightarrow p\pi^0)$	140	1.14	A2-GDH	$T(\gamma p \rightarrow p\pi^0)$	389	3.15	SAID db
$P(\gamma p \rightarrow p\pi^0)$	607	2.98	SAID db	$G(\gamma p \rightarrow p\pi^0)$	75	1.70	SAID db
$H(\gamma p \rightarrow p\pi^0)$	71	1.17	SAID db	$O_z(\gamma p \rightarrow p\pi^0)$	7	0.27	SAID db
$O_x(\gamma p \rightarrow p\pi^0)$	7	1.14	SAID db	$d\sigma/d\Omega(\gamma p \rightarrow n\pi^+)$	1583	1.53	SAID db
$d\sigma/d\Omega(\gamma p \rightarrow n\pi^+)$	484	1.45	CLAS	$E(\gamma p \rightarrow n\pi^+)$	231	1.52	A2-GDH
$d\sigma/d\Omega(\gamma p \rightarrow n\pi^+)$	408	0.55	A2-GDH	$T(\gamma p \rightarrow n\pi^+)$	661	2.87	SAID db
$\Sigma(\gamma p \rightarrow n\pi^+)$	899	2.95	SAID db	$G(\gamma p \rightarrow p\pi^+)$	86	5.67	SAID db
$P(\gamma p \rightarrow n\pi^+)$	252	2.00	SAID db	$d\sigma/d\Omega(\gamma p \rightarrow p\eta)$	100	2.26	TAPS
$H(\gamma p \rightarrow p\pi^+)$	71	4.20	SAID db	$\Sigma(\gamma p \rightarrow p\eta)$	100	2.43	GRAAL 07
$d\sigma/d\Omega(\gamma p \rightarrow p\eta)$	680	1.23	CB-ELSA				
$\Sigma(\gamma p \rightarrow p\eta)$	51	1.90	GRAAL 98				
$T(\gamma p \rightarrow p\eta)$	50	1.39	Phoenics				

Baryon Data Base

Kaon photoproduction (χ^2 analysis).

Observable	N_{data}	$\frac{\chi^2}{N_{\text{data}}}$		Observable	N_{data}	$\frac{\chi^2}{N_{\text{data}}}$	
$d\sigma/d\Omega(\gamma p \rightarrow \Lambda K^+)$	1320	0.78	CLAS09	$d\sigma/d\Omega(\gamma p \rightarrow \Sigma^0 K^+)$	1280	1.98	CLAS
$P(\gamma p \rightarrow \Lambda K^+)$	1270	1.75	CLAS09	$P(\gamma p \rightarrow \Sigma^0 K^+)$	95	1.53	CLAS
$C_x(\gamma p \rightarrow \Lambda K^+)$	160	1.44	CLAS	$C_x(\gamma p \rightarrow \Sigma^0 K^+)$	94	2.36	CLAS
$C_z(\gamma p \rightarrow \Lambda K^+)$	160	1.53	CLAS	$C_z(\gamma p \rightarrow \Sigma^0 K^+)$	94	1.62	CLAS
$\Sigma(\gamma p \rightarrow \Lambda K^+)$	66	3.32	GRAAL	$\Sigma(\gamma p \rightarrow \Sigma^0 K^+)$	42	1.80	GRAAL
$\Sigma(\gamma p \rightarrow \Lambda K^+)$	45	2.34	LEP	$\Sigma(\gamma p \rightarrow \Sigma^0 K^+)$	45	1.31	LEP
$T(\gamma p \rightarrow \Lambda K^+)$	66	1.35	GRAAL 09	$d\sigma/d\Omega(\gamma p \rightarrow \Sigma^+ K^0)$	48	3.41	CLAS
$O_x(\gamma p \rightarrow \Lambda K^+)$	66	1.70	GRAAL 09	$d\sigma/d\Omega(\gamma p \rightarrow \Sigma^+ K^0)$	72	0.67	CB-ELSA 10
$O_z(\gamma p \rightarrow \Lambda K^+)$	66	1.66	GRAAL 09	$P(\gamma p \rightarrow \Sigma^+ K^0)$	24	1.17	CB-ELSA 10
$P(\gamma p \rightarrow \Lambda K^+)$	84	0.60	GRAAL	$\Sigma(\gamma p \rightarrow \Sigma^+ K^0)$	15	1.39	CB-ELSA 10

Baryon Data Base

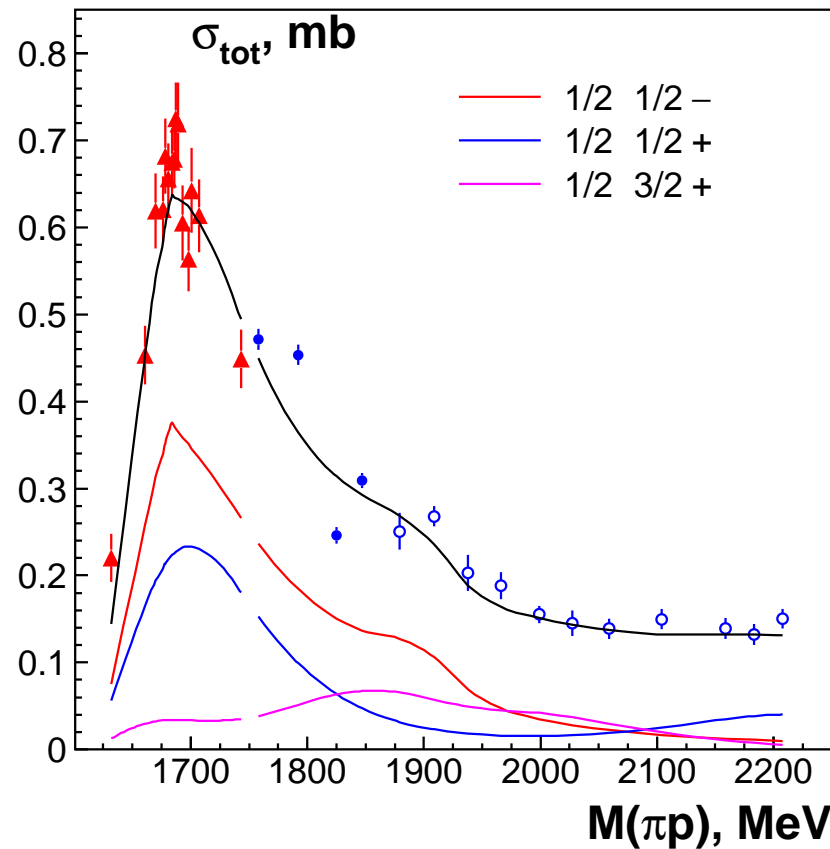
Multi-meson final states (maximum likelihood analysis).

$d\sigma/d\Omega(\pi^- p \rightarrow n\pi^0\pi^0)$	CBALL					
$d\sigma/d\Omega(\gamma p \rightarrow p\pi^0\pi^0)$	CB-ELSA (1.4 GeV)	$E(\gamma p \rightarrow p\pi^0\pi^0)$	16	1.91	MAMI	
$d\sigma/d\Omega(\gamma p \rightarrow p\pi^0\eta)$	CB-ELSA (3.2 GeV)	$\Sigma(\gamma p \rightarrow p\pi^0\eta)$	180	2.37	GRAAL	
$d\sigma/d\Omega(\gamma p \rightarrow p\pi^0\pi^0)$	CB-ELSA (3.2 GeV)	$\Sigma(\gamma p \rightarrow p\pi^0\pi^0)$	128	0.96	GRAAL	
$d\sigma/d\Omega(\gamma p \rightarrow p\pi^0\eta)$	CB-ELSA (3.2 GeV)	$\Sigma(\gamma p \rightarrow p\pi^0\eta)$	180	2.37	GRAAL	
$I_c(\gamma p \rightarrow p\pi^0\eta)$	CB-ELSA (3.2 GeV)	$I_s(\gamma p \rightarrow p\pi^0\eta)$	CB-ELSA (3.2 GeV)			

The fit of the the $\pi^- p \rightarrow K\Lambda$ reaction

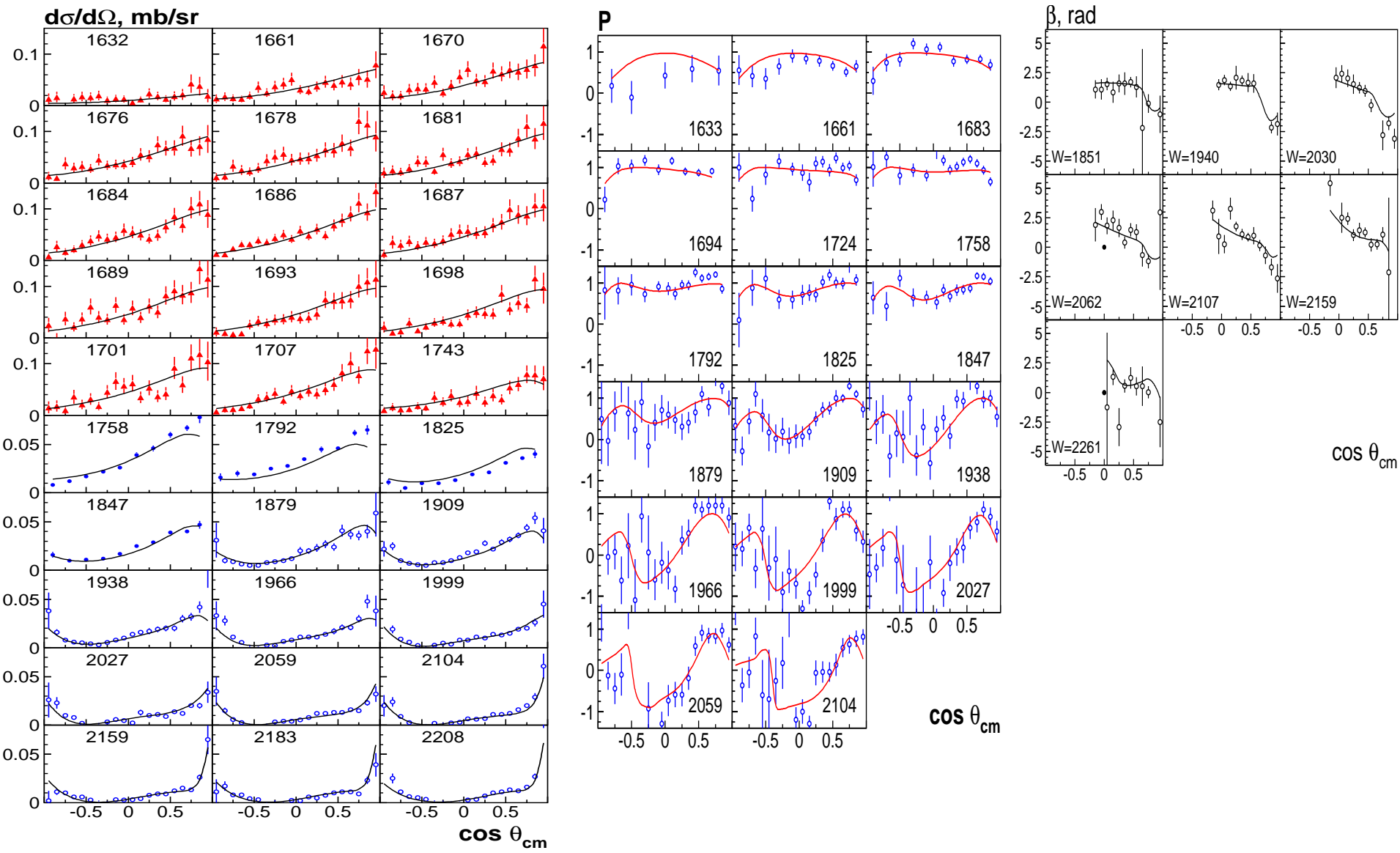
Full experiment for $\pi N \rightarrow K\Lambda$:
differential cross section, analyzing
power, rotation parameter.

A clear evidence for resonances which
are hardly seen (or not seen) in
the elastic reactions: $N(1710)P_{11}$,
 $N(1900)P_{13}$,

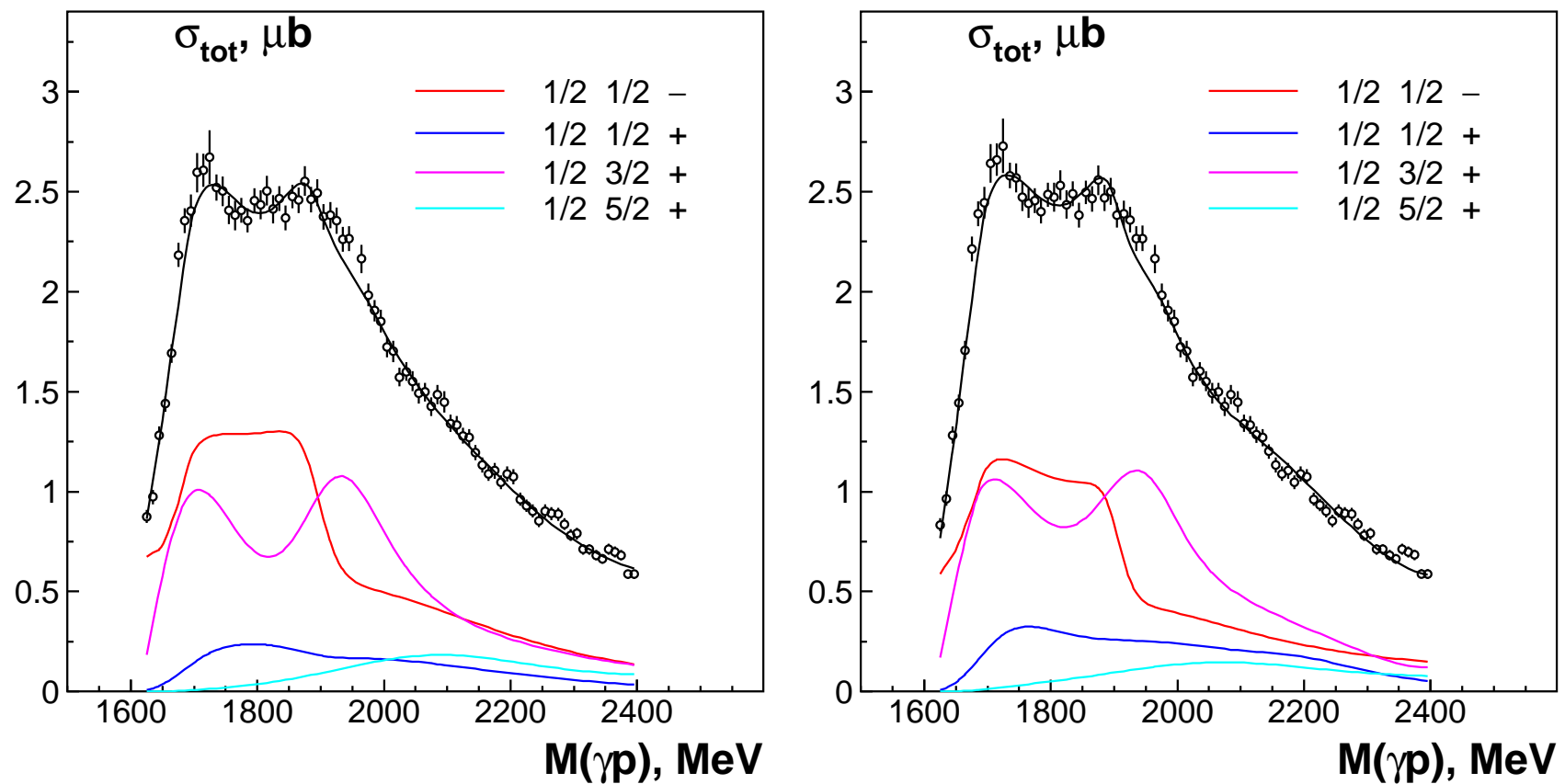


The total cross section for the reaction
 $\pi^- p \rightarrow K^0\Lambda$ **and contributions from**
leading partial waves.

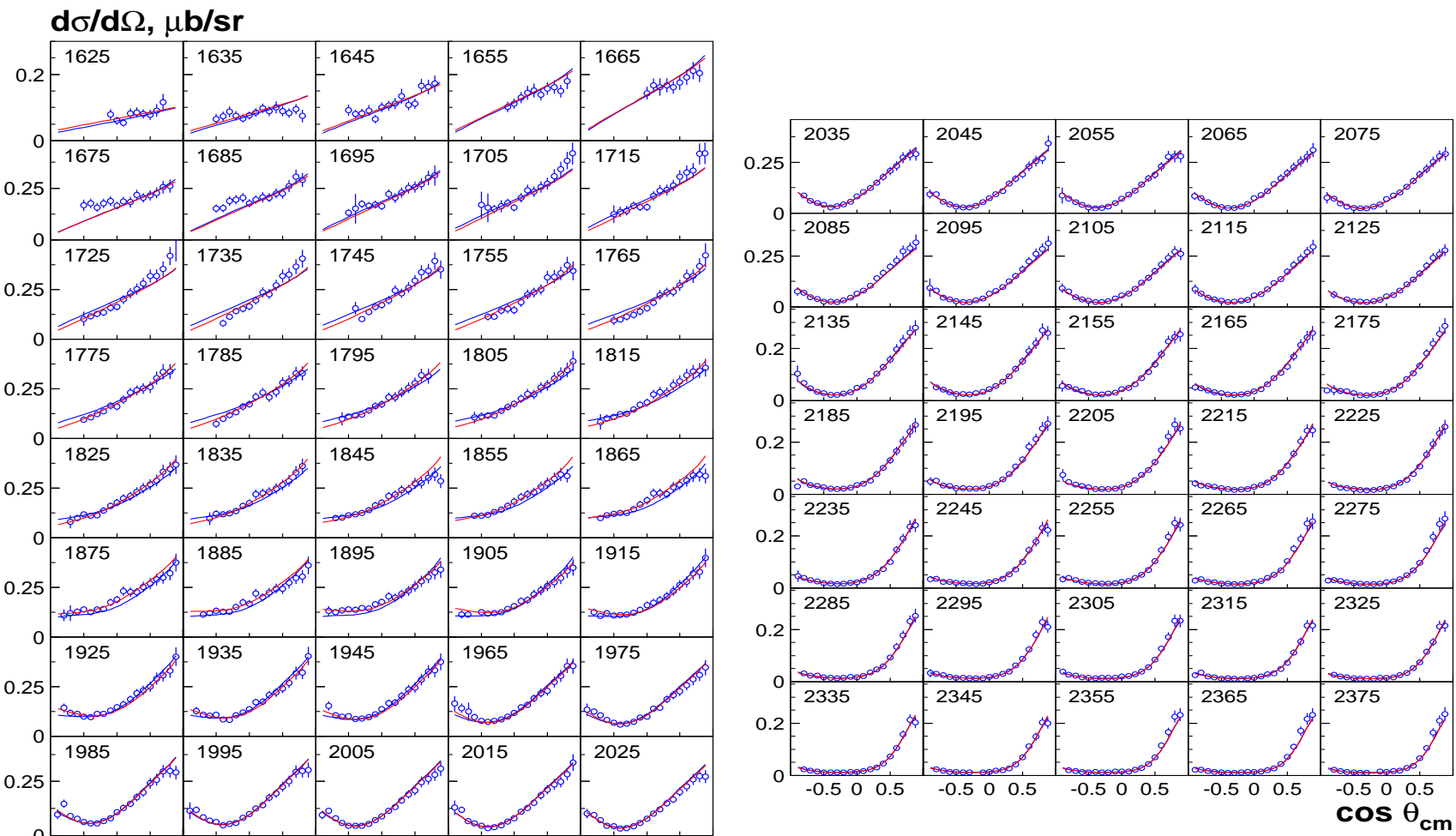
$$\pi^- p \rightarrow K\Lambda \text{ (} d\sigma/d\Omega, P, \beta \text{)}$$



The $\gamma p \rightarrow K\Lambda$ reaction (CLAS 2009)

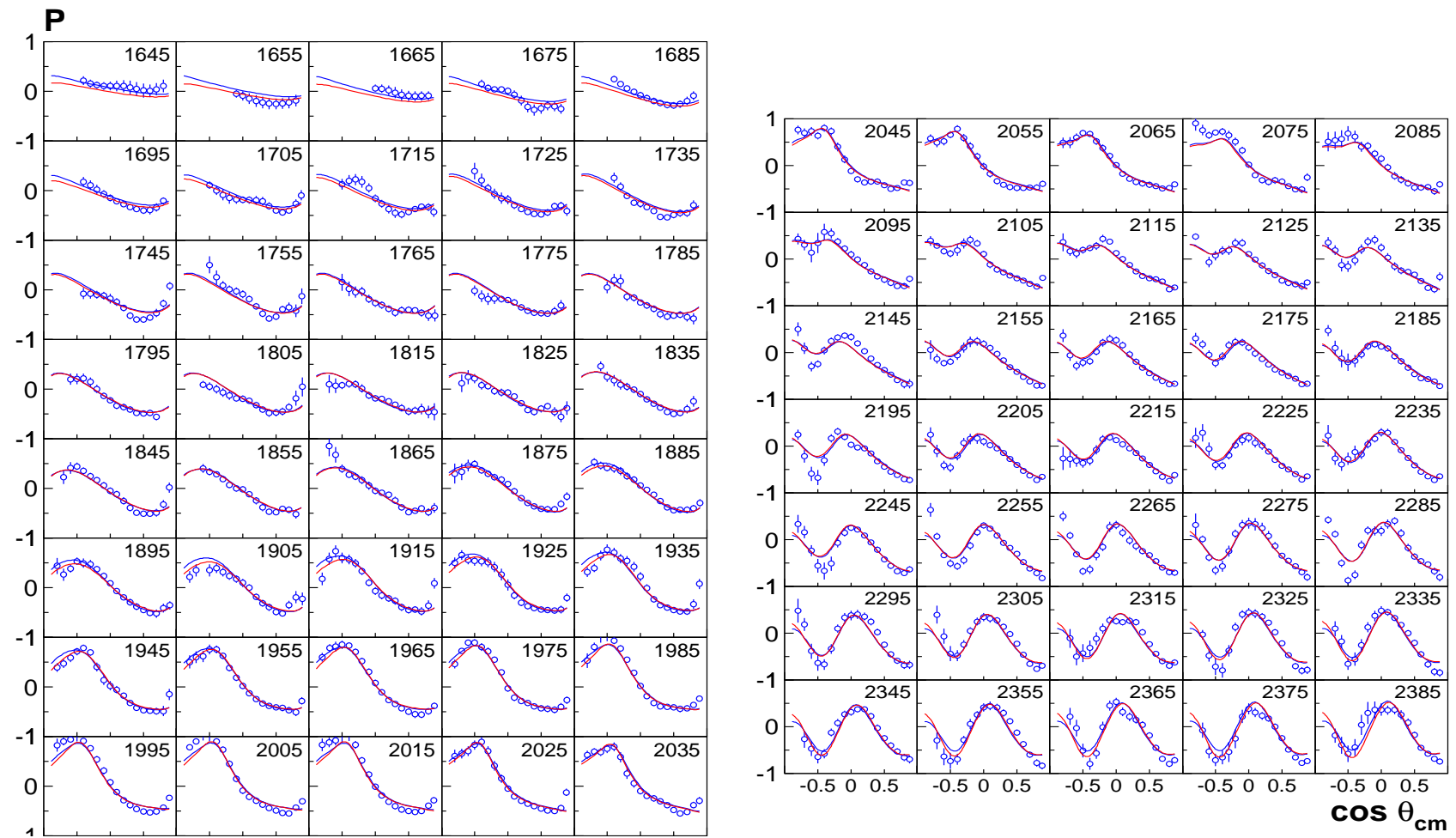


**The fit of the $\gamma p \rightarrow K\Lambda$ differential cross section
(CLAS 2009)**

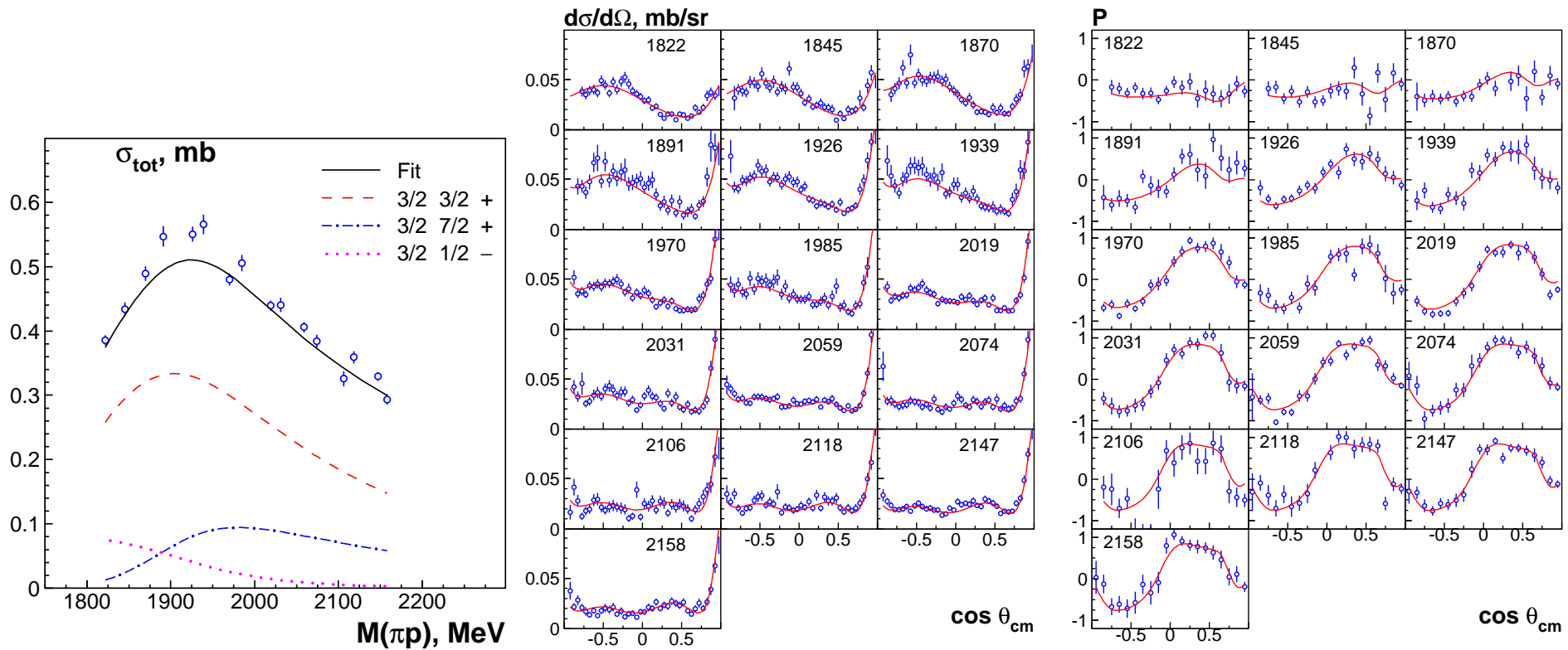


The fit of the $\gamma p \rightarrow K\Lambda$ recoil asymmetry

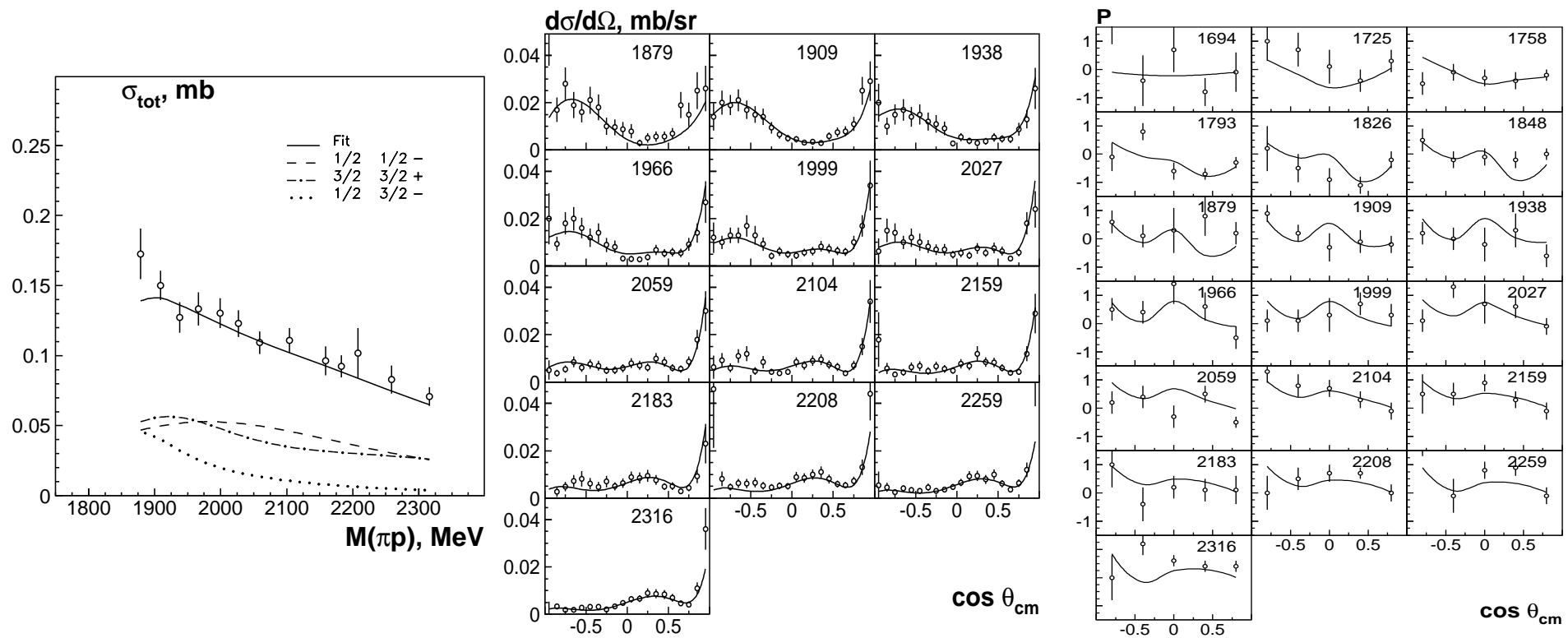
(CLAS 2009)

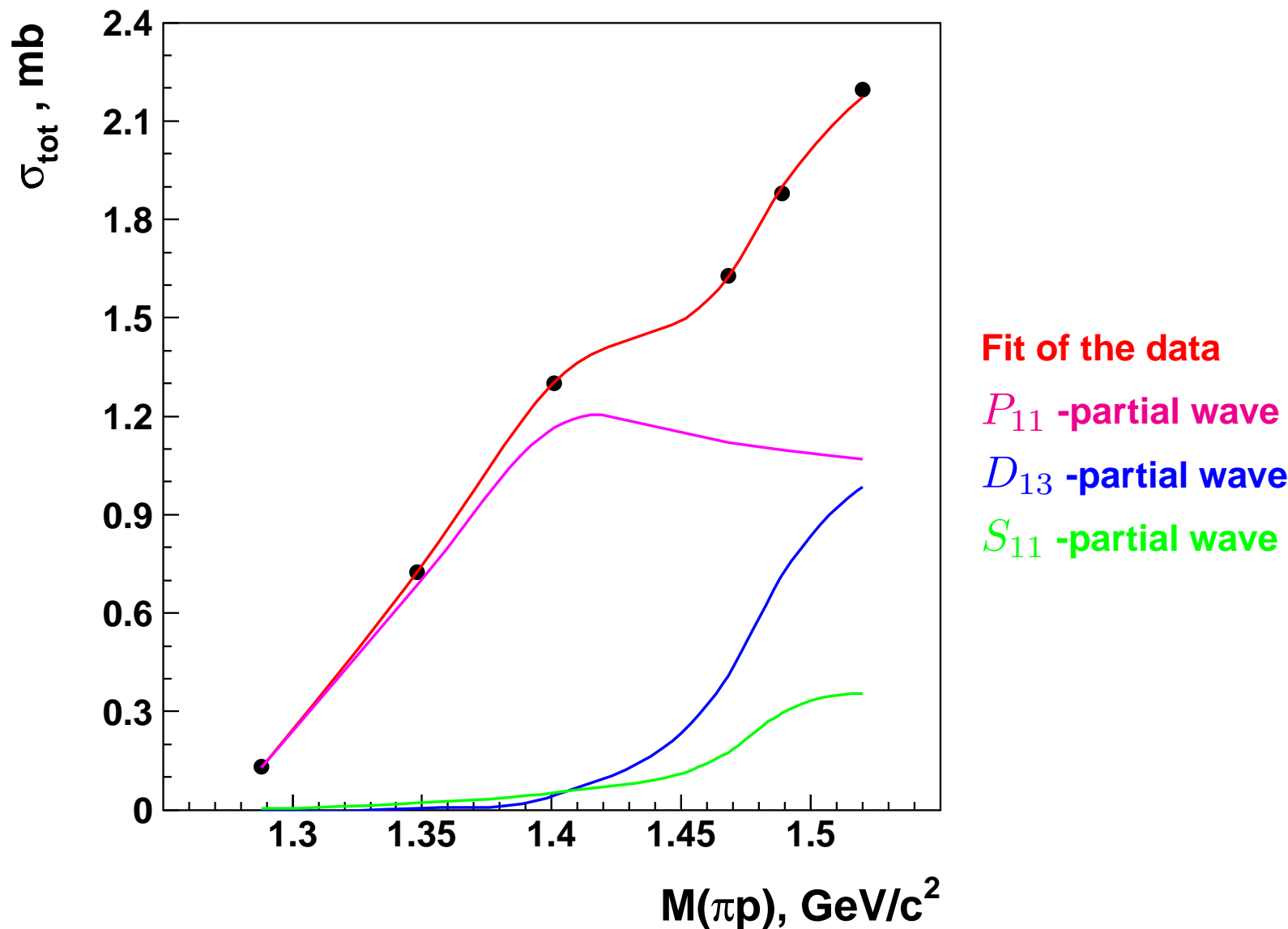


The fit of the the $\pi^+ p \rightarrow K^+ \Sigma^+$ reaction



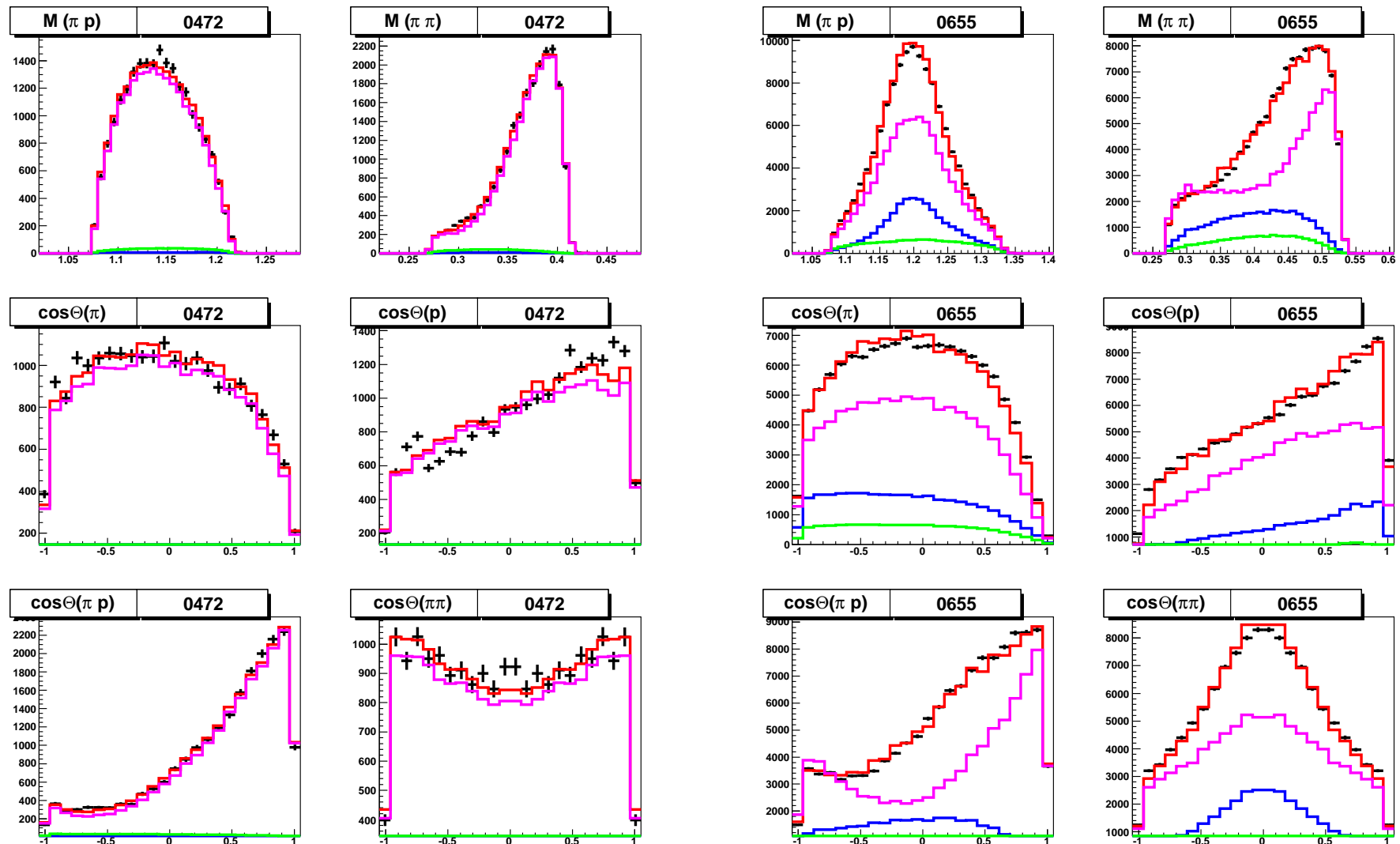
The fit of the the $\pi^- p \rightarrow K^0 \Sigma^0$ reaction



$\pi^- p \rightarrow n\pi^0\pi^0$ (Crystal Ball) total cross section

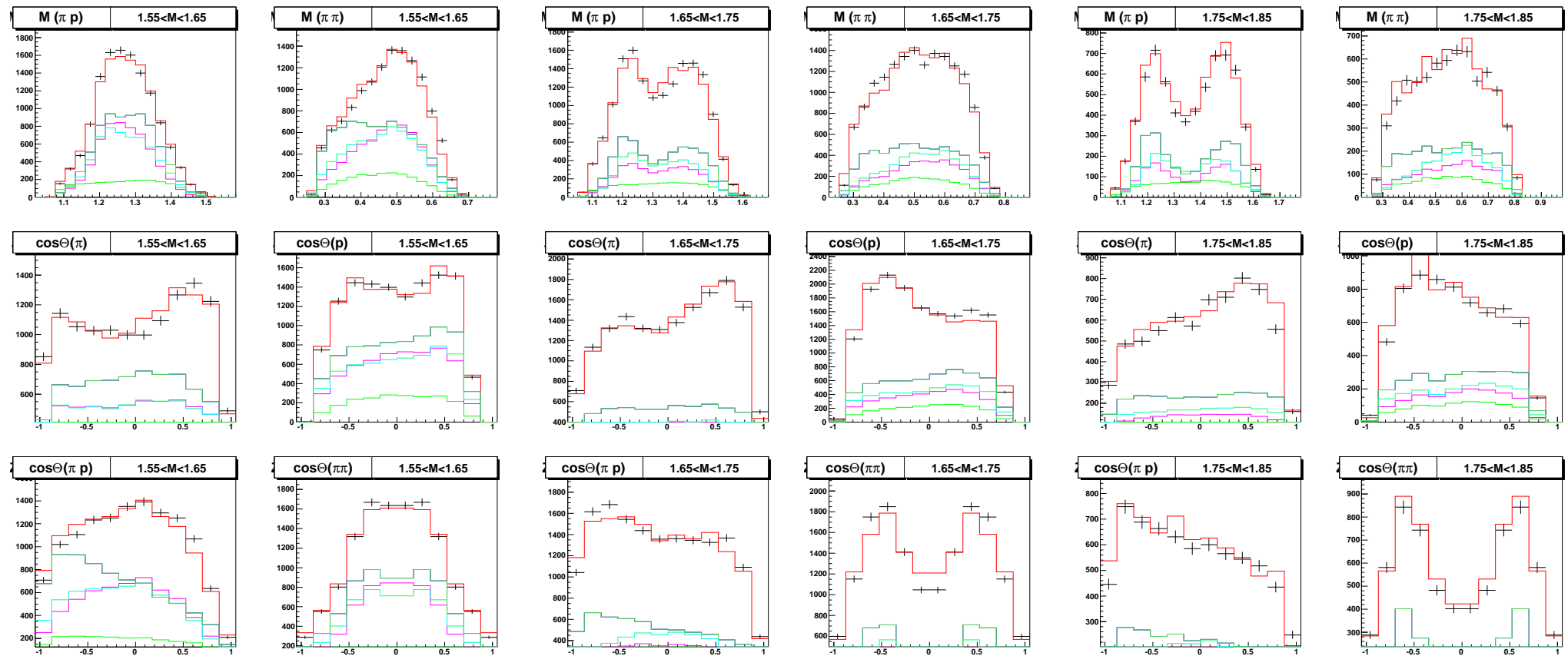
$$\pi^- p \rightarrow n \pi^0 \pi^0$$
 (Crystal Ball)

Differential cross sections for 472 and 665 MeV/c data.

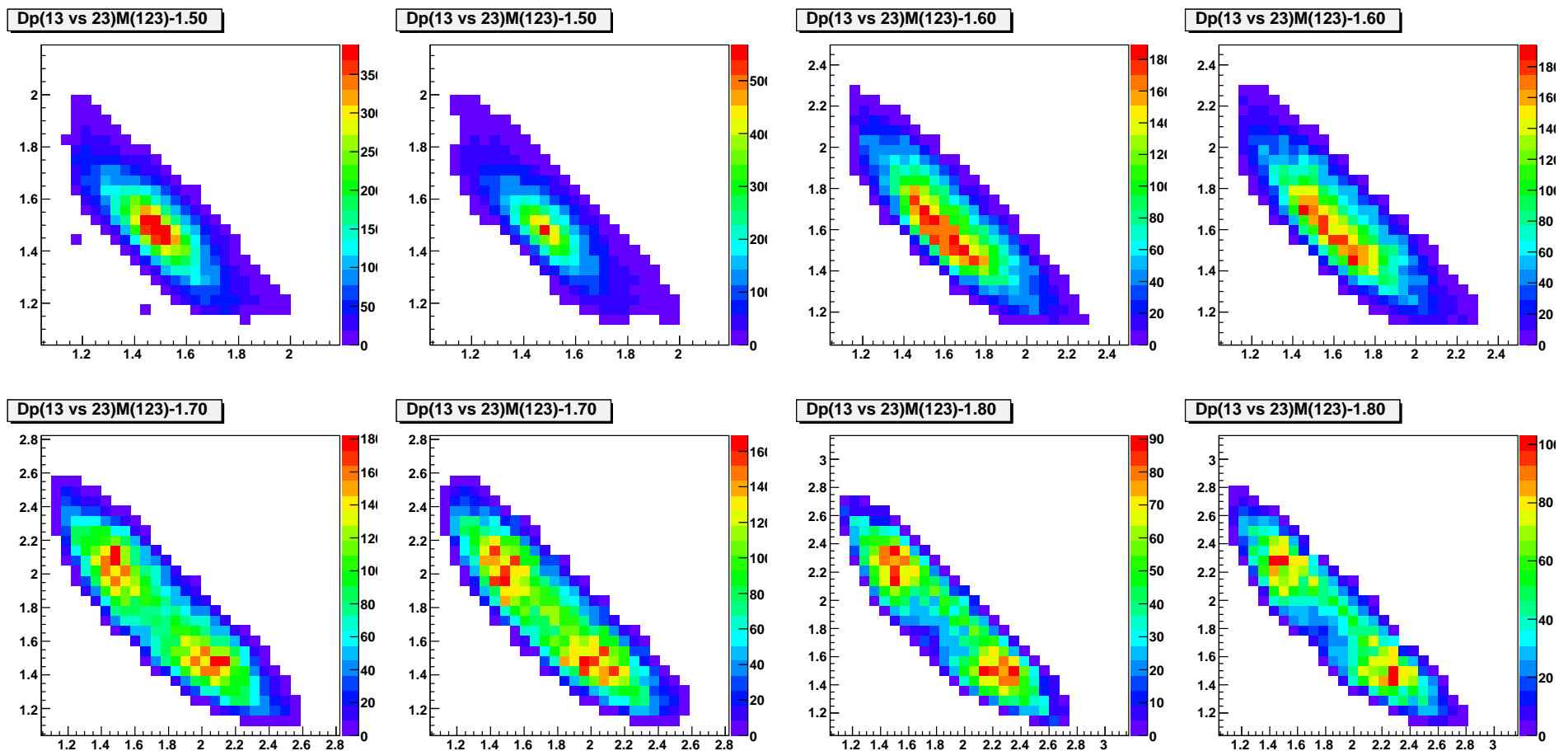


$\gamma p \rightarrow p\pi^0\pi^0$ (Crystal Barrel)

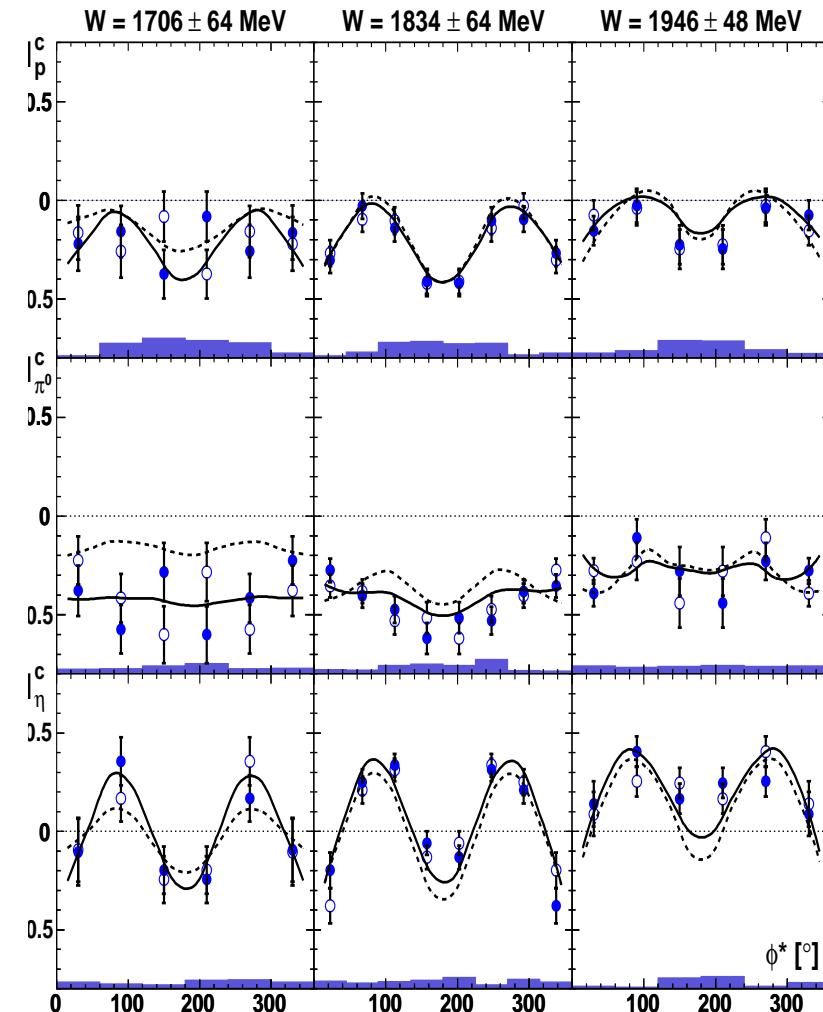
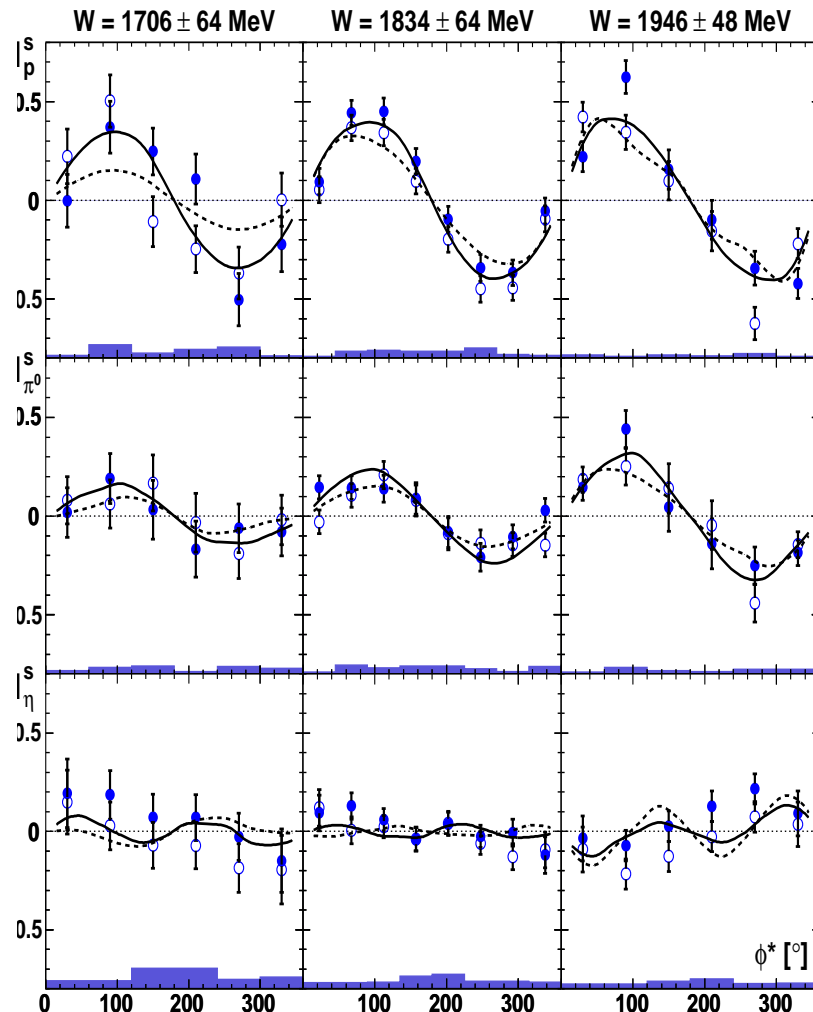
Differential cross sections.



$\gamma p \rightarrow p\pi^0\pi^0$ (Crystal Barrel)
Dalitz plots W=1.5, 1.6, 1.7, 1.8 GeV.



I^c and *I^s* for $\gamma p \rightarrow p\pi^0\eta$ (CB-ELSA)



List of resonances used in the combined analysis of the data. Known states are listed by the PDG names

$N(1535)S_{11}$	$N(1650)S_{11}$	$N(1440)P_{11}$	$N(1710)P_{11}$
$N(1520)D_{13}$	$N(1700)D_{13}$	$N(1720)P_{13}$	$N(1675)D_{15}$
$N(1680)F_{15}$	$\Delta(1620)S_{31}$	$\Delta(1232)P_{33}$	$\Delta(1600)P_{33}$
$N_{1/2^-}(1890)$	$N_{3/2^-}(1875)$	$N_{3/2^-}(2130)$	$N_{1/2^+}(1860)$
$N_{3/2^+}(1900)$	$N_{5/2^-}(2070)$	$N(2000)F_{15}$	$N(1990)F_{17}$
$N(2190)G_{17}$	$\Delta(1900)S_{31}$	$\Delta(1910)P_{31}$	$\Delta(1920)P_{33}$
$\Delta(1905)F_{35}$	$\Delta(1950)F_{37}$	$\Delta(1700)D_{33}$	$\Delta(1940)D_{33}$
$\Delta_{3/2^-}(2200)$	$\Delta(1905)F_{35}$	$\Delta(1950)F_{37}$	

Background amplitudes used in the combined analysis of the data.

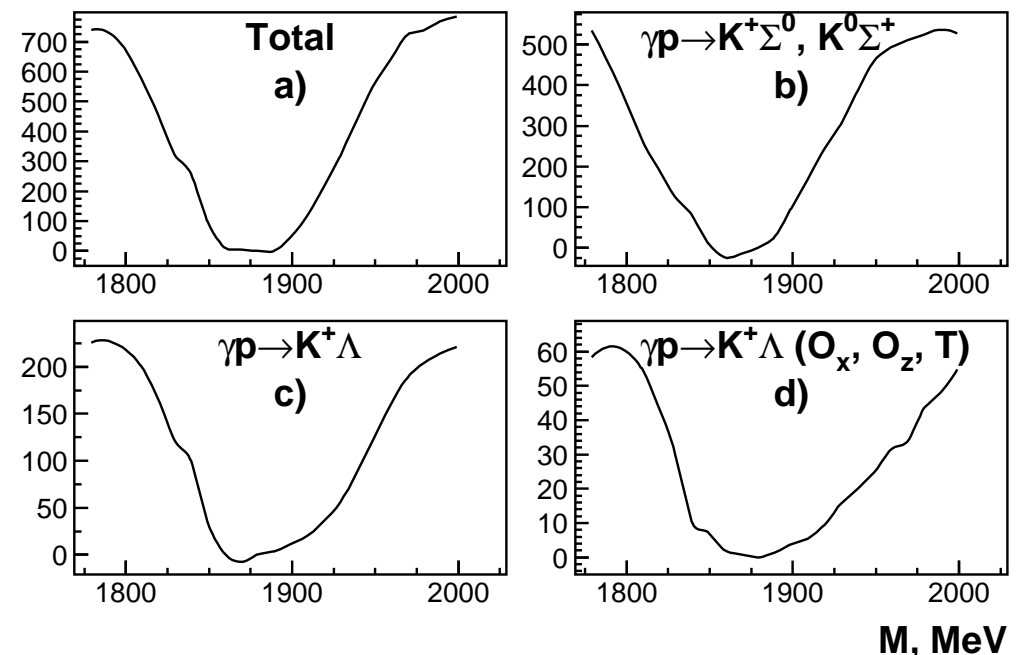
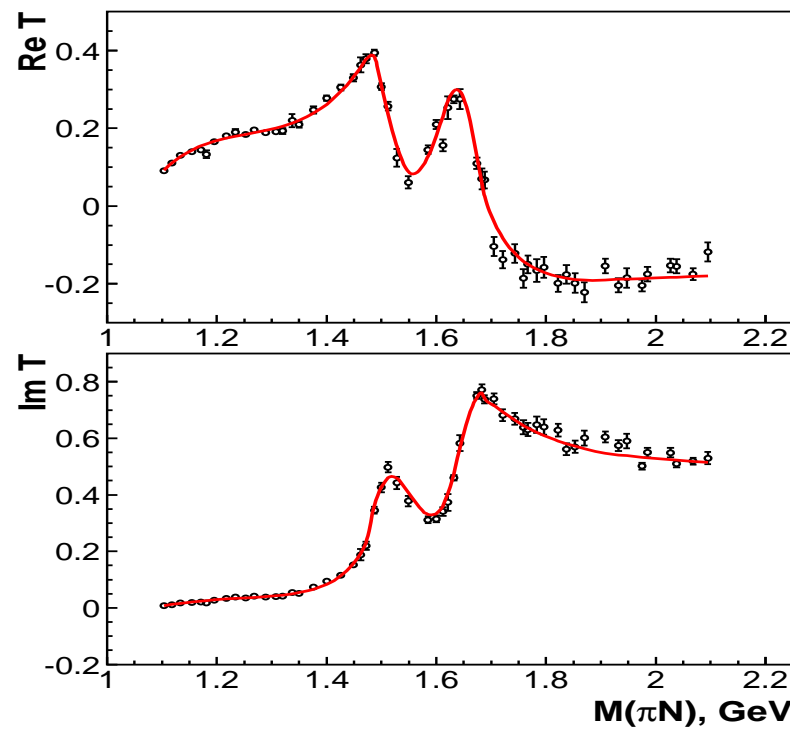
	pion-induced	photo-induced
t-channel exchange		$\pi^\pm, \rho^0/\omega, \rho^\pm$
	$K^{*0}, K^{*\pm}$	$K^\pm, K^{*0}, K^{*\pm}$
u-channel exchange		$N(938), \Lambda, \Sigma^0, \Sigma^\pm$
Direct production of final-state particles		

Pole position of baryon states (Re and -2Im) in the mass region 1900-2300 MeV

State		Solution 1	Solution 2	Arndt	Hoehler	Cutcosky
$N(1875)\frac{1}{2}^+$	Re	1860 ± 20	1850^{+20}_{-50}		1885 ± 30 (Manley)	
**	-2Im	110^{+30}_{-10}	360 ± 40		113 ± 44 (Manley)	
$N(1890)\frac{1}{2}^-$	Re		1895 ± 8	—	1880 ± 20	—
**	-2Im		82 ± 10	—	95 ± 30	—
$N(1880)\frac{3}{2}^-$	Re		1860 ± 12	—	—	1880 ± 100
***	-2Im		185 ± 16	—	—	180 ± 60
$N(2130)\frac{3}{2}^-$	Re		2130 ± 45	—	2081 ± 20	2050 ± 70
***	-2Im		340 ± 45	—	265 ± 40	200 ± 60
$N(1900)\frac{3}{2}^+$	Re	1910 ± 40	1920 ± 50	—	—	—
***	-2Im	270 ± 50	300 ± 60	—	—	—
$N(2000)\frac{5}{2}^+$	Re		1800 – 1950	1807	1882 ± 10	—
*	-2Im		100 – 300	109	95 ± 20	—
$N(2100)\frac{5}{2}^+$	Re		2100 ± 25	—	—	—
**	-2Im		550 ± 40	—	—	—
$N(2070)\frac{5}{2}^-$	Re		2060 ± 8	—	—	2100 ± 60
***	-2Im		370 ± 15	—	—	360 ± 80
$N(1990)\frac{7}{2}^+$	Re	1975 ± 15	2090 ± 15	—	~ 1935	1900 ± 30
**	-2Im	170 ± 50	260 ± 20	—	~ 260	260 ± 60
$N(2190)\frac{7}{2}^-$	Re		2160 ± 20	2070	2042	2100 ± 50
***	-2Im		310 ± 25	520	480	400 ± 160

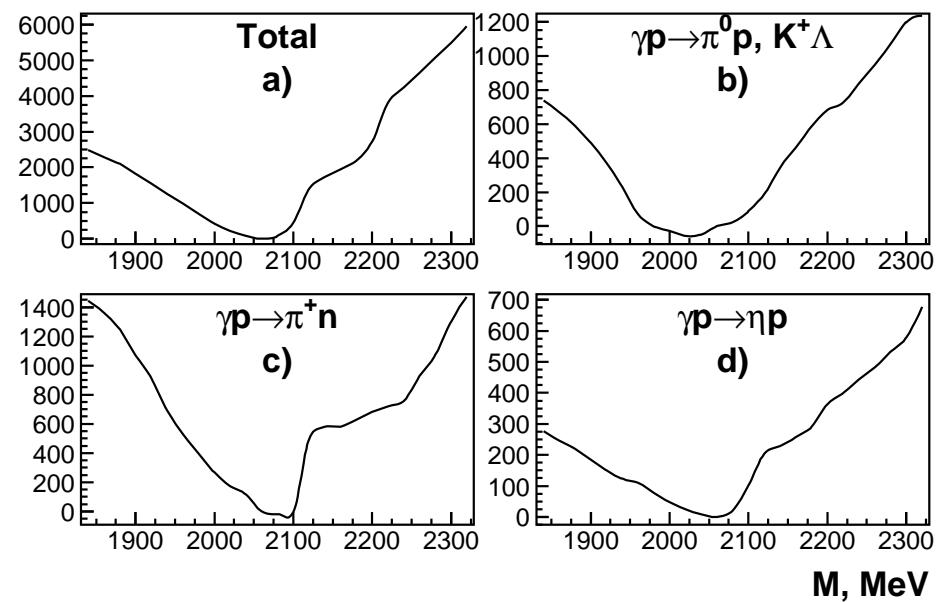
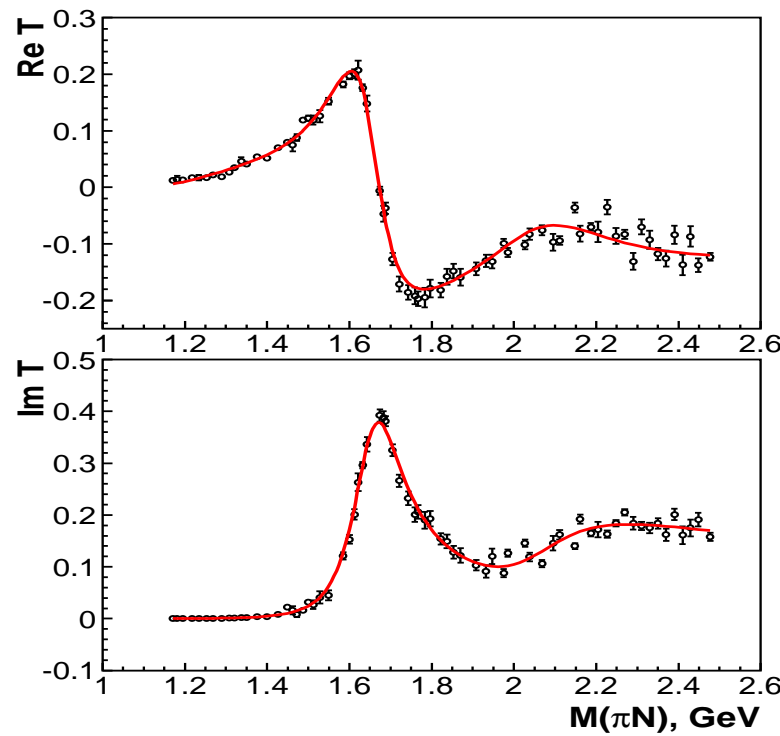
S_{11} : pole position and Breit-Wigner parameters

State		Solution 1	Solution 2	Arndt	Hoehler	Cutcosky
$N(1890) \frac{1}{2}^-$	Re	1895 \pm 8				
**	-2Im	82 \pm 10				
BW	M	1900 \pm 10			1880 \pm 20	
parameters	Γ	77 \pm 15			95 \pm 30	



D_{15} : pole position and Breit-Wigner parameters

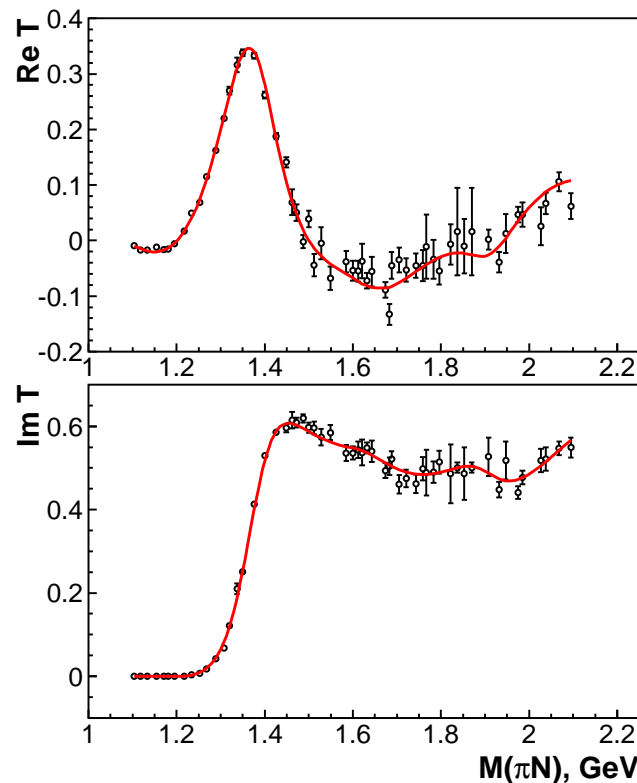
State		Solution 1	Solution 2	Arndt	Hoehler	Cutcosky
$N(2070) \frac{5}{2}^-$	Re	2060 ± 8		—	—	2100 ± 60
***	-2Im	370 ± 15		—	—	360 ± 80
BW	M	2075 ± 12			2228 ± 30	2180 ± 80
parameters	Γ	365 ± 20			310 ± 50	400 ± 100



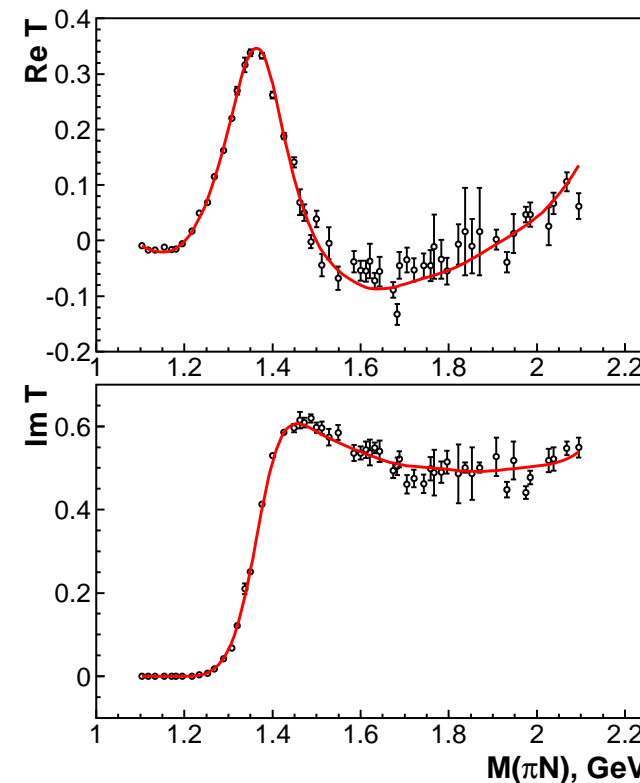
P_{11} : pole position and Breit-Wigner parameters

State		Solution 1	Solution 2	Manley
$N(1875) \frac{1}{2}^+$	Re	1860 ± 20	1850^{+20}_{-50}	1885 ± 30
*	-2Im	110^{+30}_{-10}	360 ± 40	113 ± 44
BW	M	1864 ± 10	1863 ± 20	
parameters	Γ	115 ± 20	320 ± 30	

BG2011-01

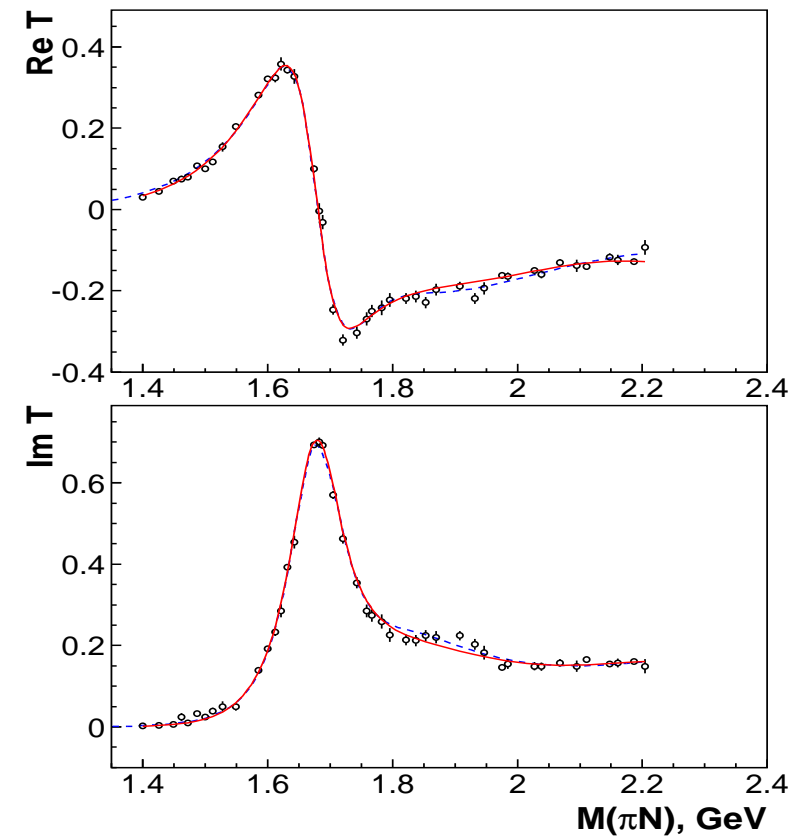
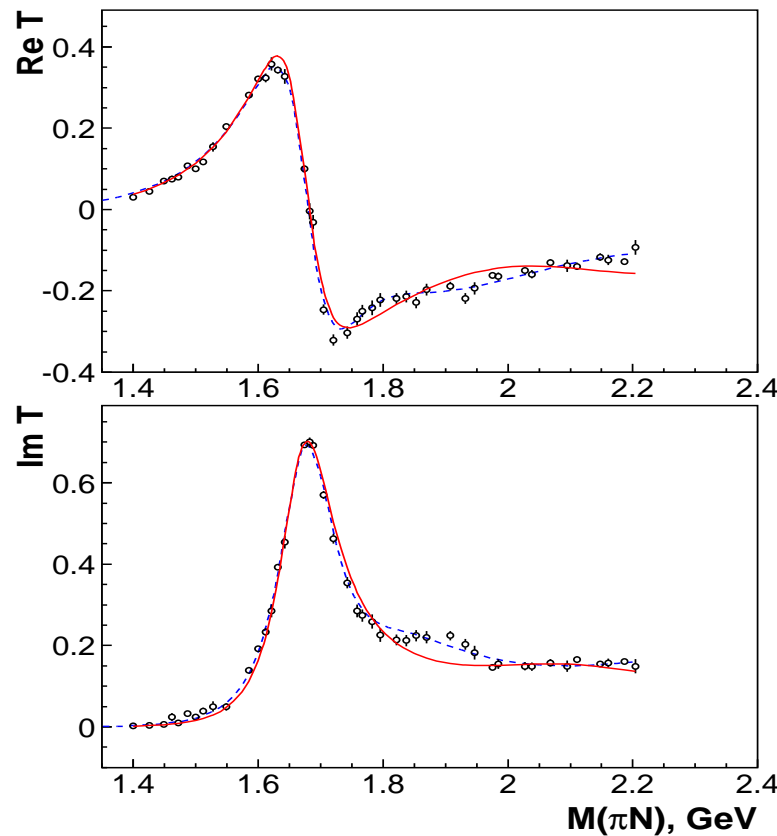


BG2011-02



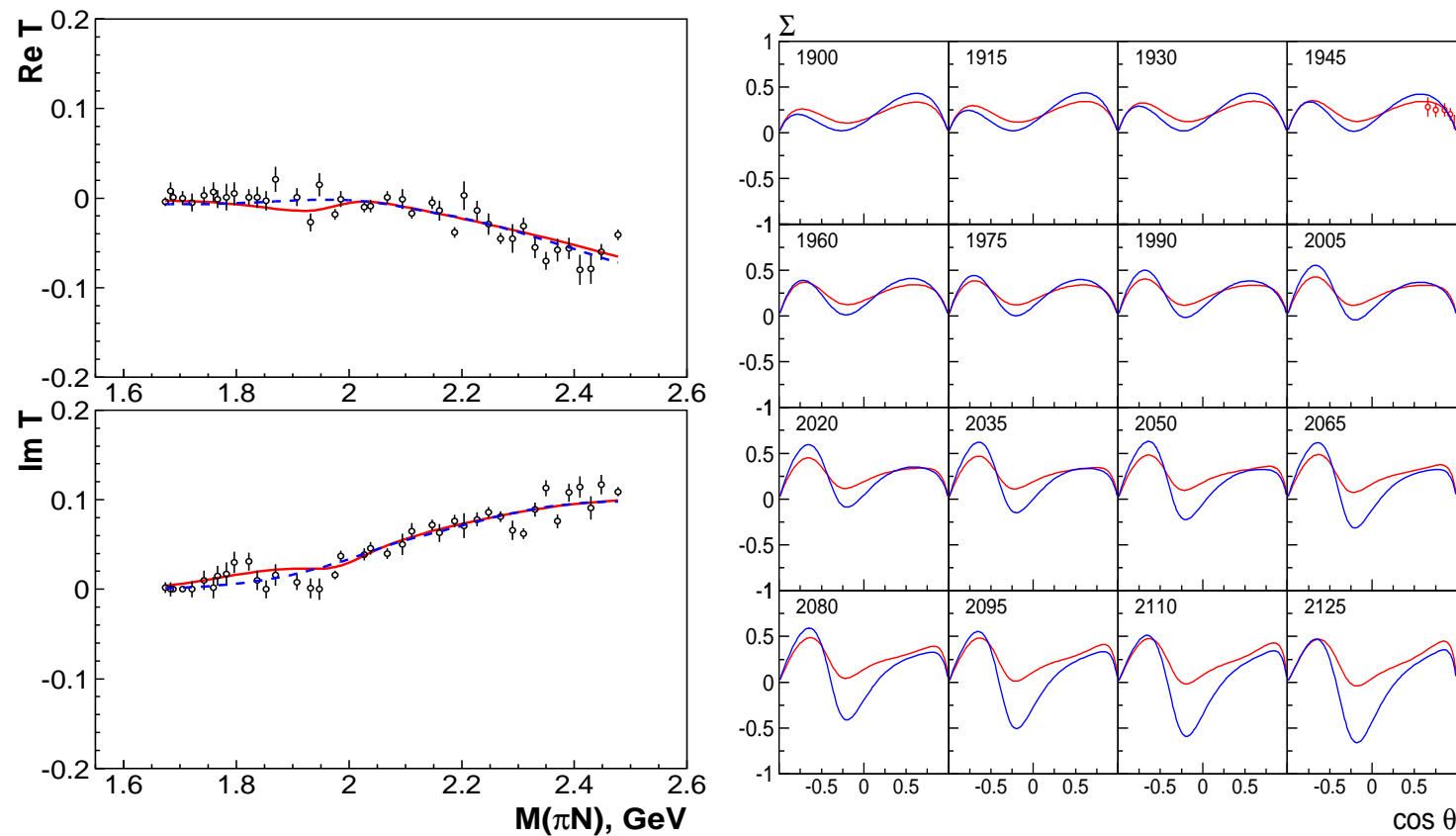
Pole position of F_{15} : two and three pole solution

State		Solution 1	Solution 2	Arndt	Hoehler	Cutcosky
$N(2000)\frac{5}{2}^+$	Re	1800 – 1950	1800 – 1950	1807	1882 ± 10	–
**	-2Im	100 – 300	100 – 300	109	95 ± 20	–
$N(2100)\frac{5}{2}^+$	Re	2090^{+20}_{-40}	2110^{+20}_{-80}	–	–	–
	-2Im	560 ± 100	540 ± 100	–	–	–



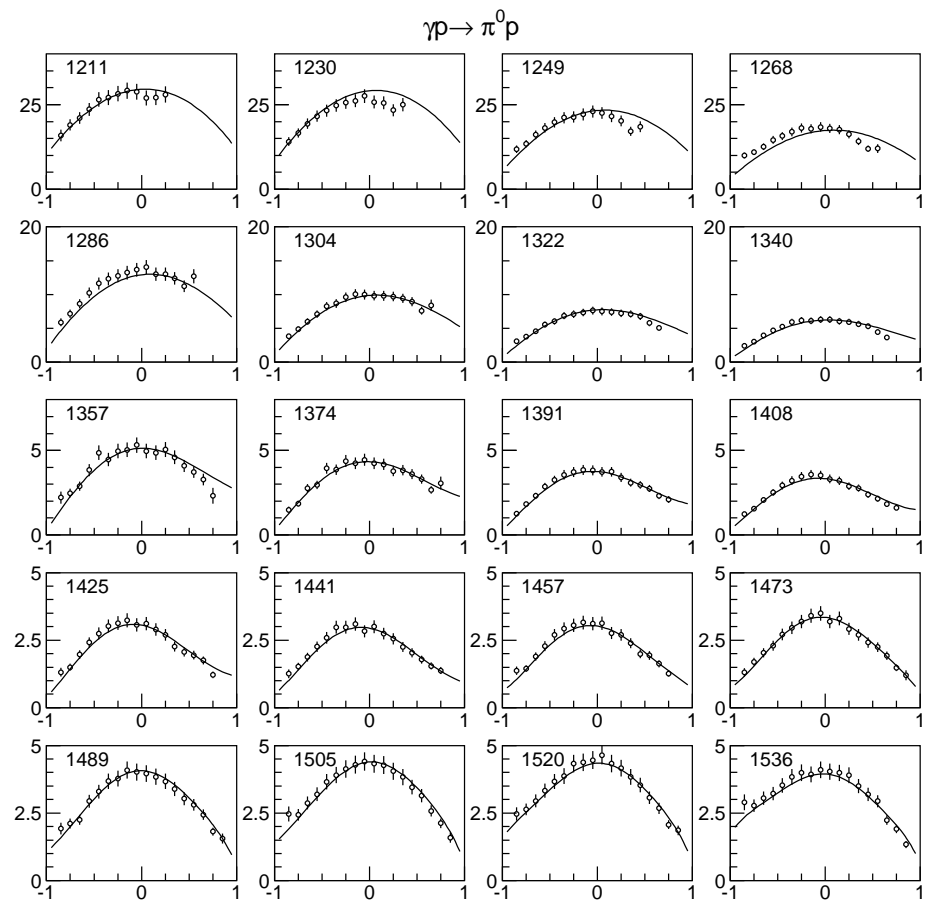
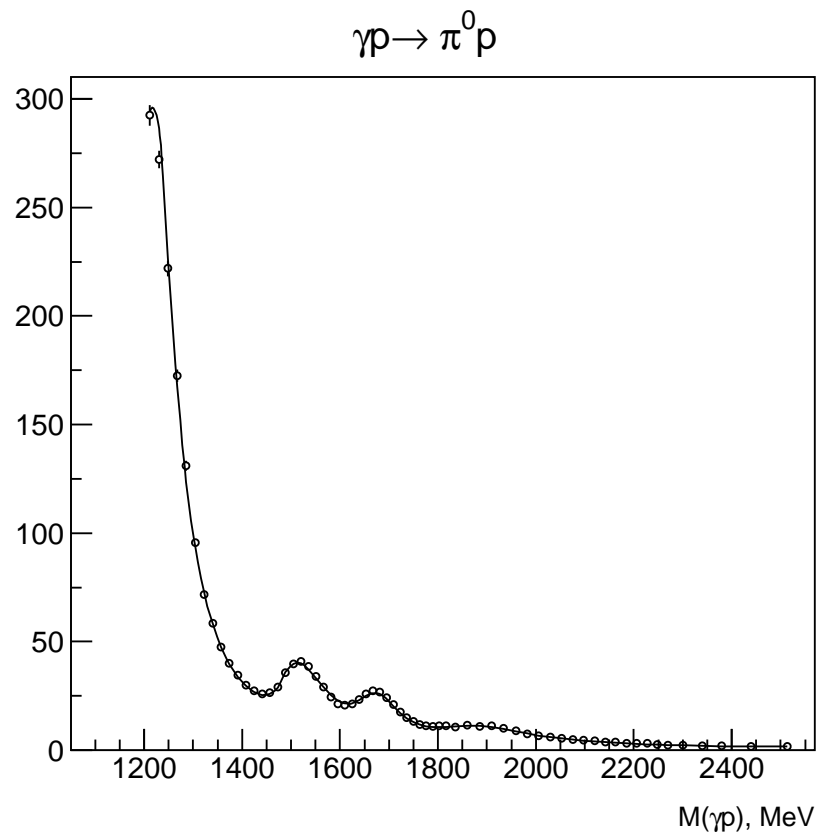
Pole position of F_{17} and helicity couplings (absolute value (10^{-3} GeV $^{\frac{1}{2}}$)/phase (degrees))

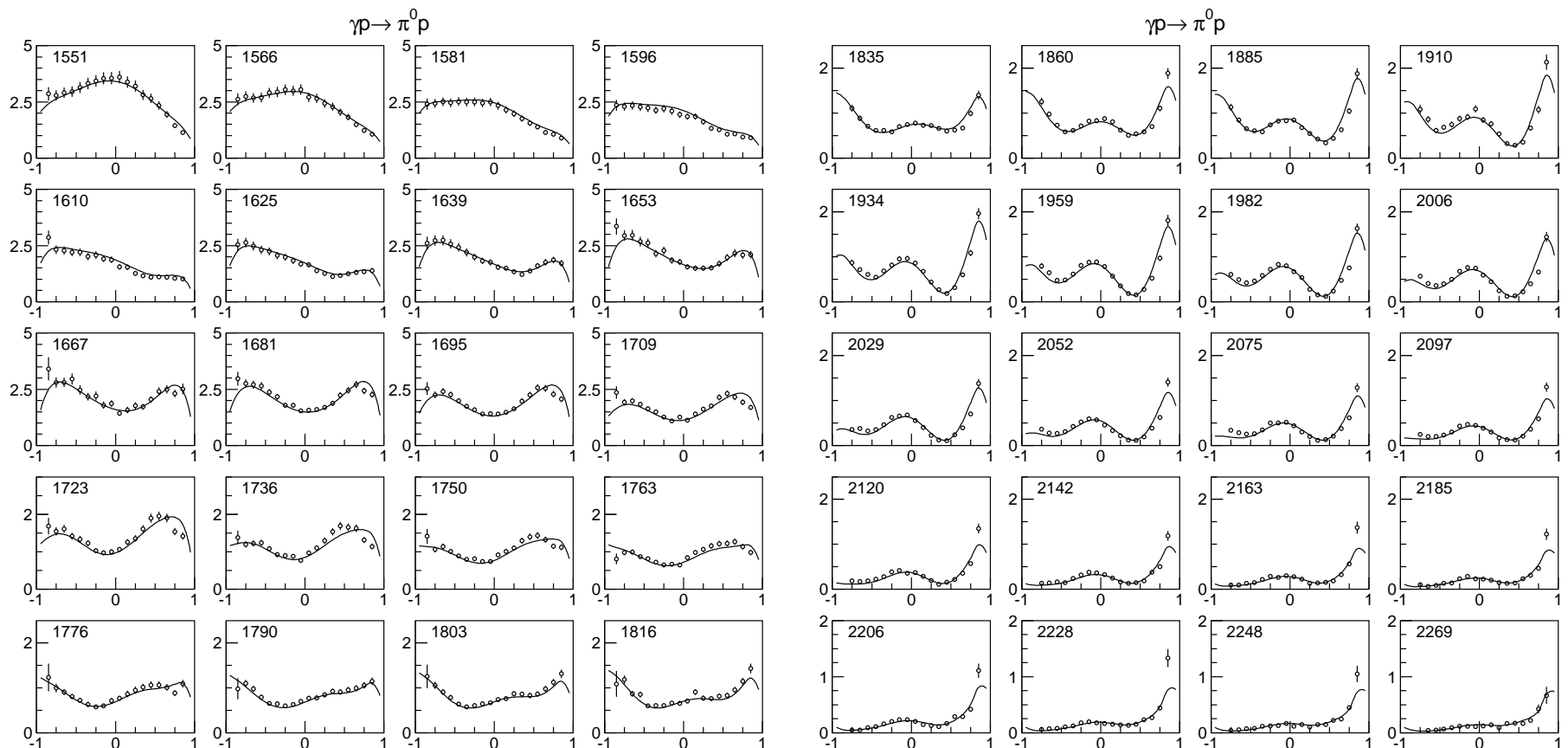
State		Solution 1	$A(\frac{1}{2})/A(\frac{3}{2})$	Solution 2	$A(\frac{1}{2})/A(\frac{3}{2})$
$N(1990)\frac{7}{2}^{+}$	Re	1980 ± 25	$15/14^o$	2100 ± 30	$76/50^o$
**	-2Im	180 ± 30	$28/3^o$	300 ± 60	$78/45^o$

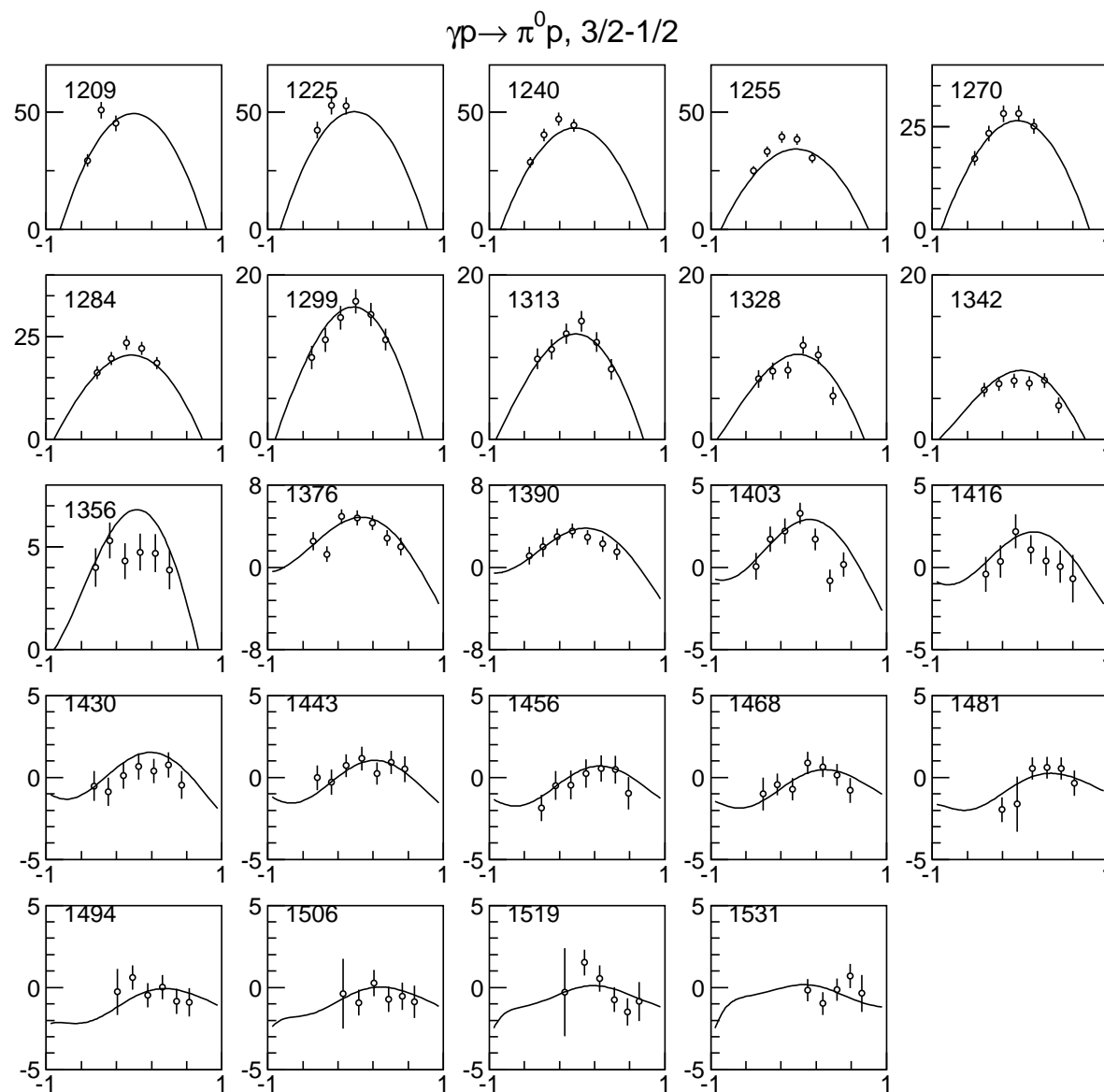


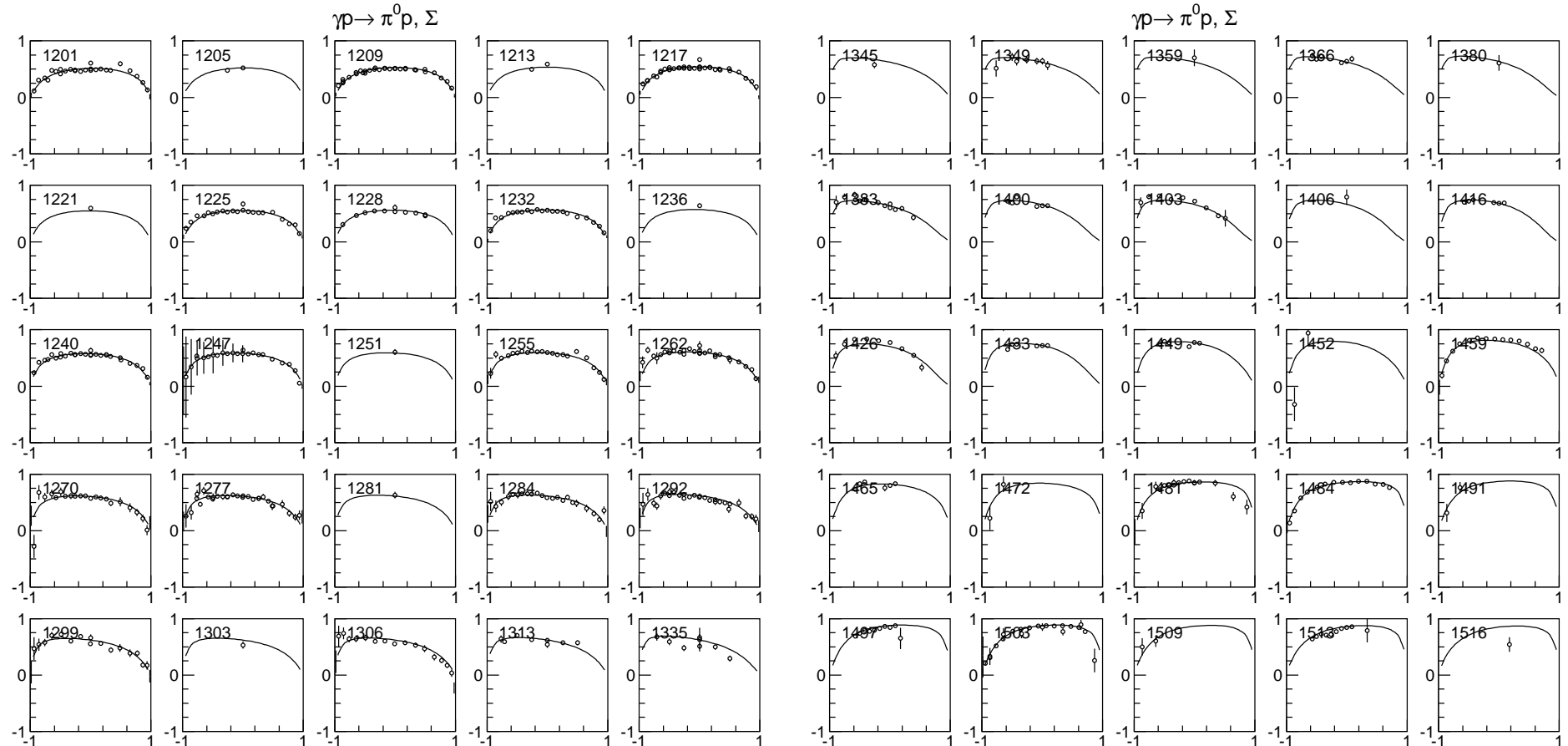
Summary

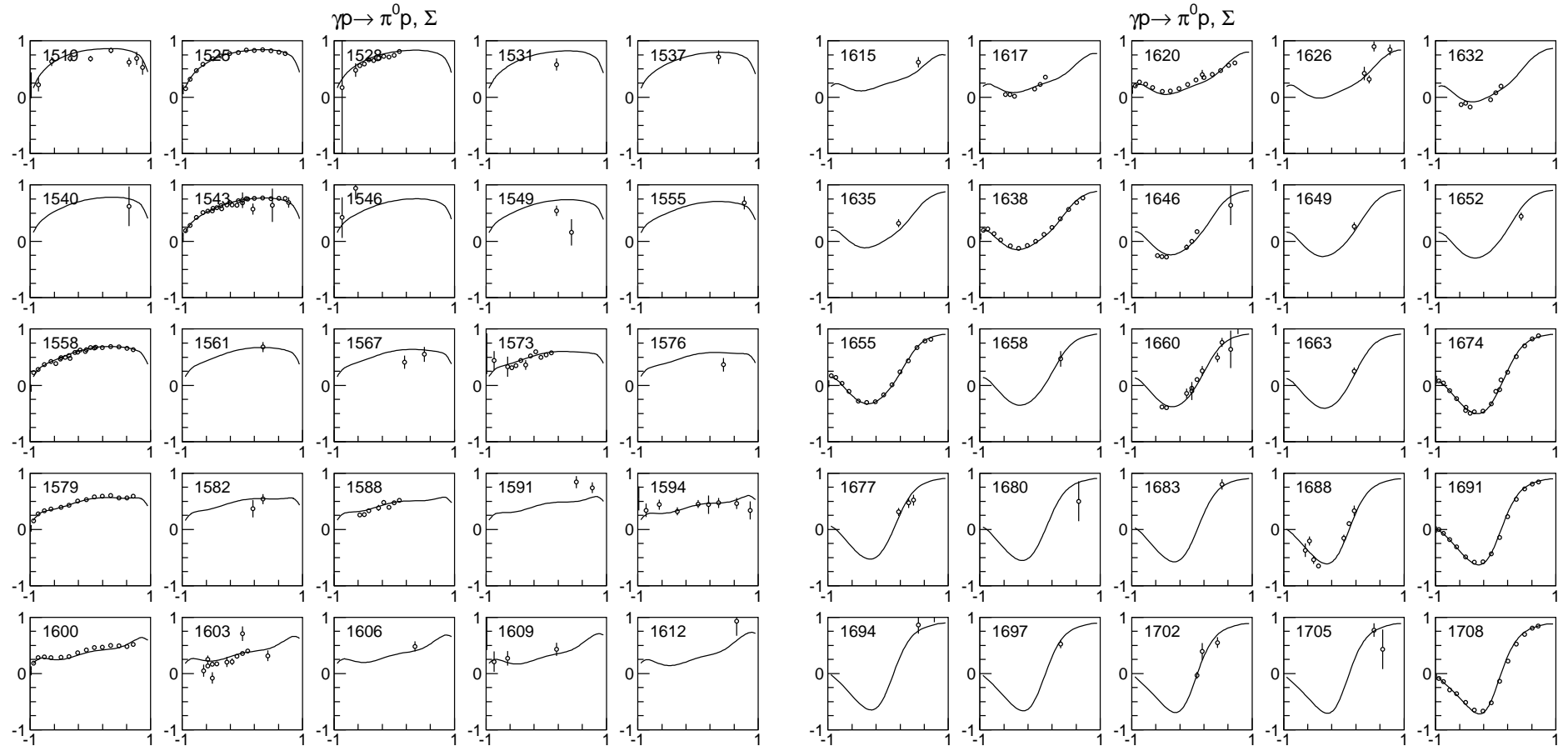
- The analysis of (almost) all available data for production of baryons in the pion and photo induced reaction is completed.
- We have observed a set of new states in the region 1800-2150 MeV, however, this number is much less than that predicted by the classical quark model.
- There are two solutions for the $N_{\frac{7}{2}^+}$ lowest state which should be distinguished from analysis of beam asymmetry data on photoproduction of hyperon-kaon final states.
- The situation for $N(\frac{5}{2}^+)$ can be resolved with reanalysis of πN elastic data and an analysis of new data on double pion photoproduction (with charged pions).

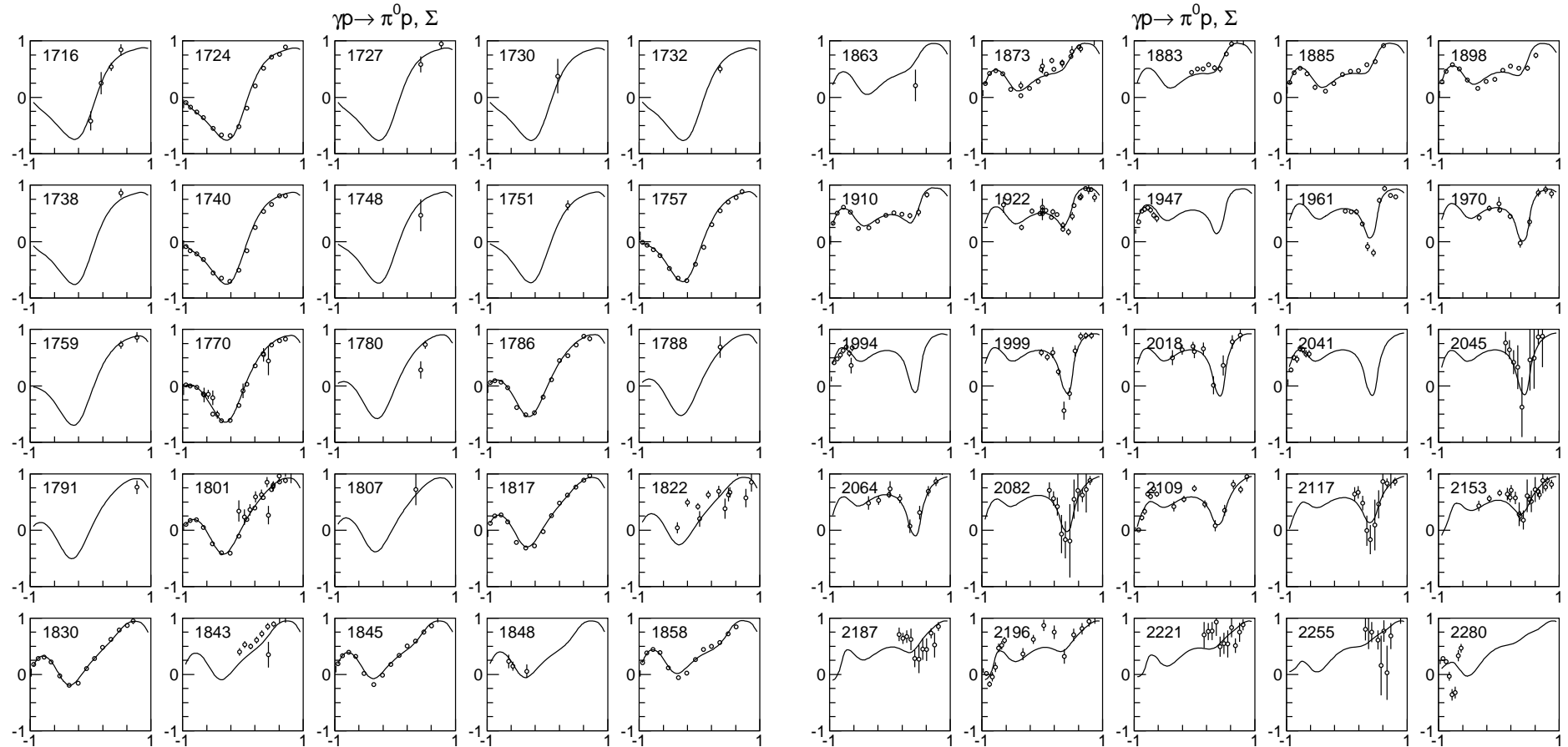


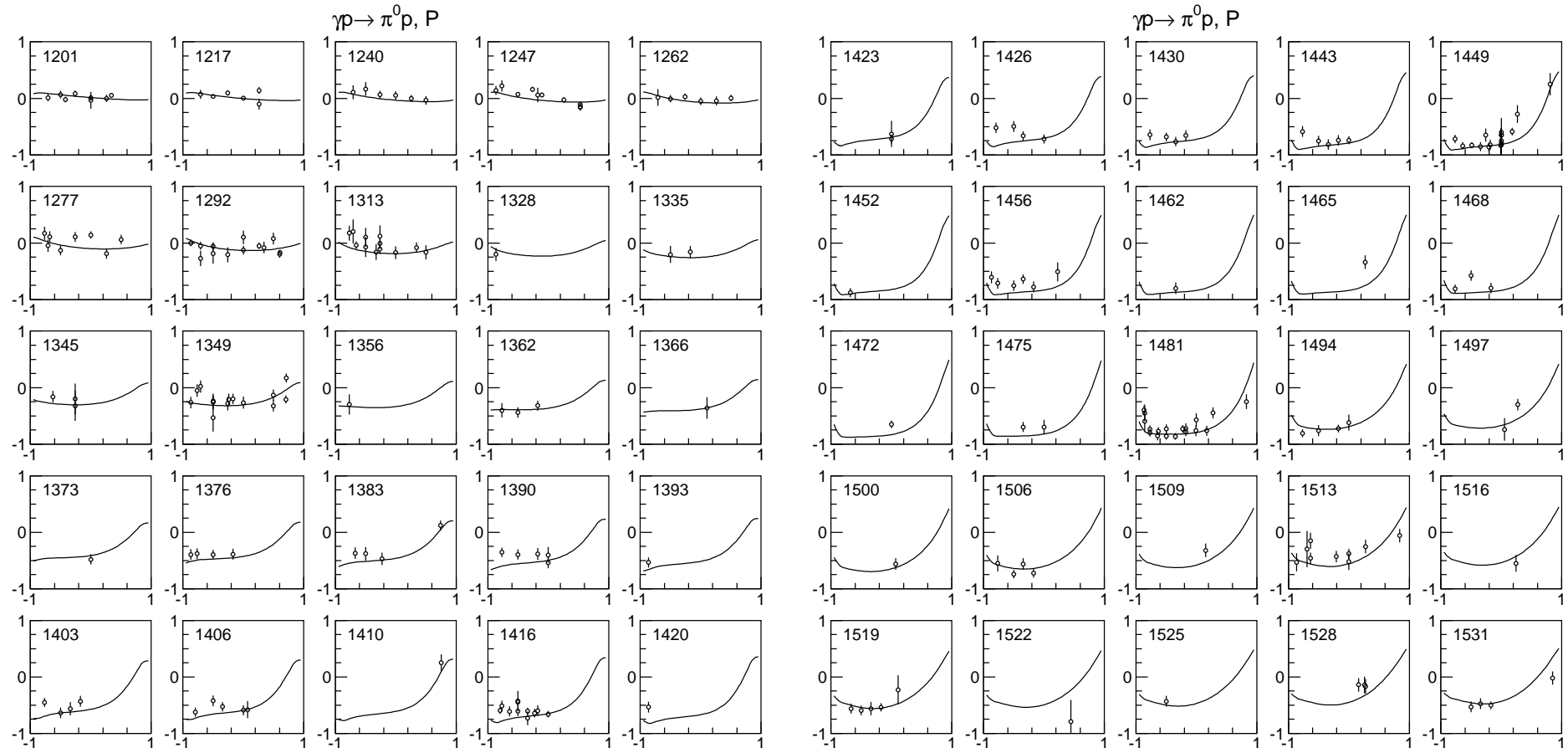


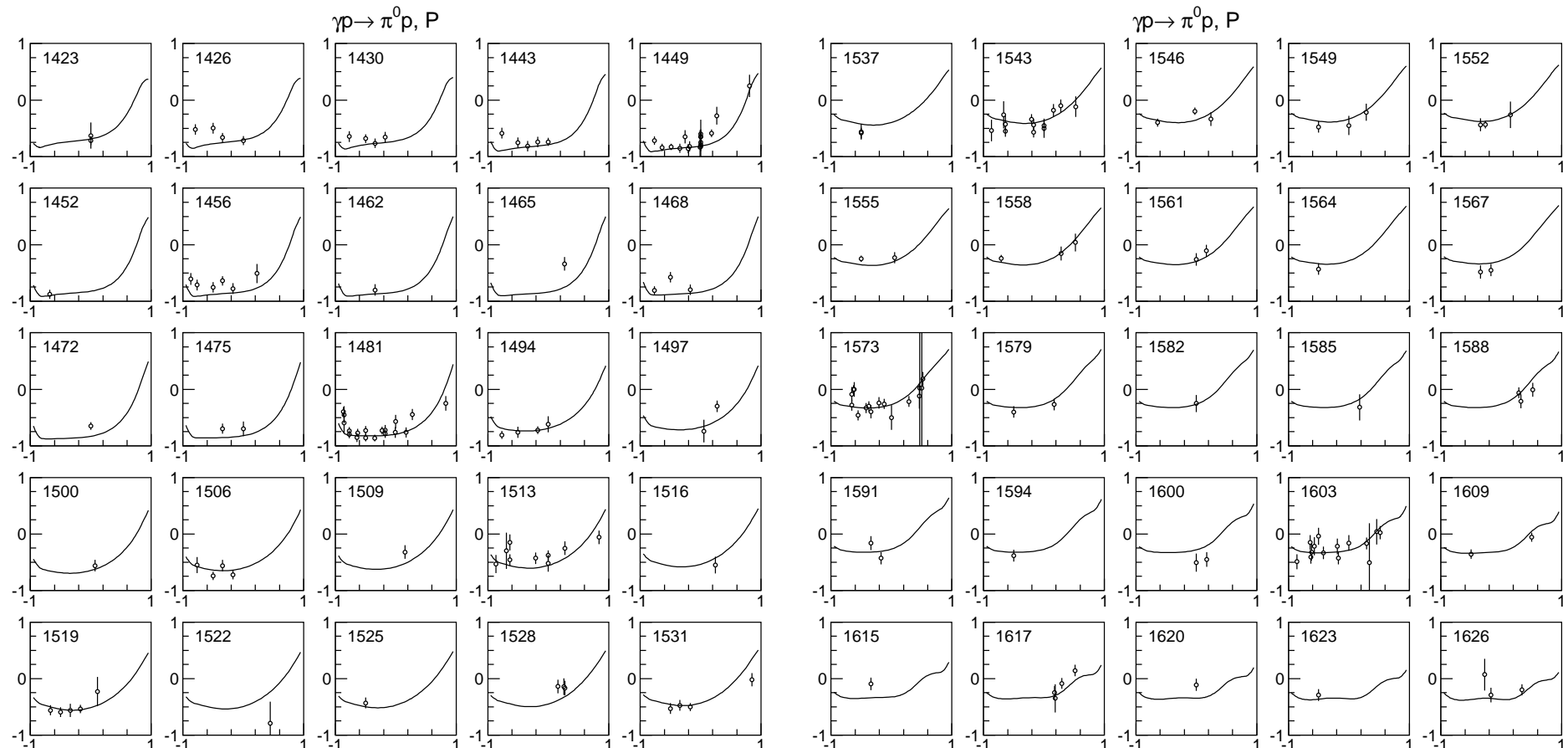


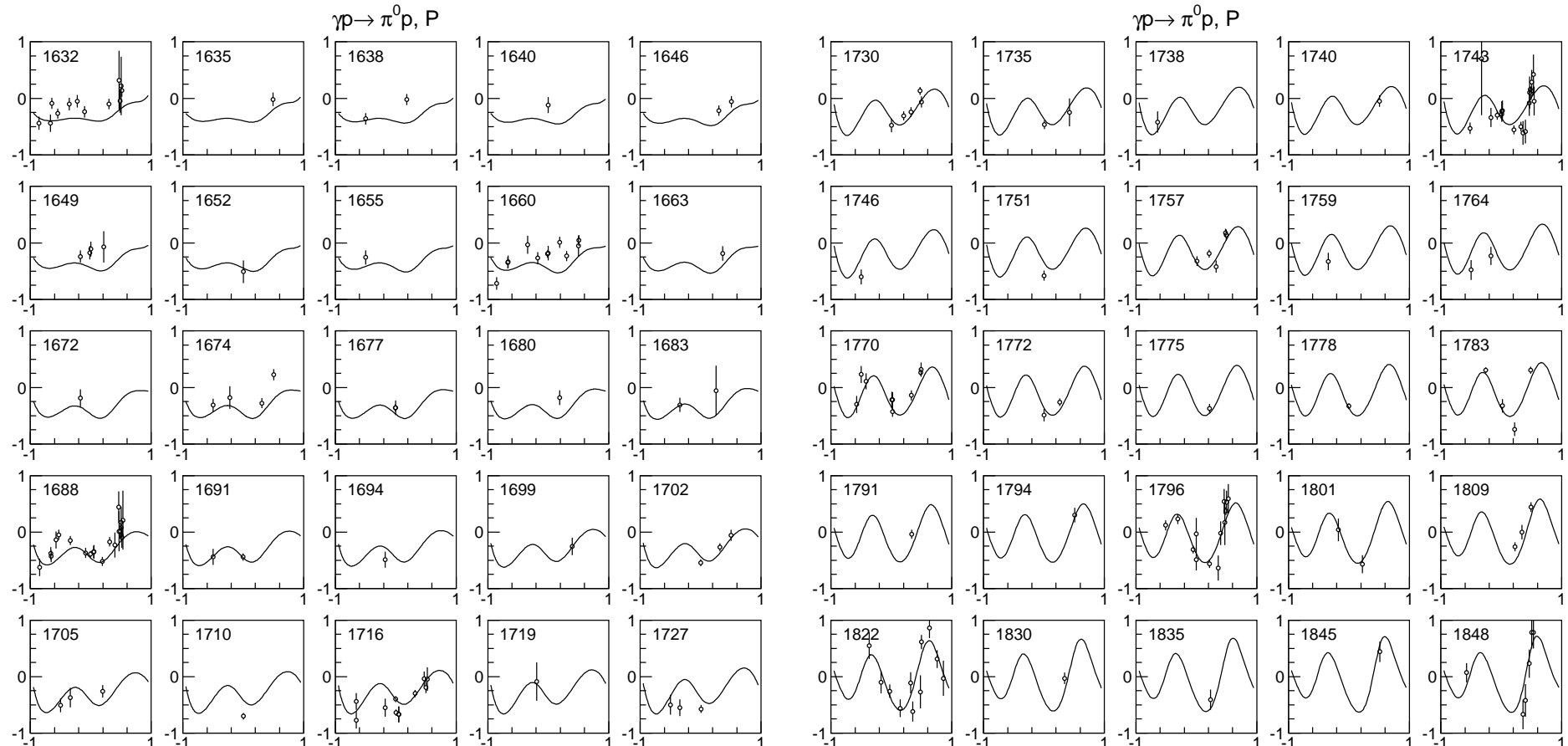


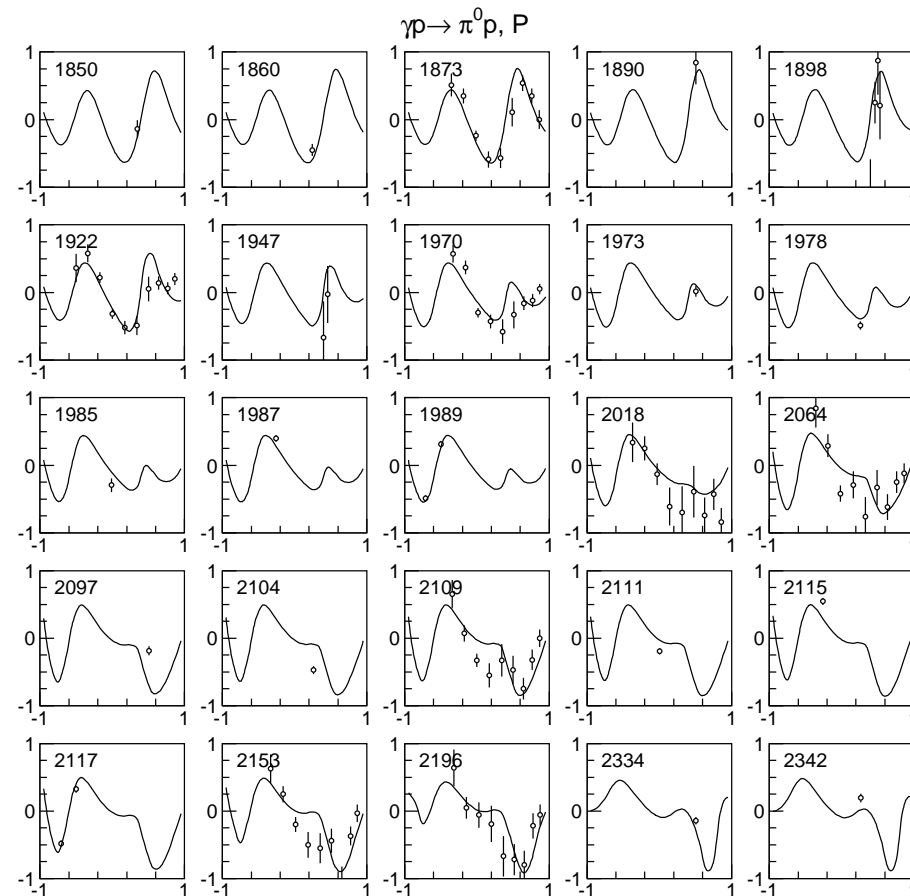


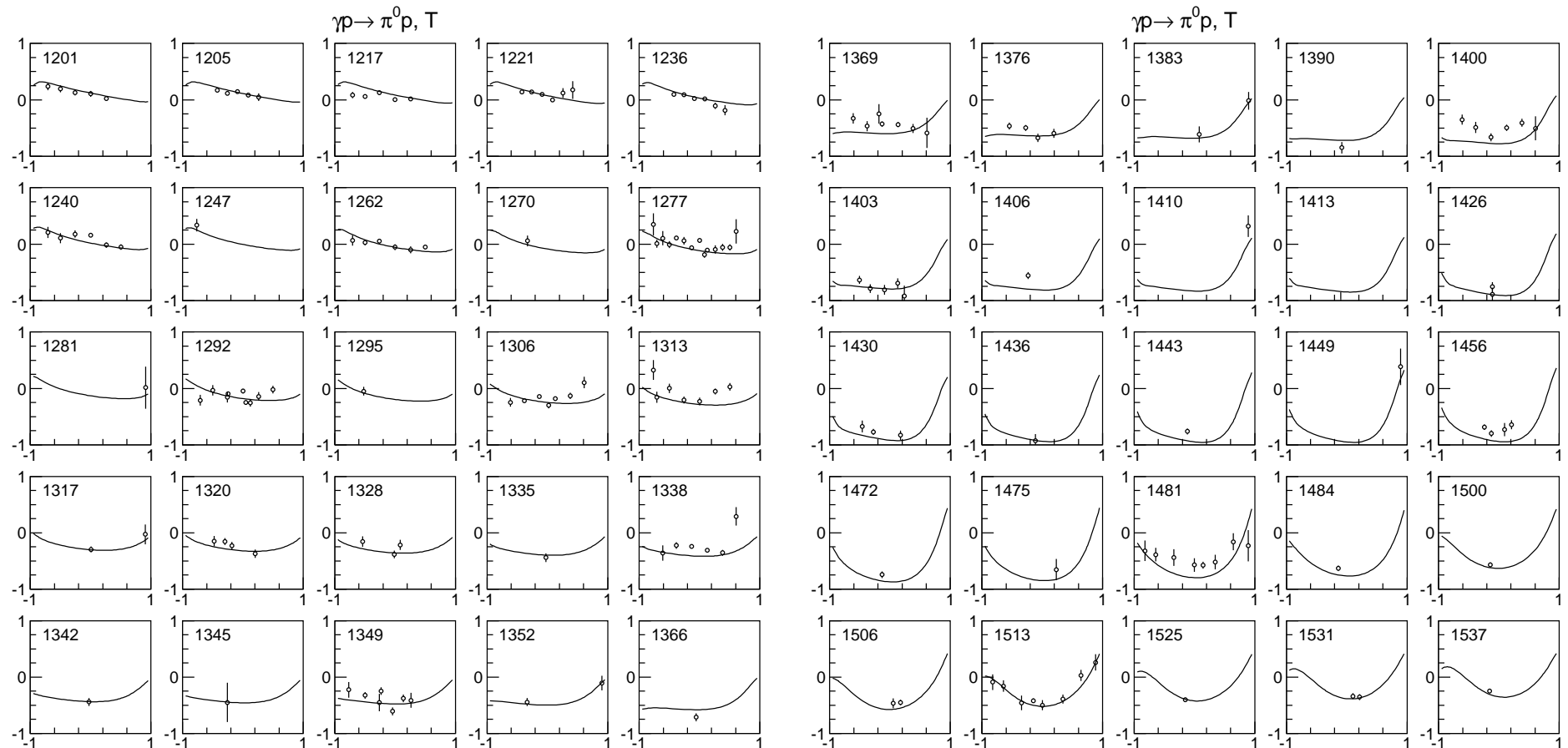


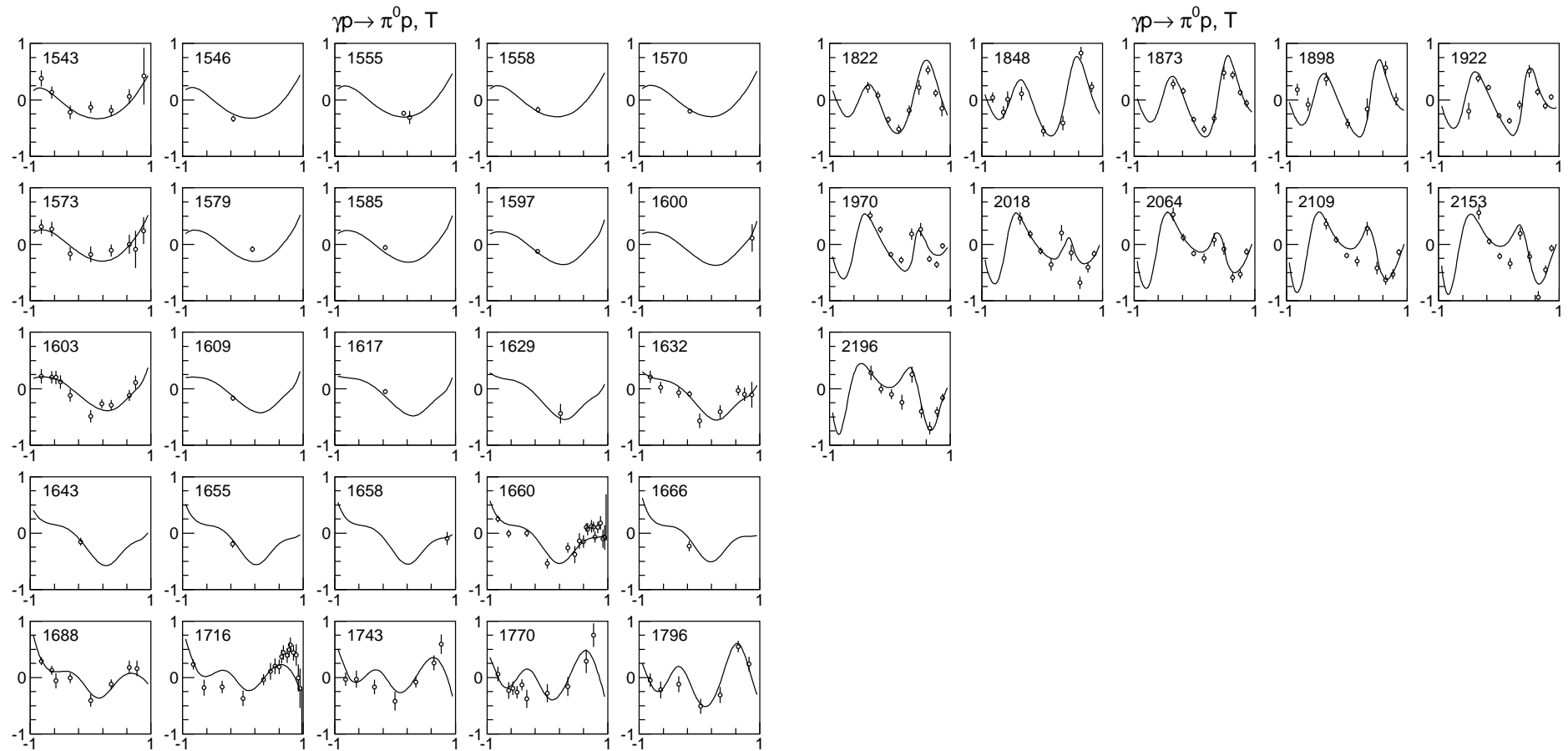


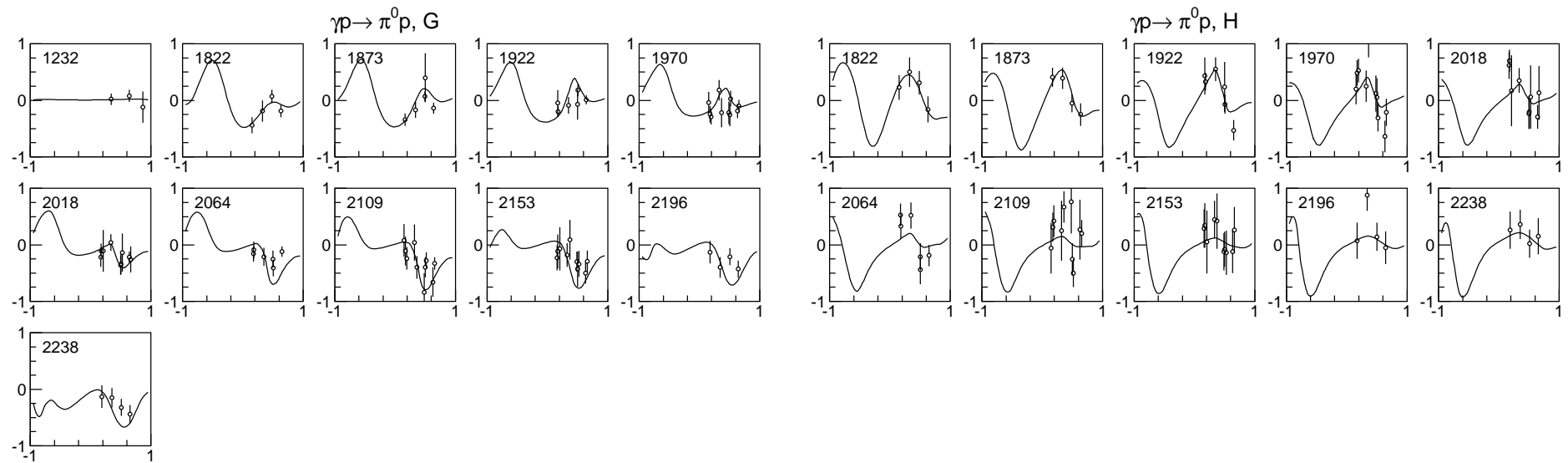


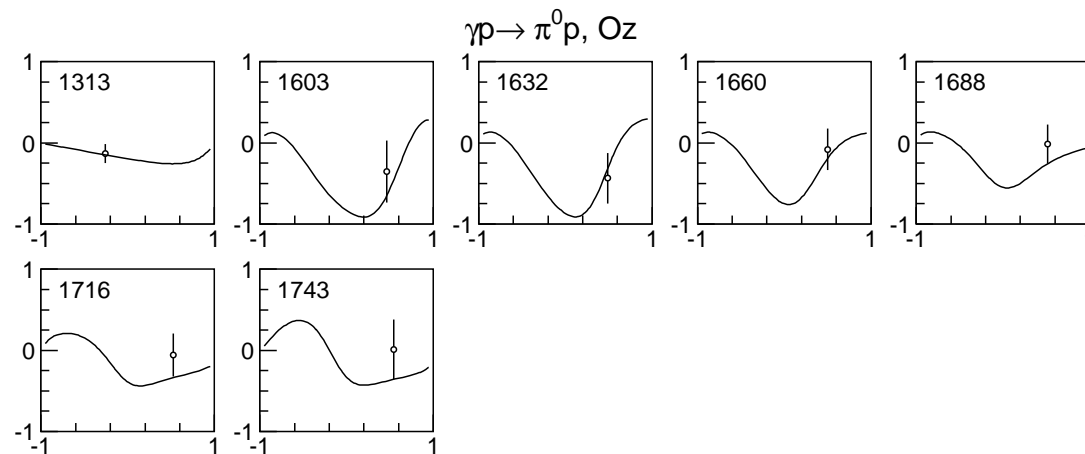
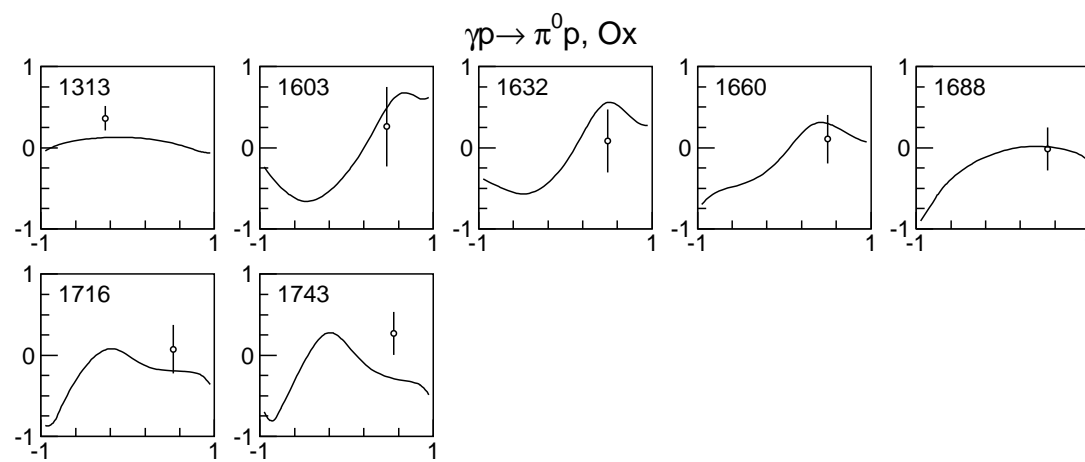


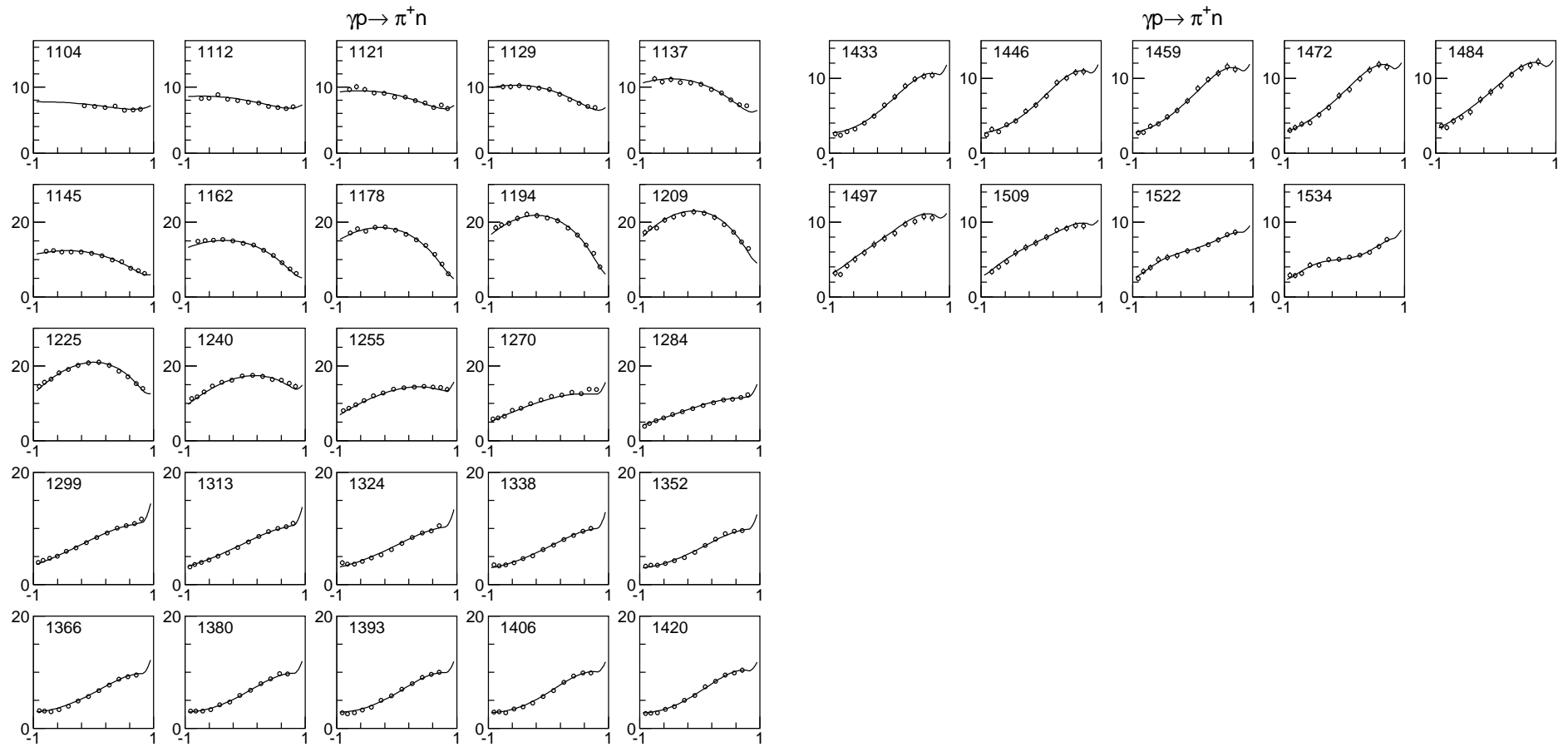


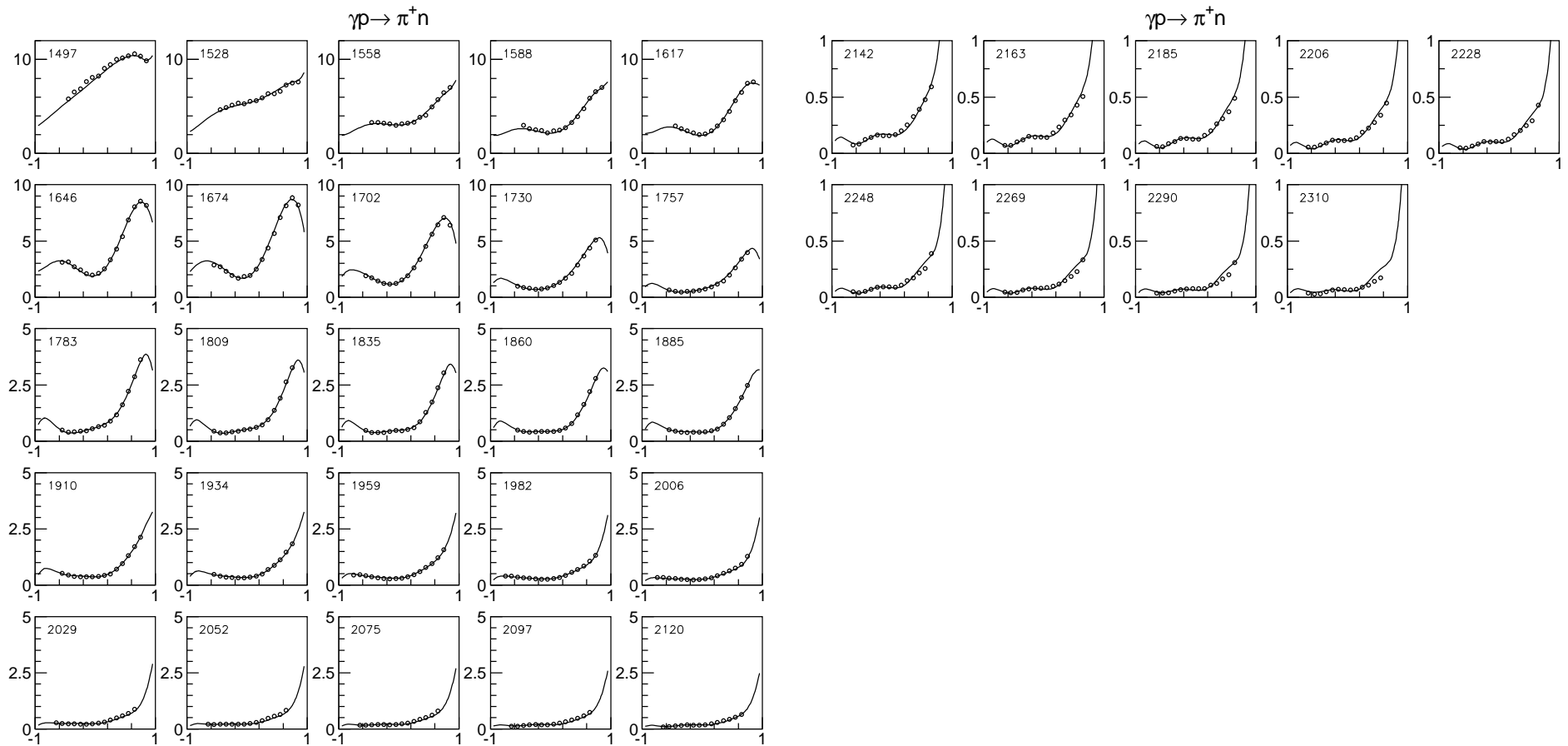


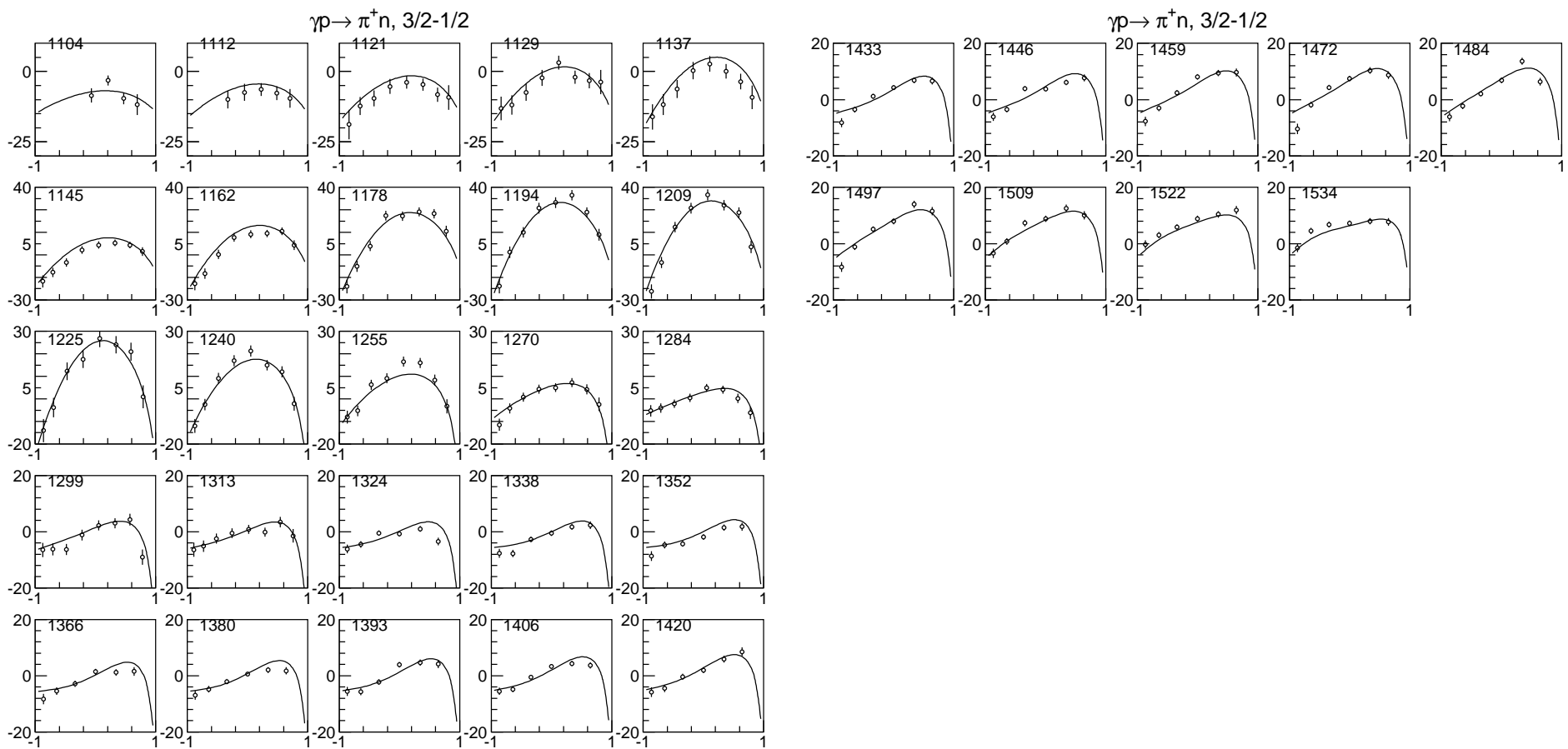


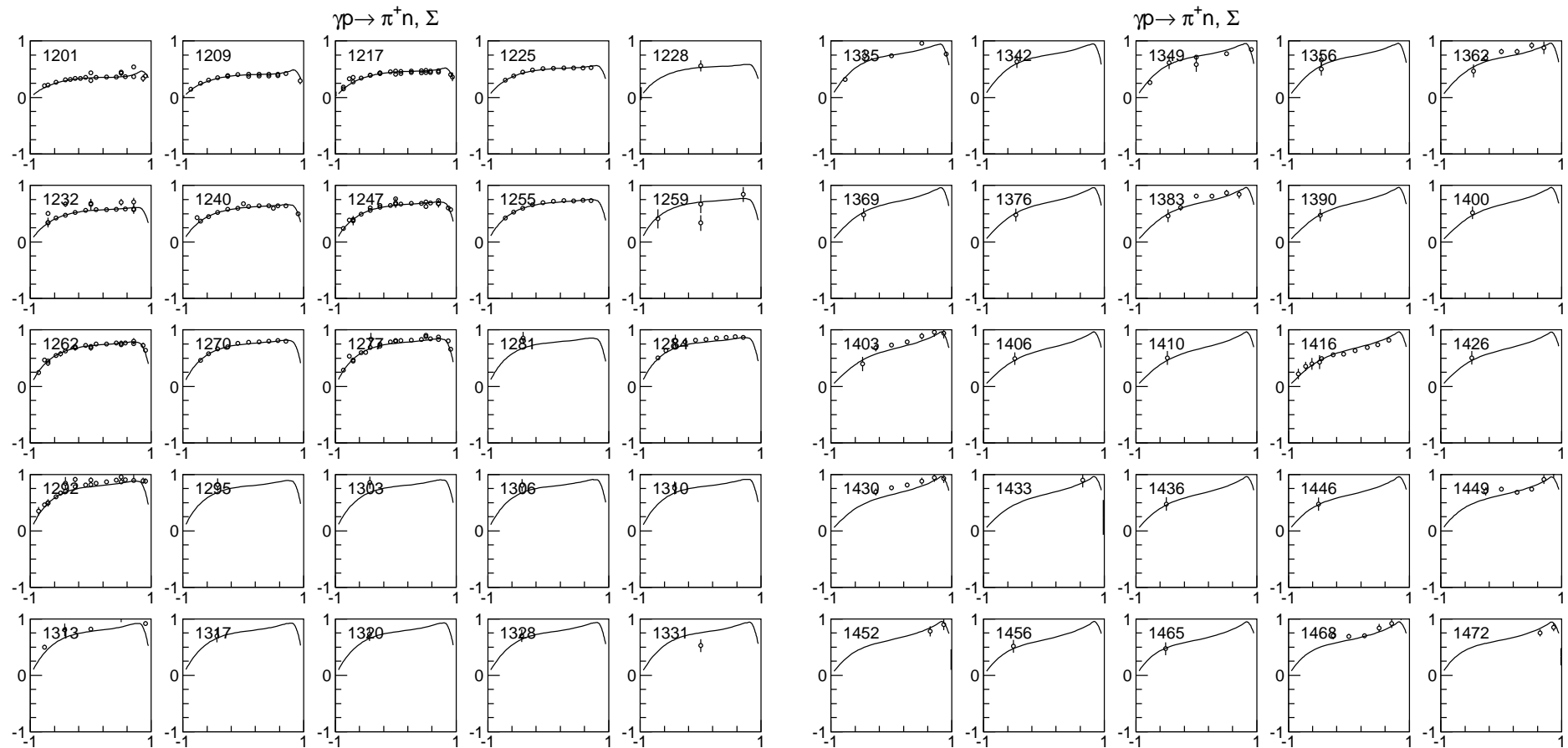


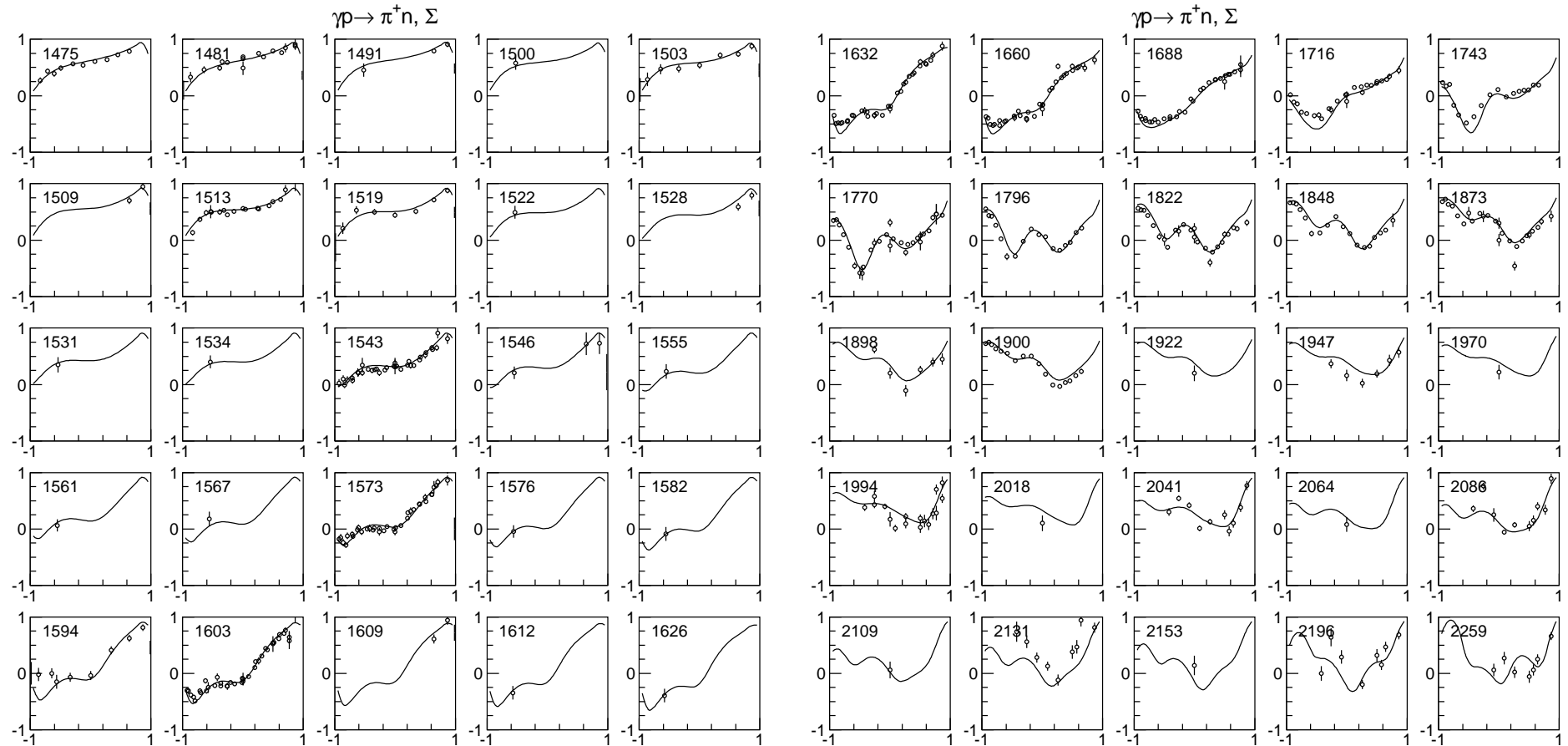


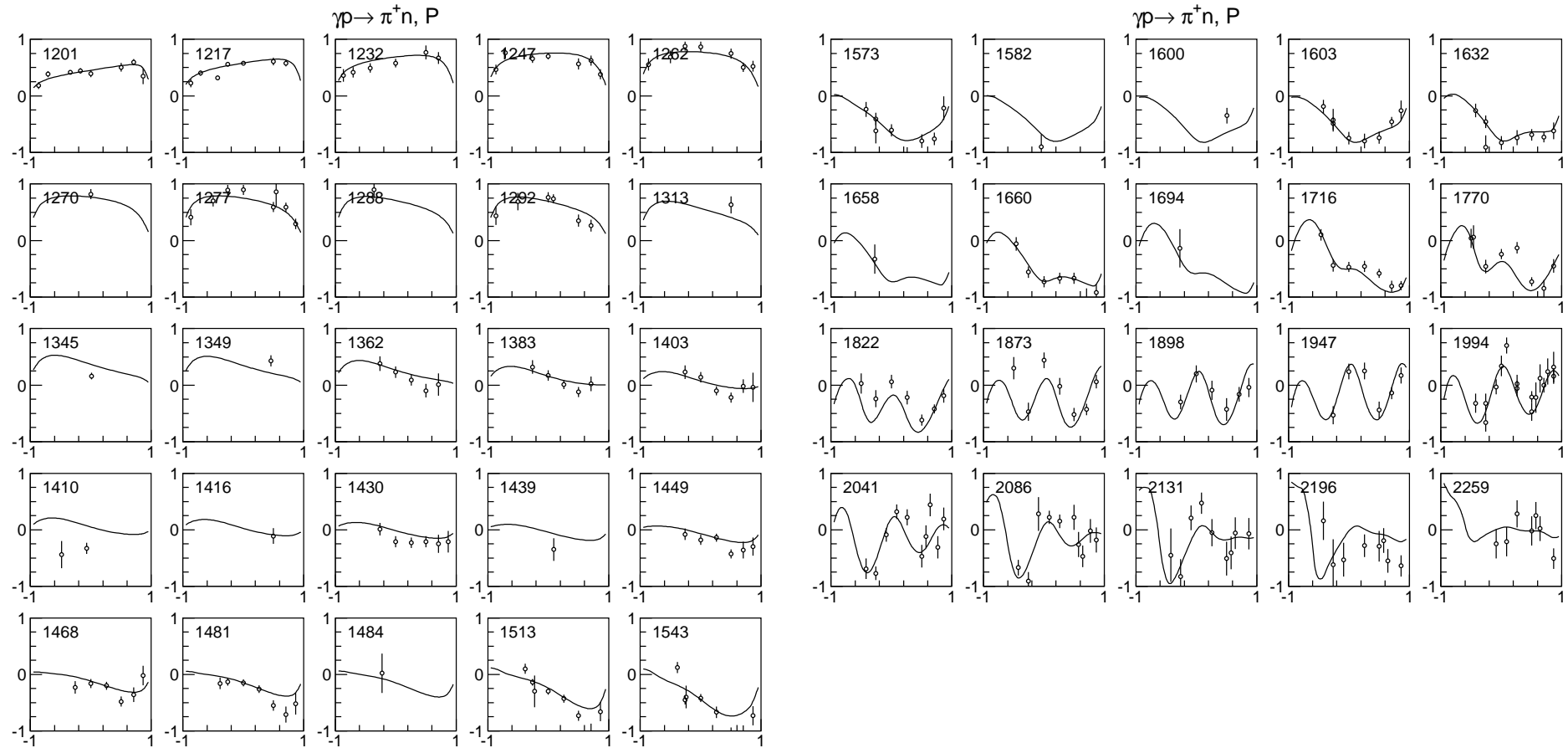


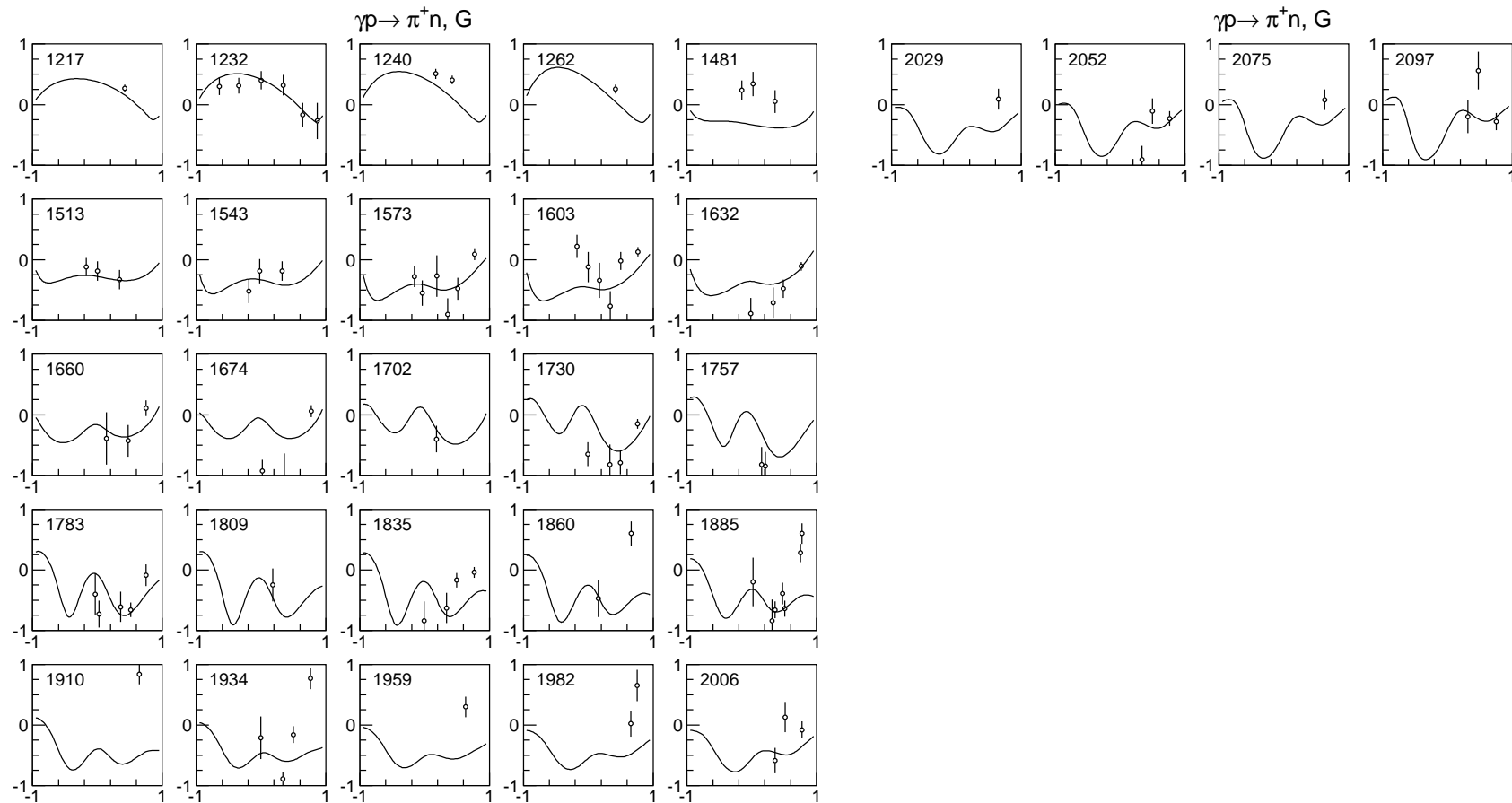


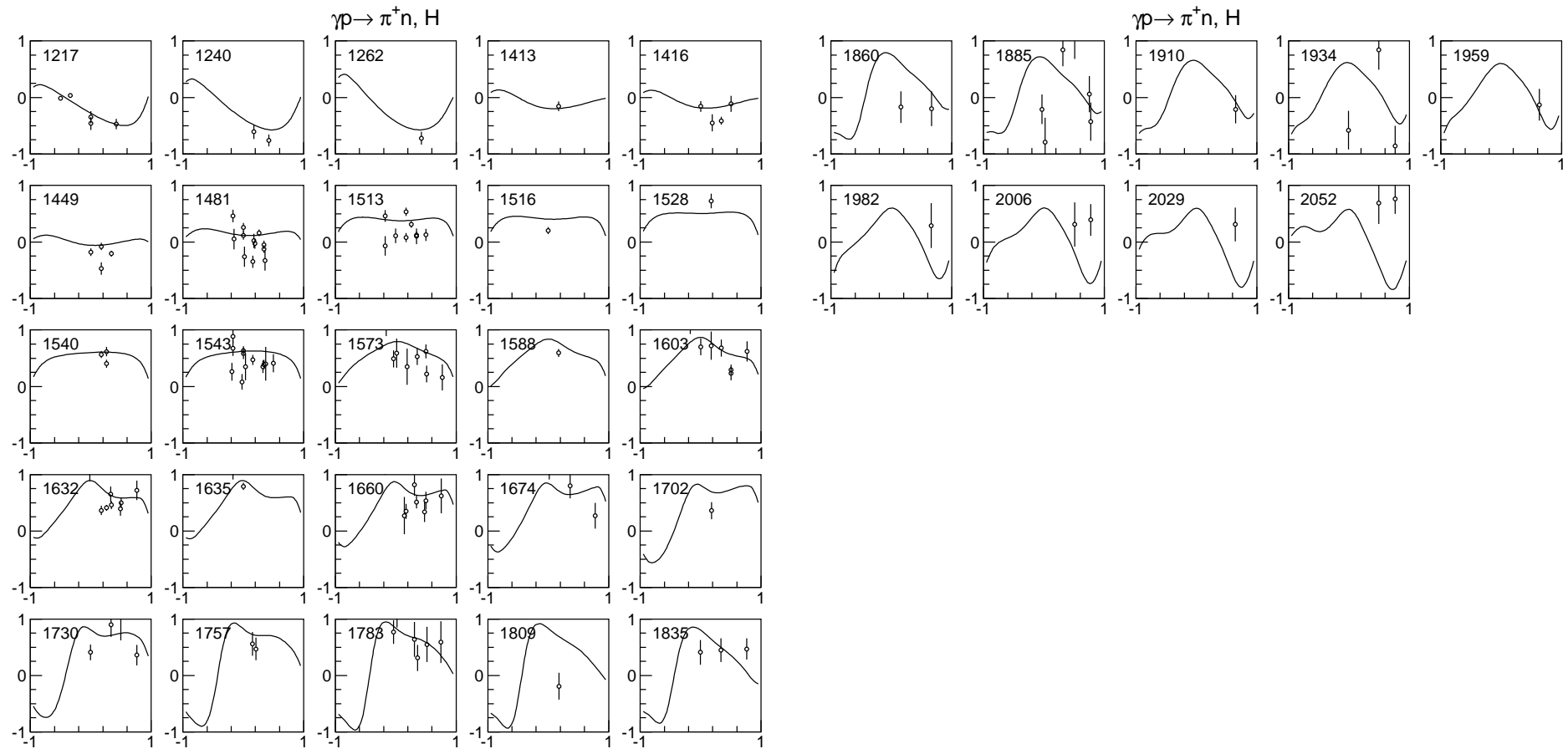


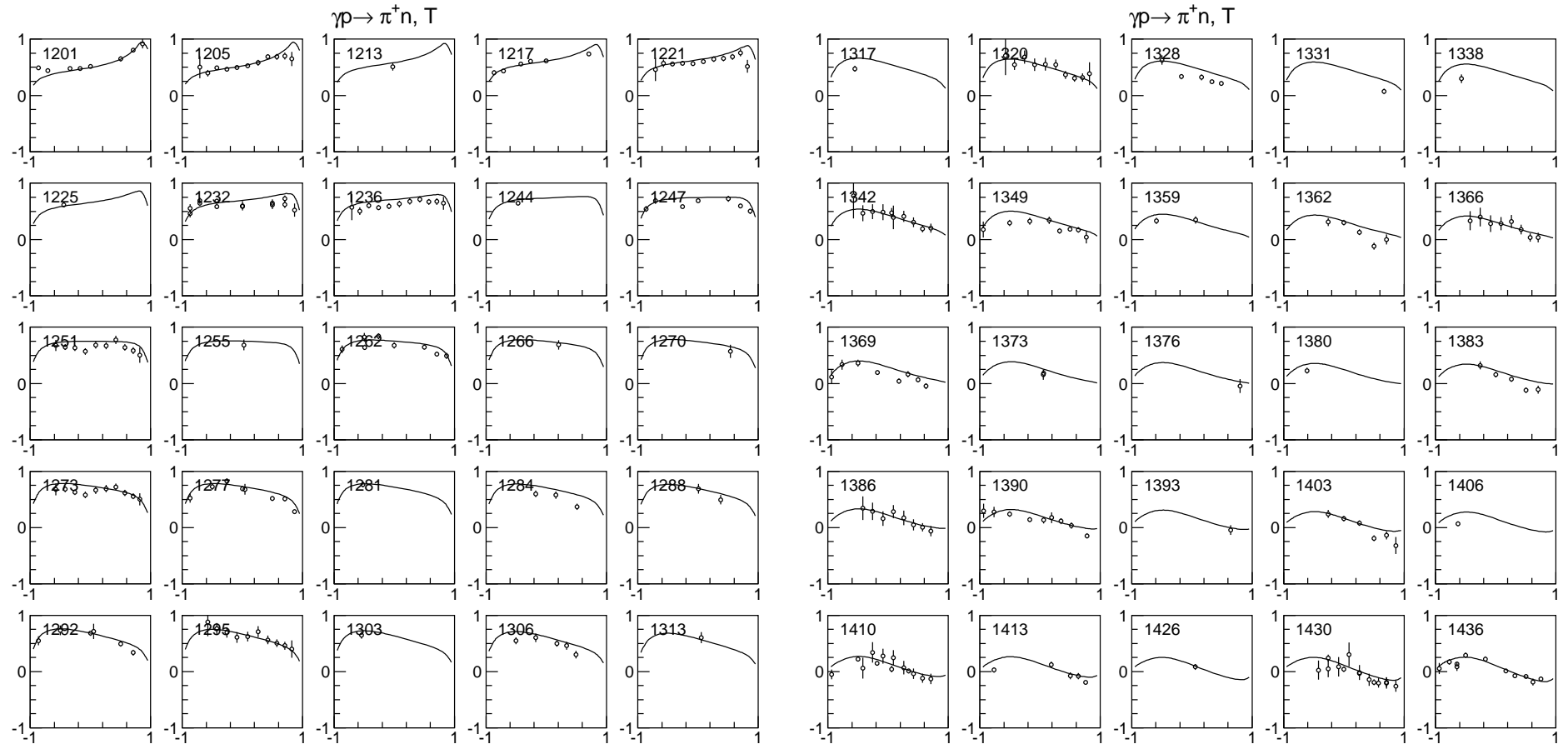


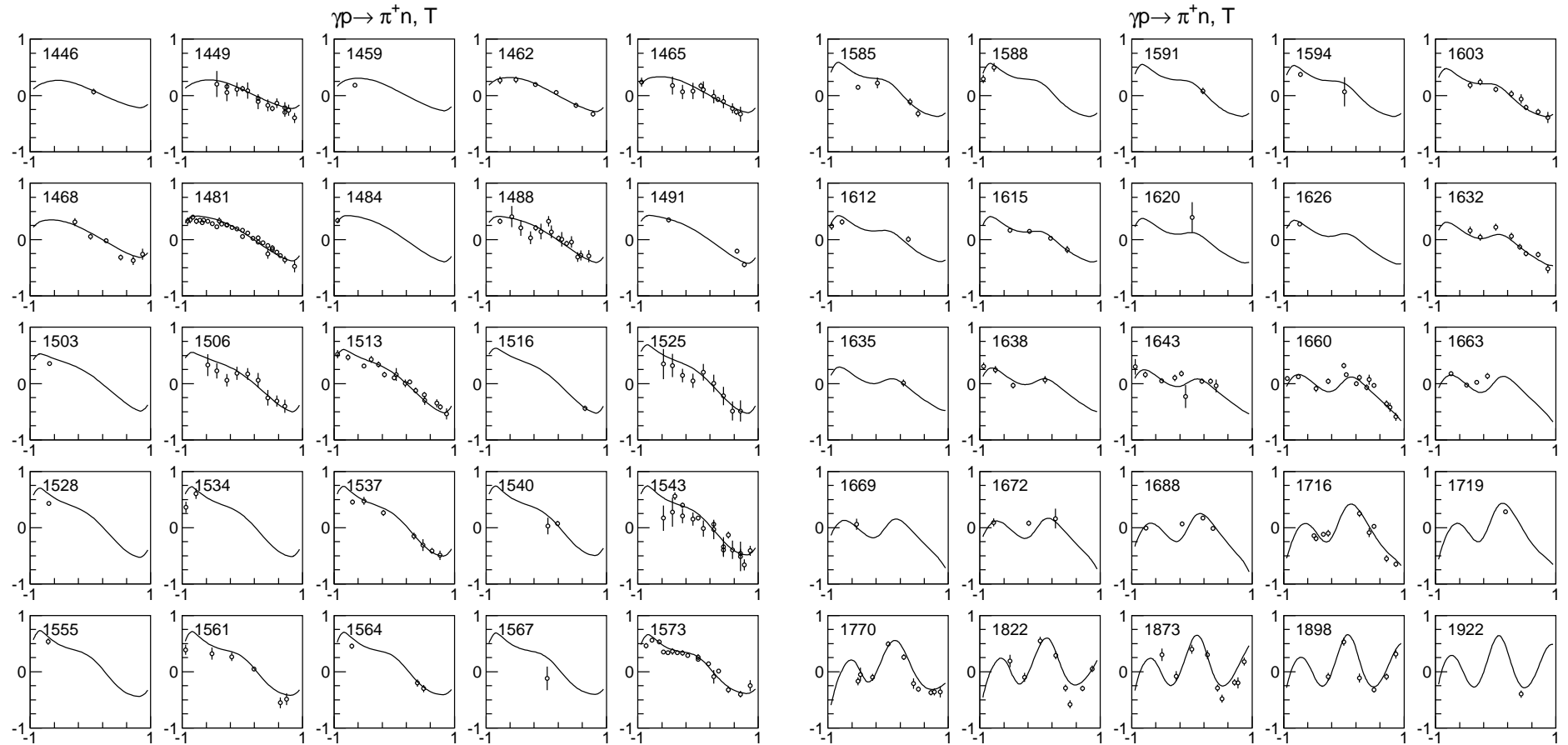


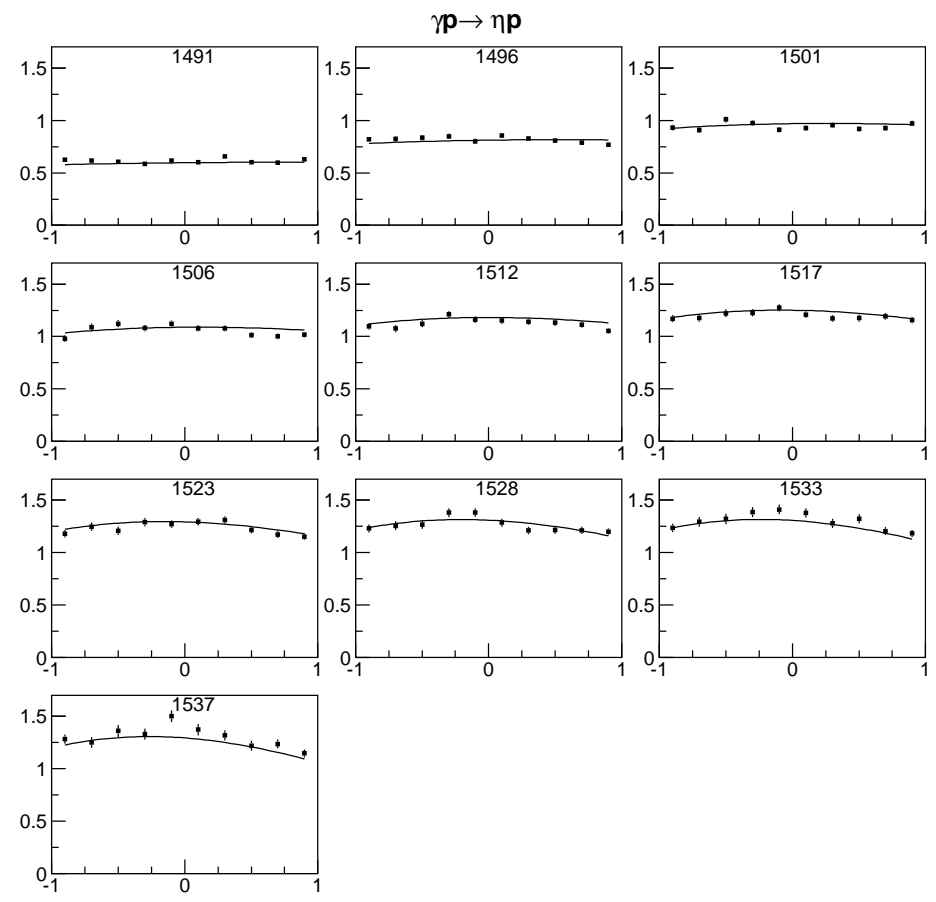
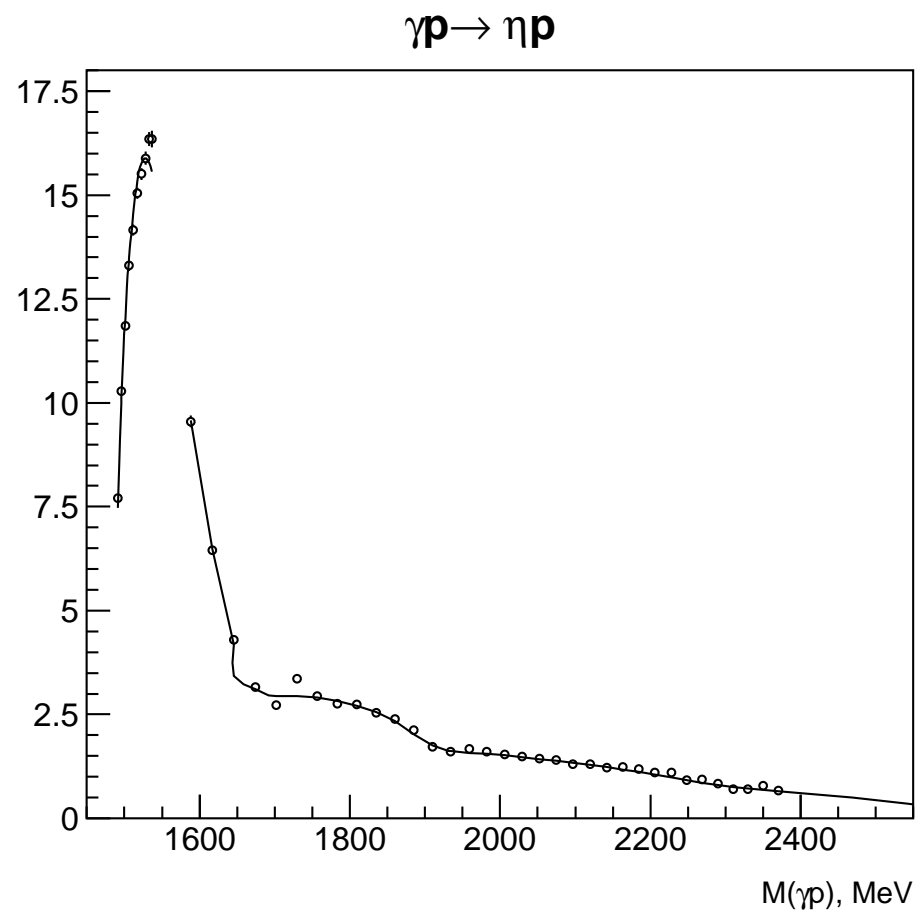


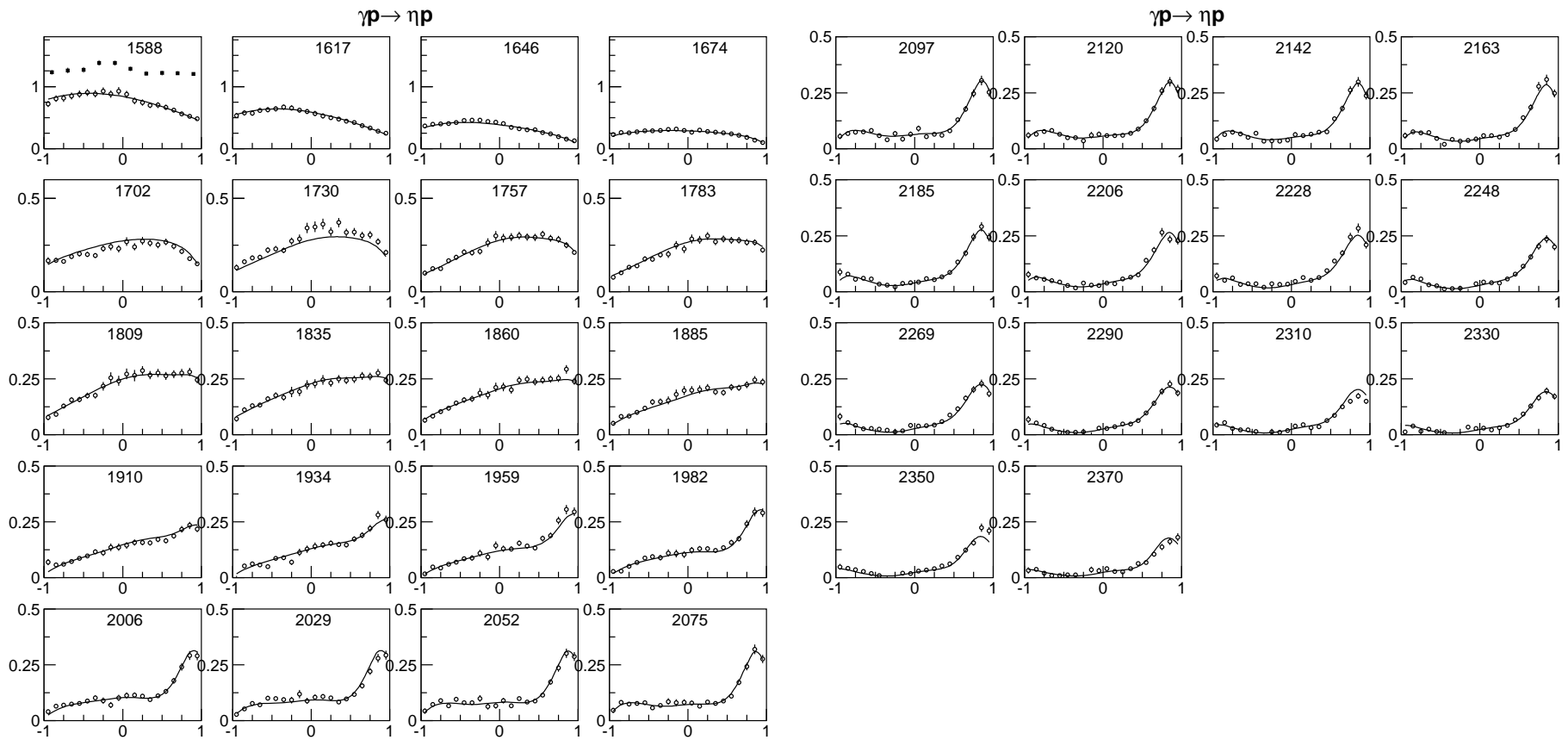


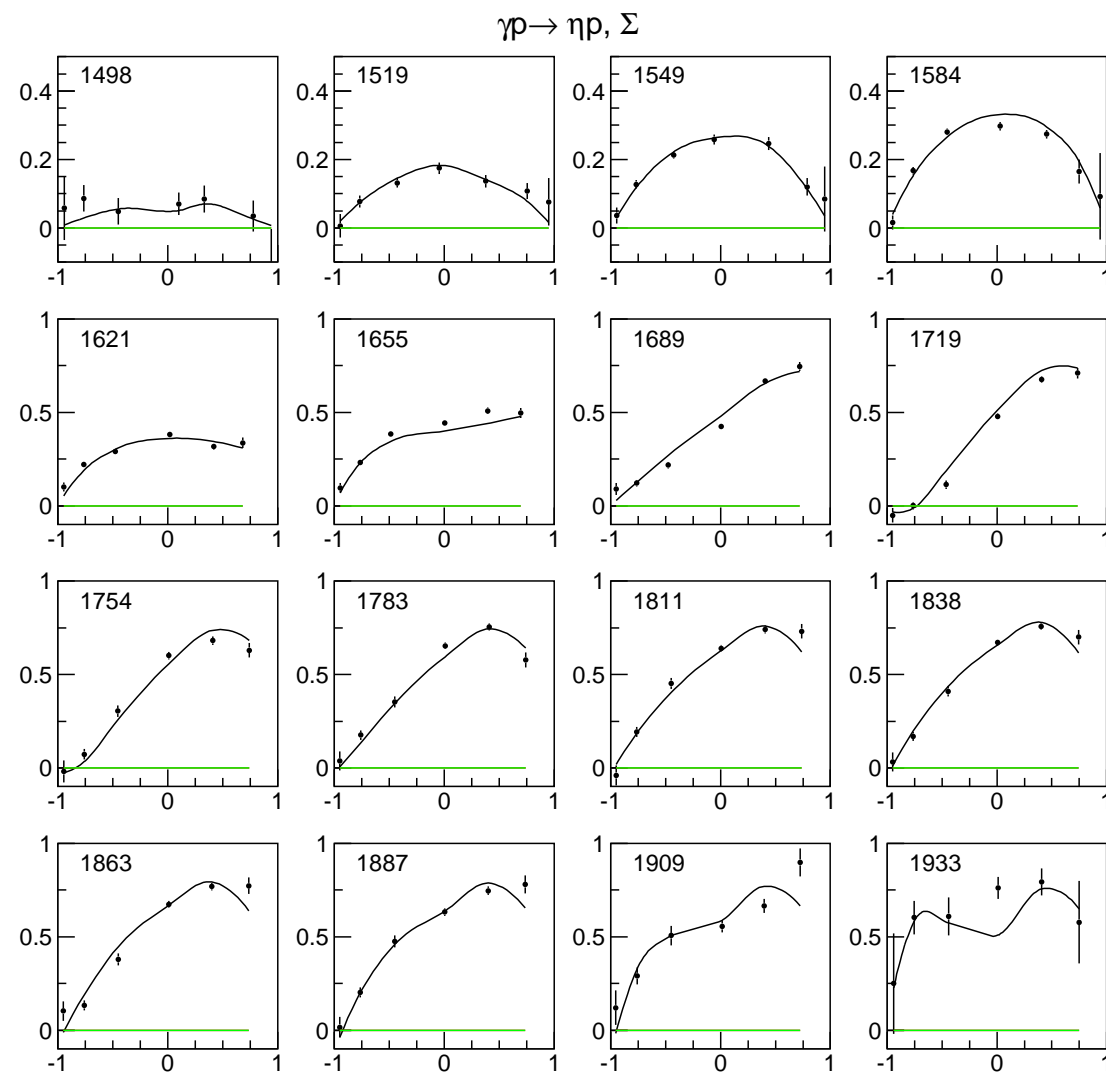


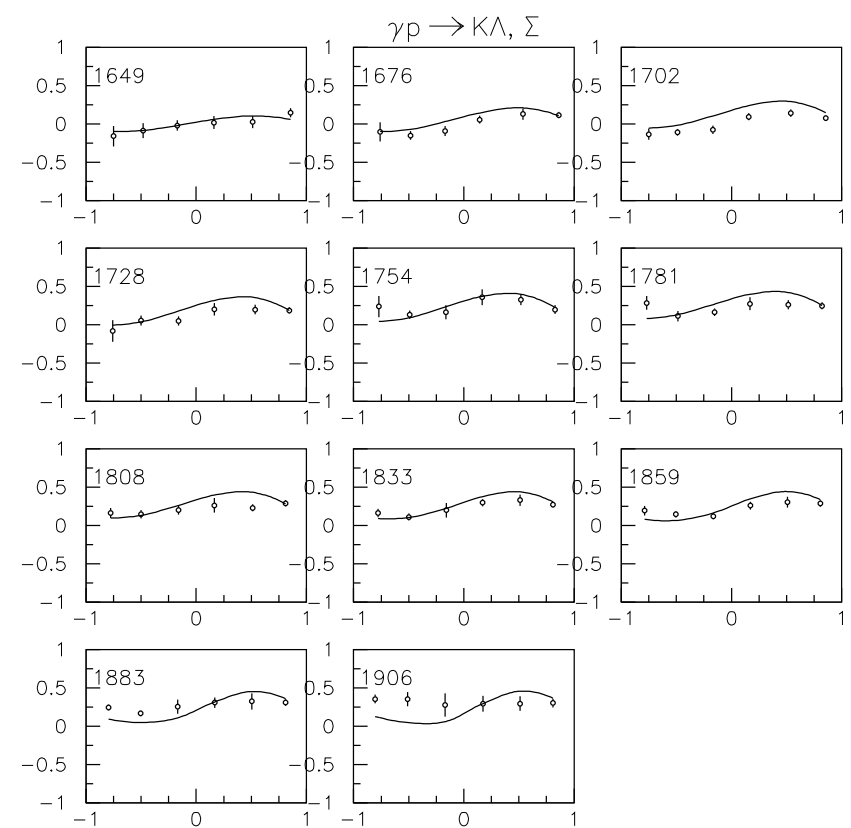
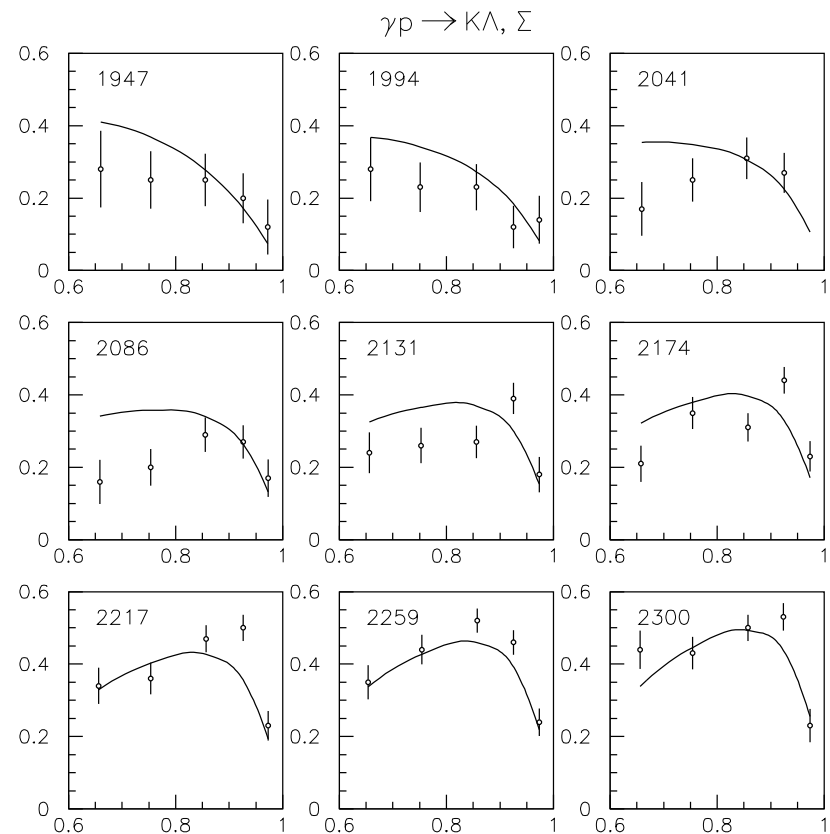


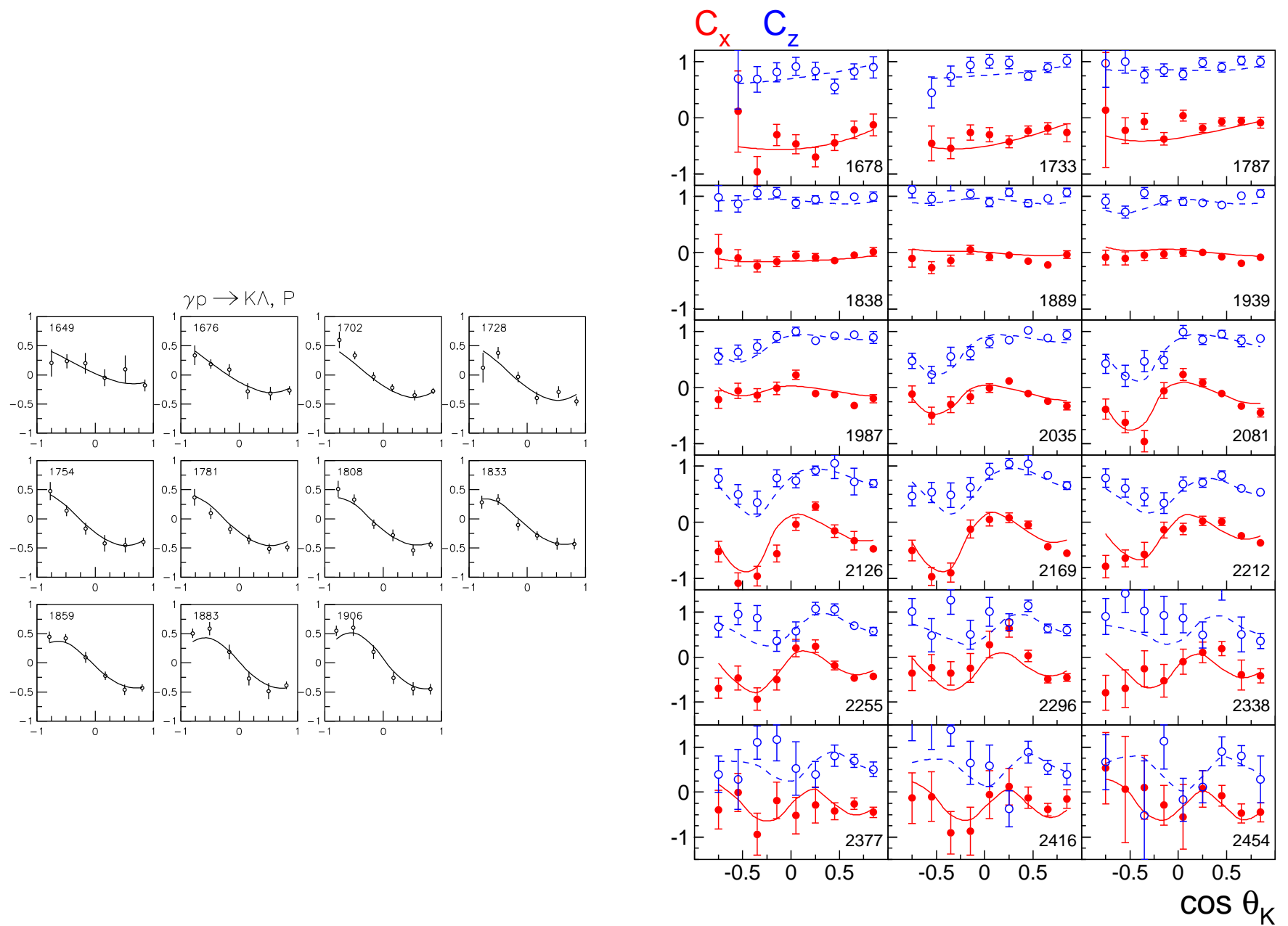


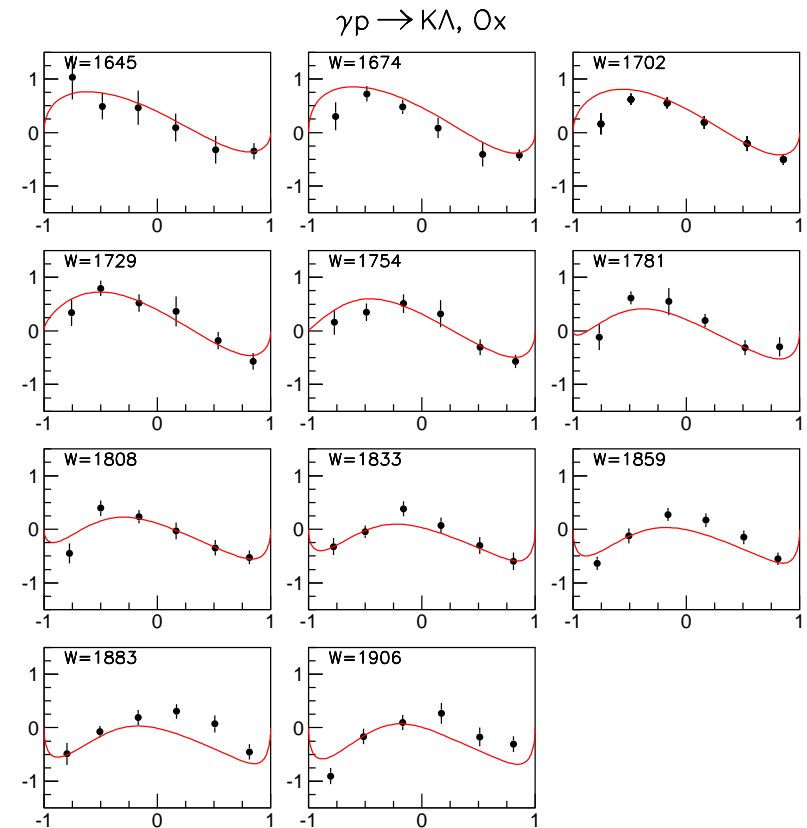
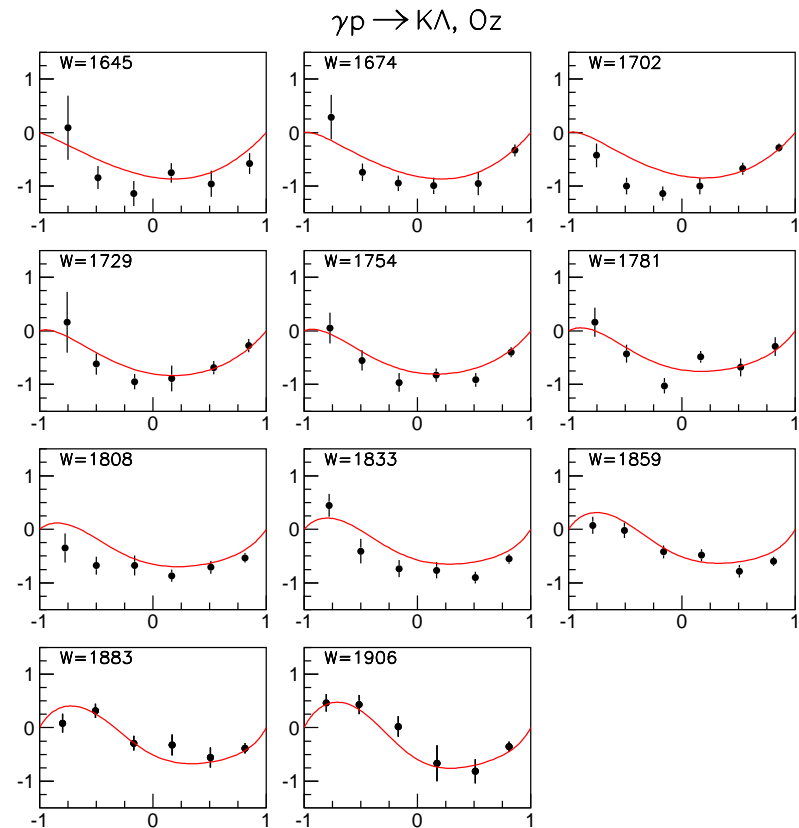


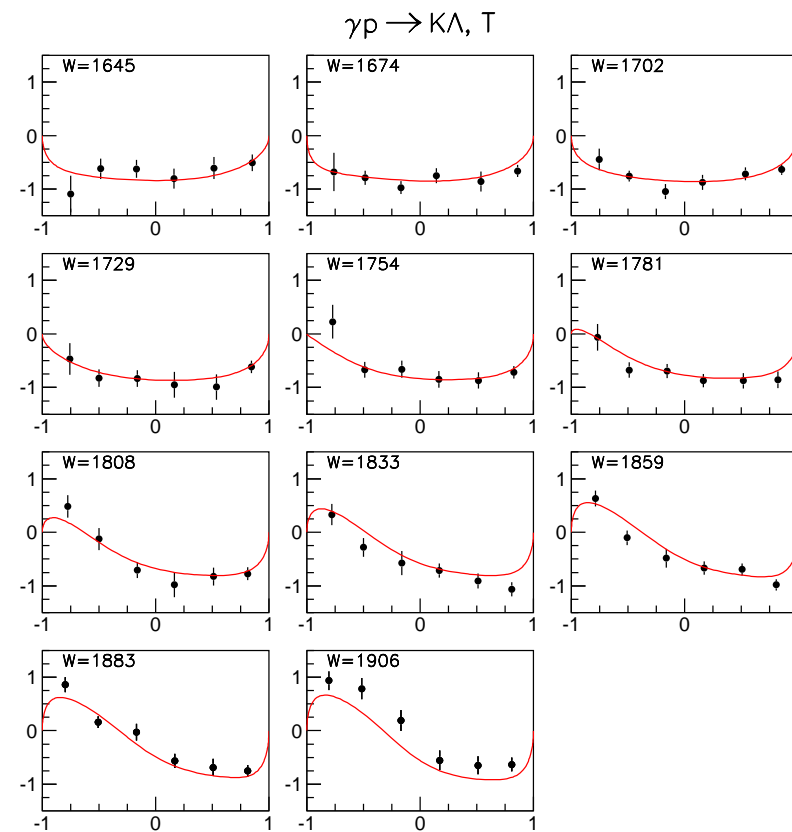


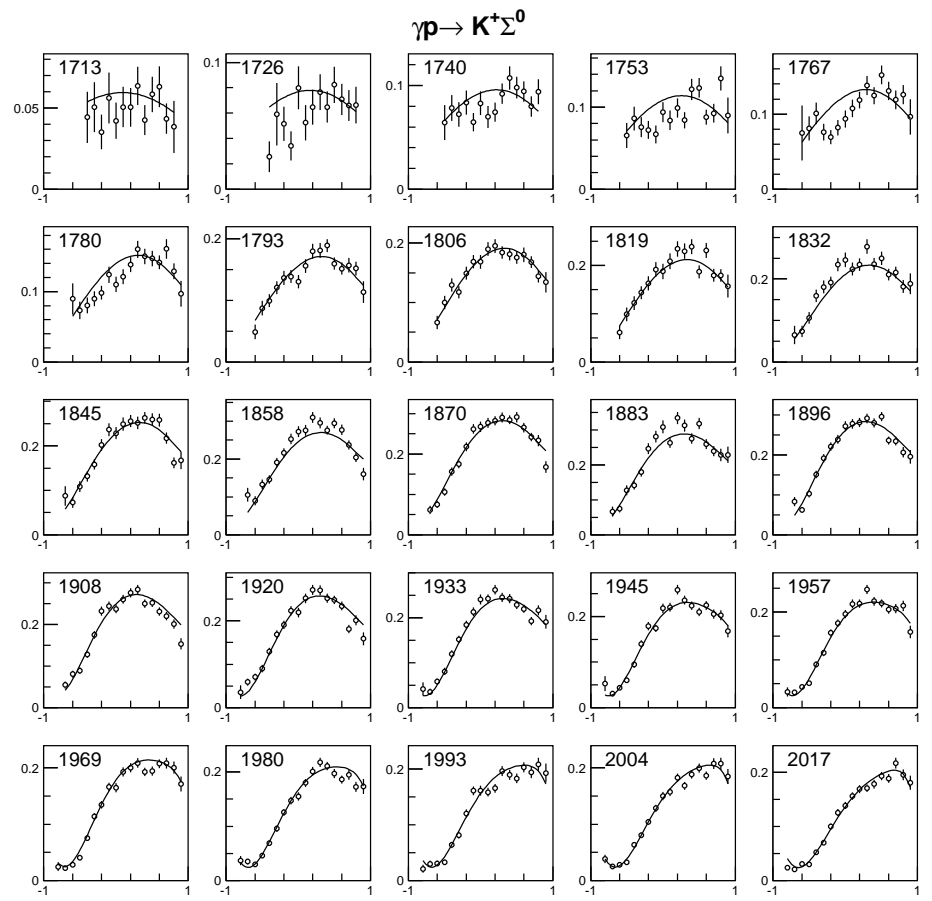
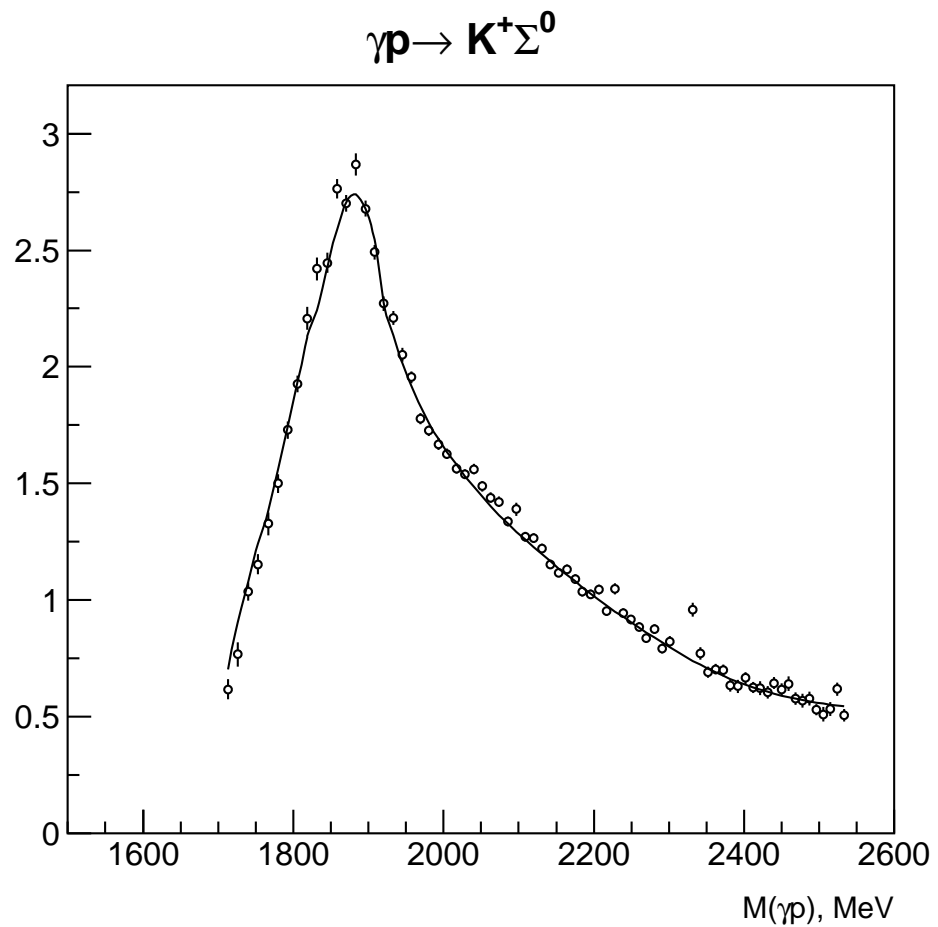


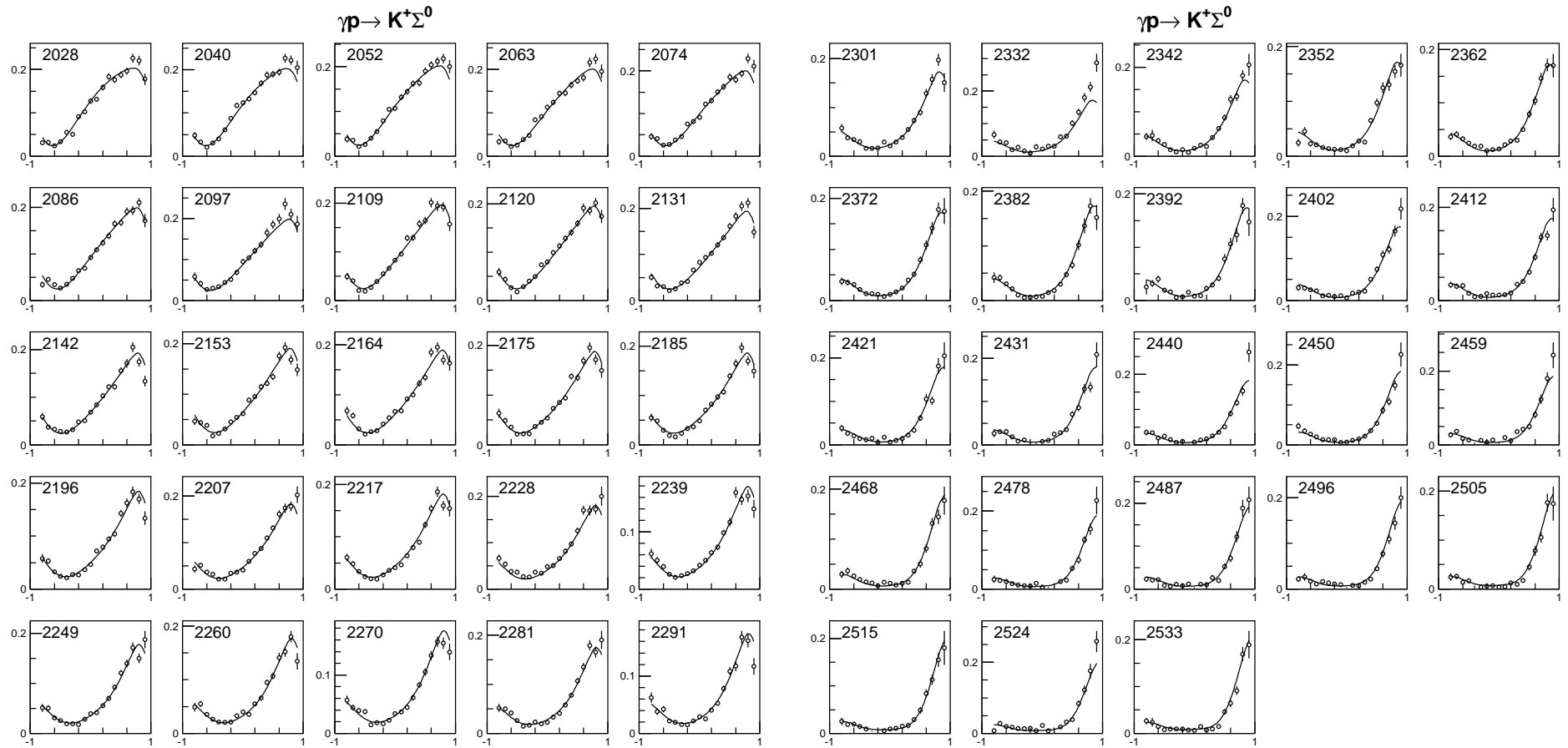


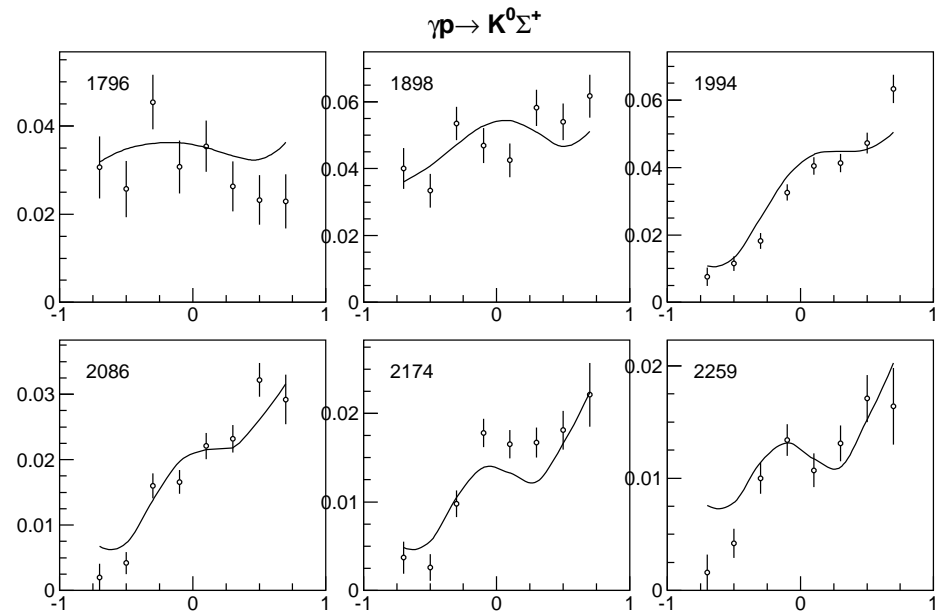
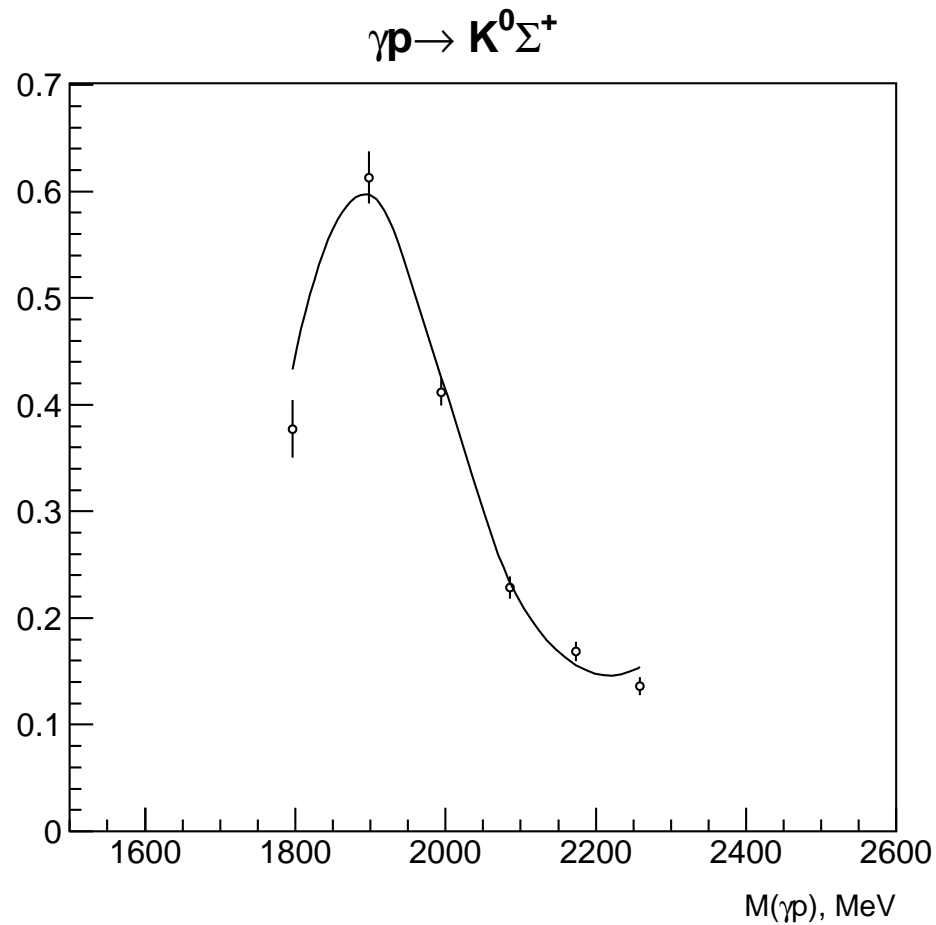


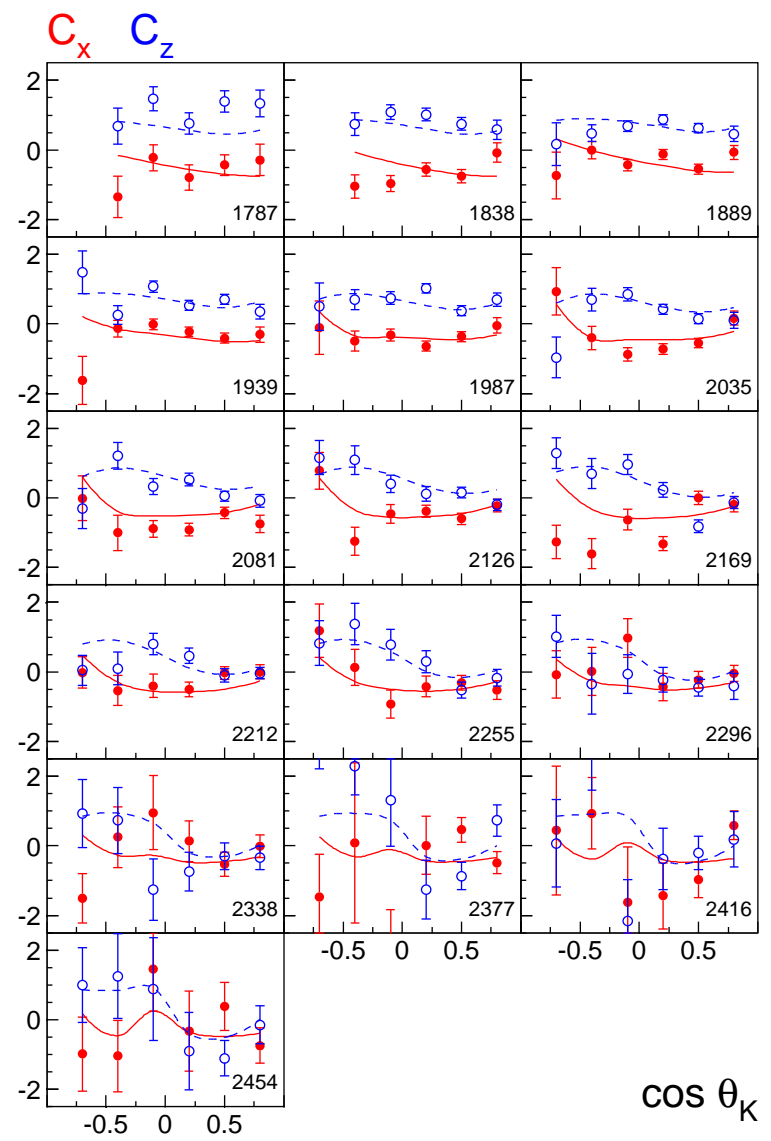
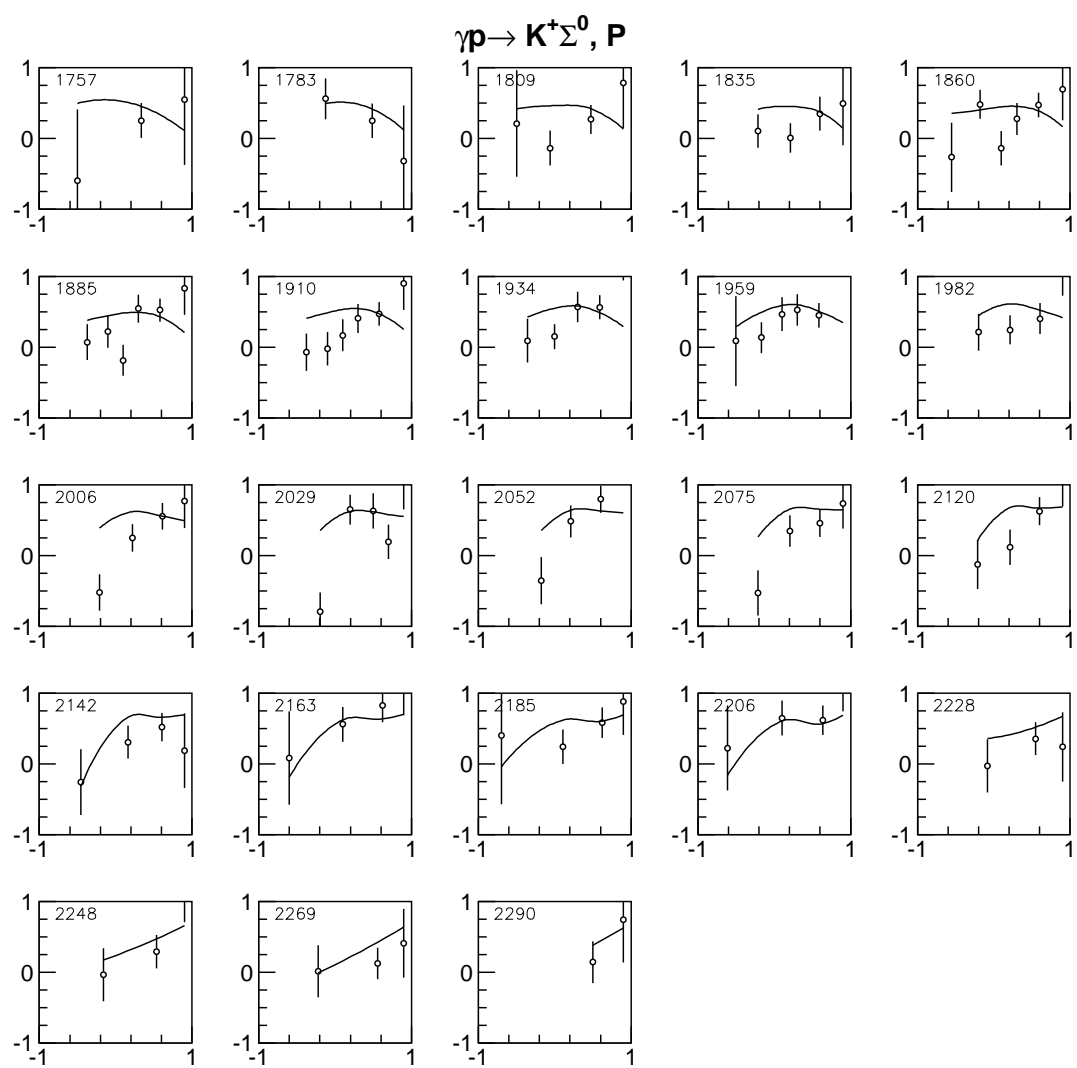


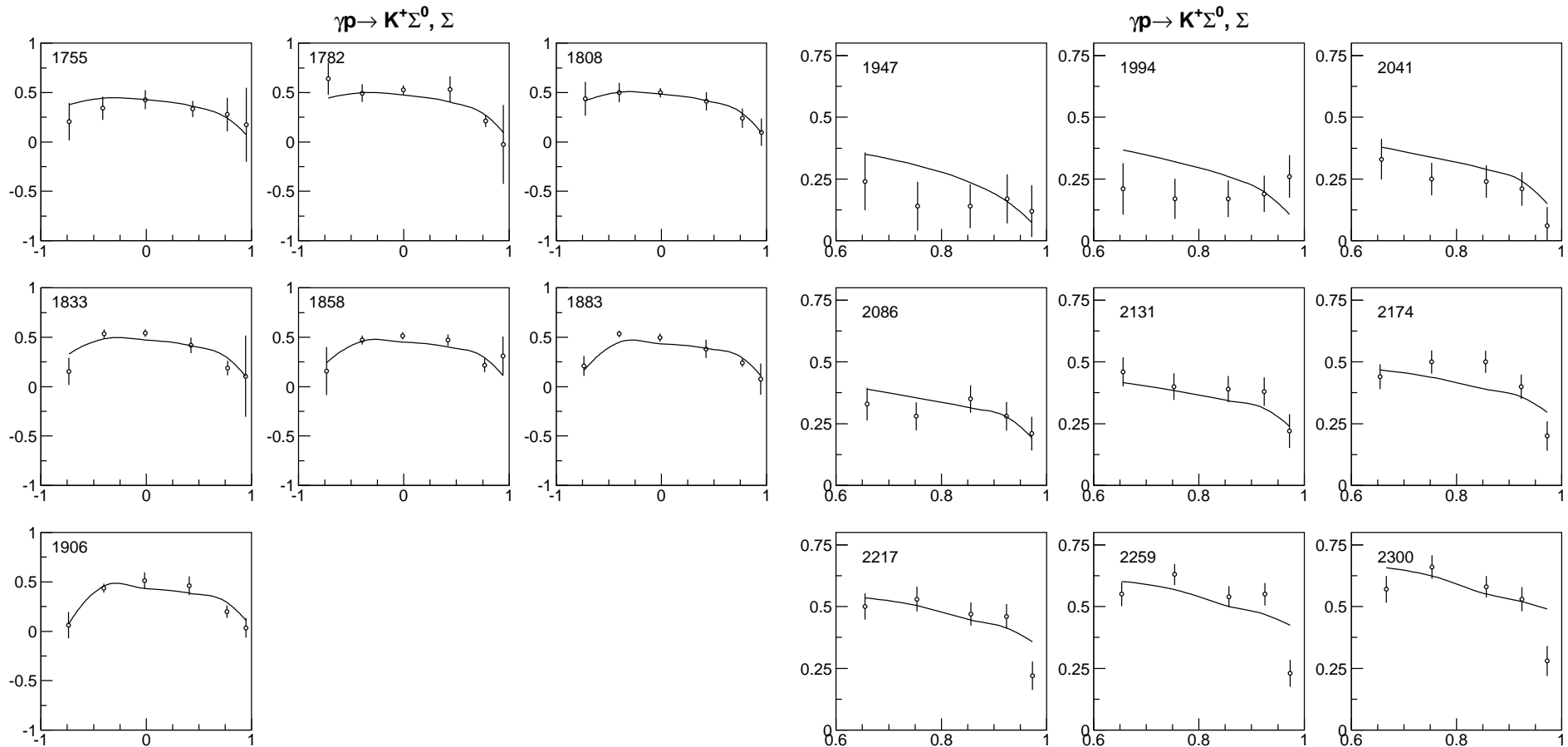


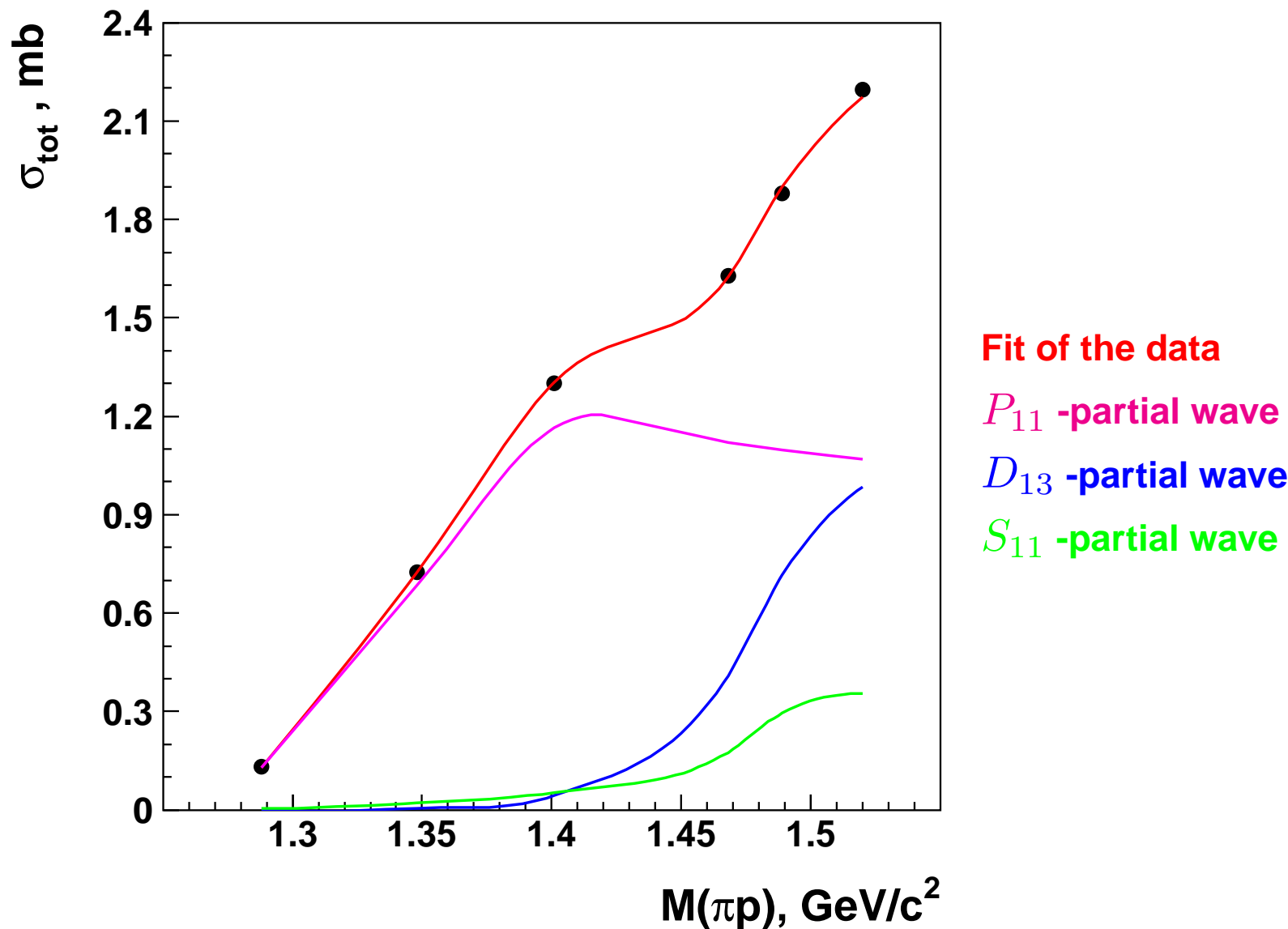






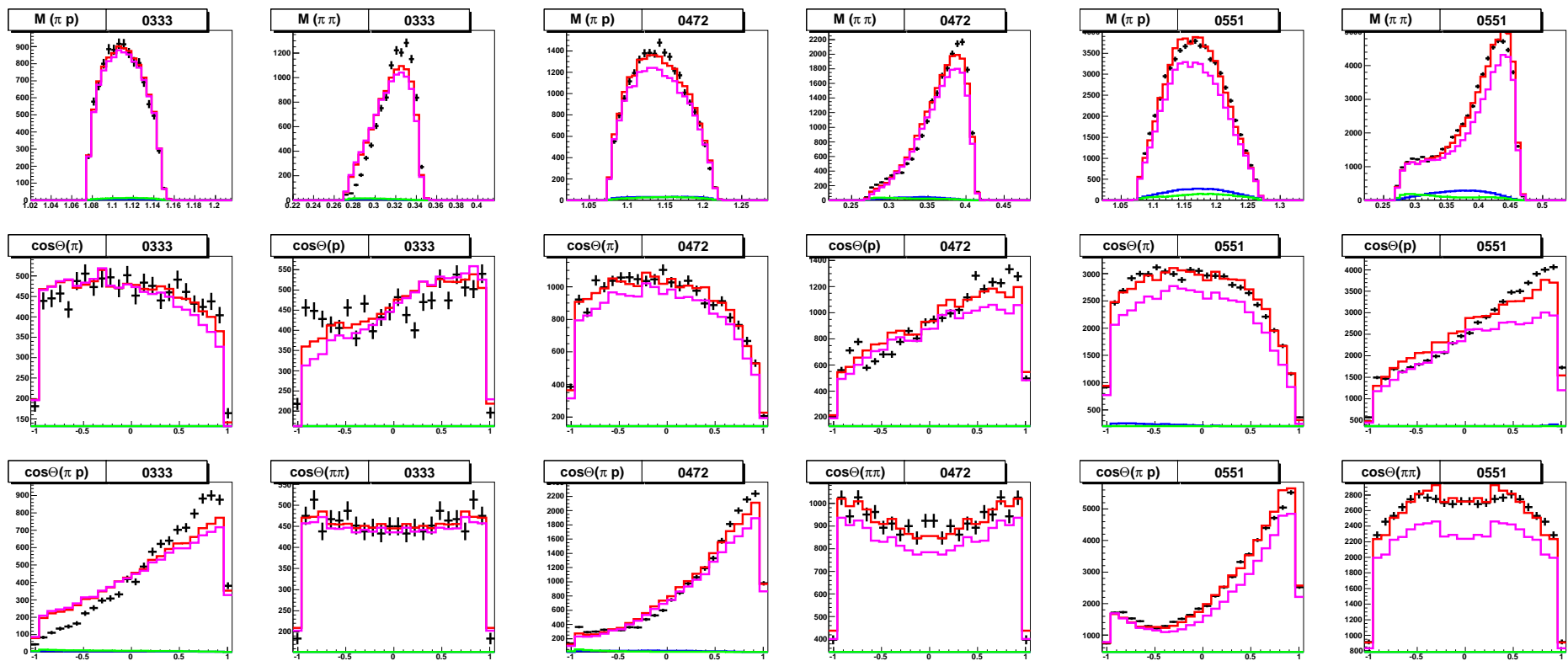




$\pi^- p \rightarrow n\pi^0\pi^0$ (Crystal Ball) total cross section

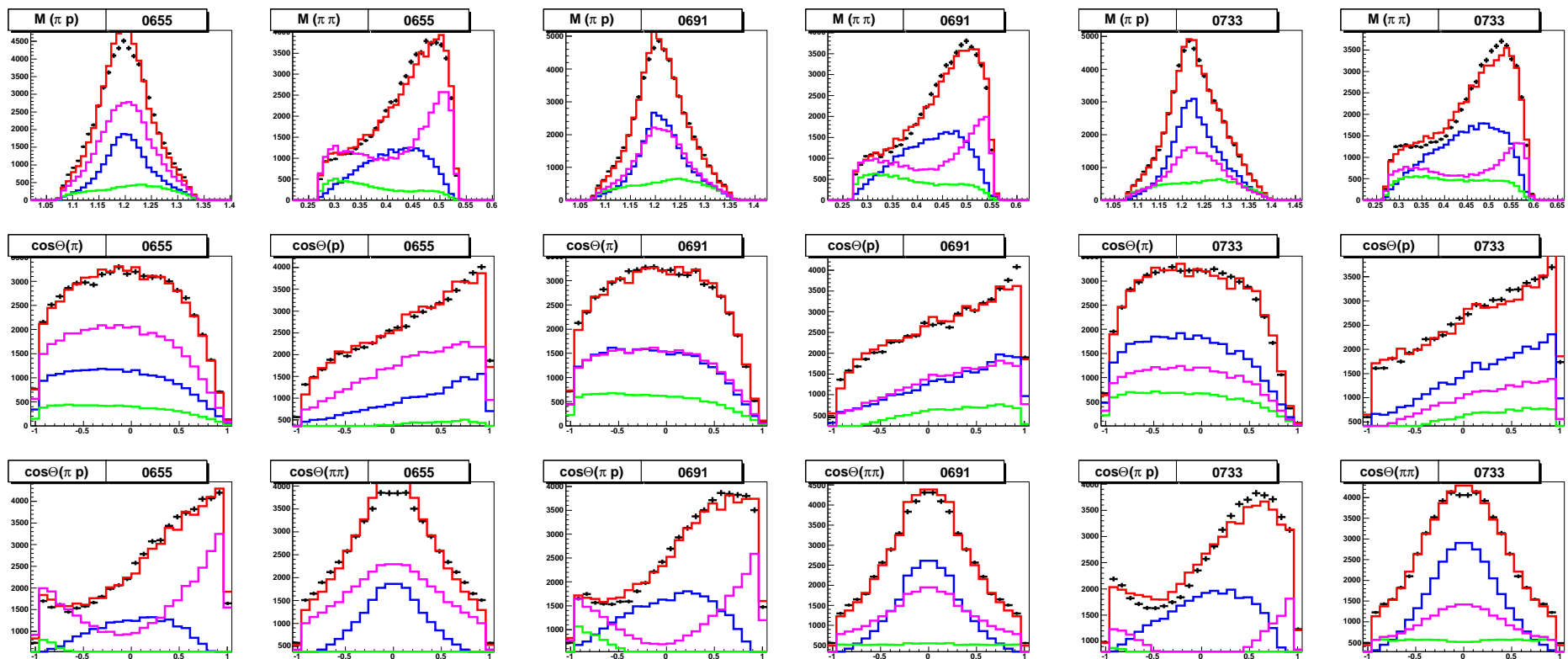
$$\pi^- p \rightarrow n \pi^0 \pi^0 \text{ (Crystal Ball)}$$

Differential cross sections for 333,472 and 551 MeV/c data.



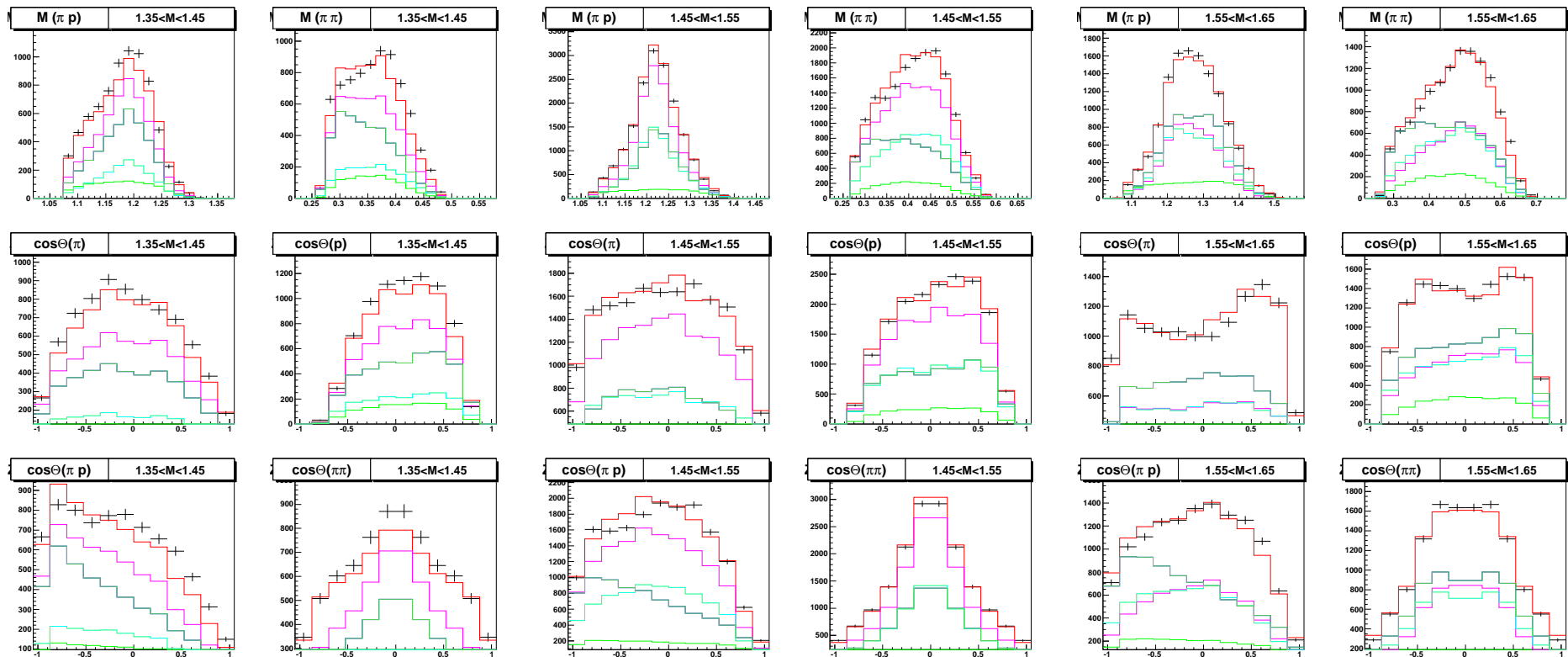
$\pi^- p \rightarrow n\pi^0\pi^0$ (Crystal Ball)

Differential cross sections for 655, 691 and 733 MeV/c data.



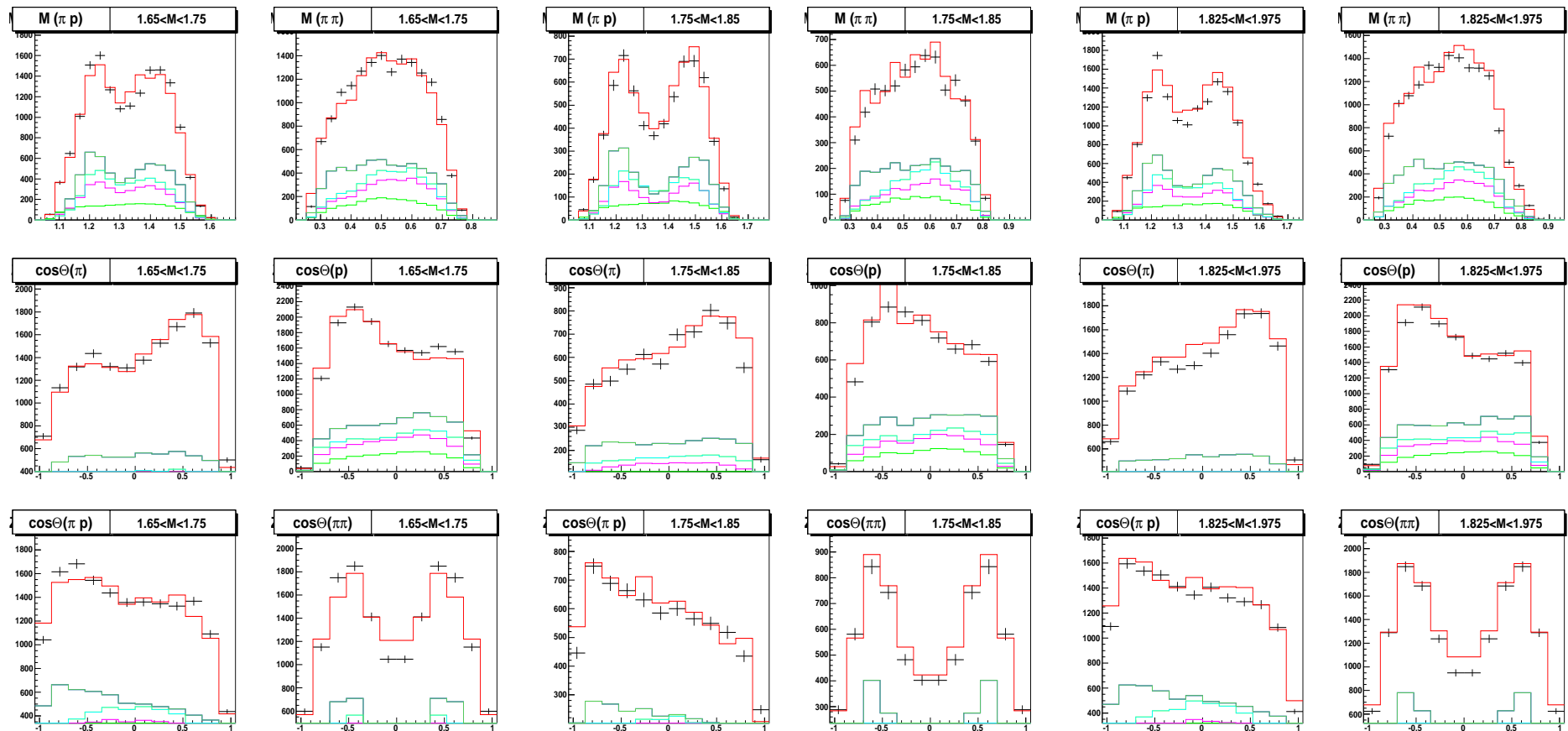
$\gamma p \rightarrow p\pi^0\pi^0$ (CB-ELSA)

Differential cross sections for W=1400, 1500 and 1600 MeV data.



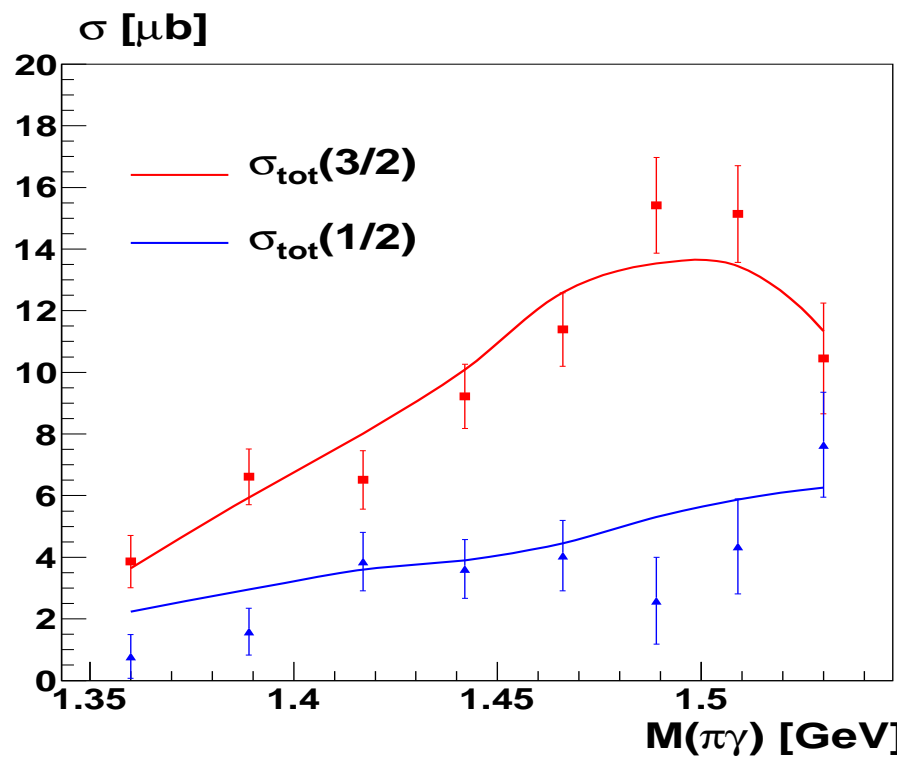
$\gamma p \rightarrow p\pi^0\pi^0$ (CB-ELSA)

Differential cross sections for W=1700, 1800 and 1900 MeV data.



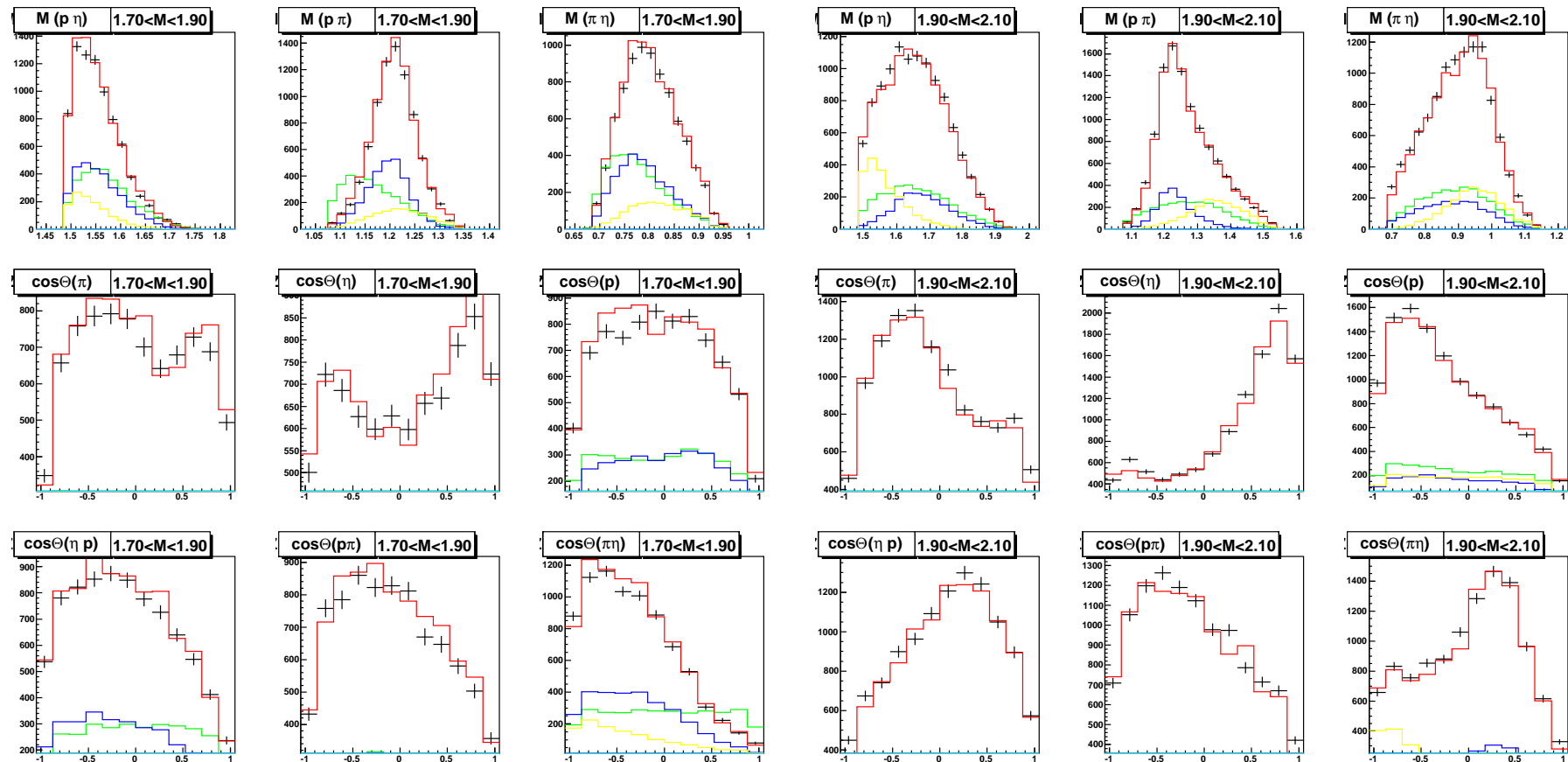
$\gamma p \rightarrow p\pi^0\pi^0$ (**MAMI**)

Differential cross sections $S = 3/2$ and $S = 1/2$.



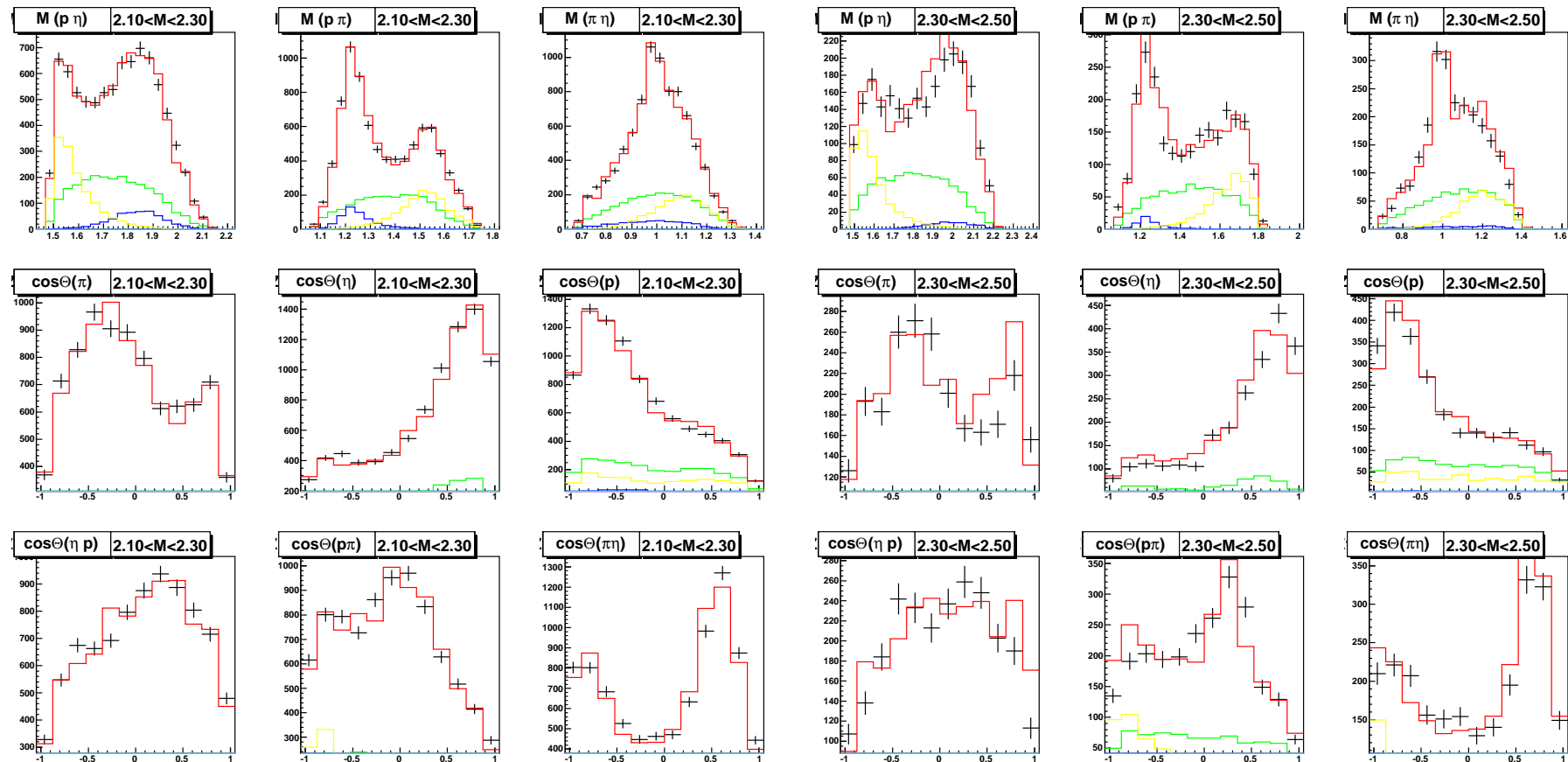
$$\gamma p \rightarrow p\eta\pi^0 \text{ (CB-ELSA)}$$

Differential cross sections for W=1700 and 1800 MeV data.



$$\gamma p \rightarrow p\eta\pi^0 \text{ (CB-ELSA)}$$

Differential cross sections for W=1900 and 2000 MeV data.



$\gamma p \rightarrow p\eta\pi^0$ (CB-ELSA)

Beam asymmetry data.
